

10-2-2015

Label-free surface-enhanced Raman spectroscopy-linked immunosensor assay (SLISA) for environmental surveillance

vinay bhardwaj

Florida International University, vbhar002@fiu.edu

DOI: 10.25148/etd.FIDC000166

Follow this and additional works at: <https://digitalcommons.fiu.edu/etd>

 Part of the [Analytical, Diagnostic and Therapeutic Techniques and Equipment Commons](#), [Biochemical and Biomolecular Engineering Commons](#), [Bioimaging and Biomedical Optics Commons](#), [Biological Engineering Commons](#), [Biomaterials Commons](#), [Biomedical Devices and Instrumentation Commons](#), [Biotechnology Commons](#), [Environmental Engineering Commons](#), [Environmental Health Commons](#), [Environmental Microbiology and Microbial Ecology Commons](#), [Nanomedicine Commons](#), [Nanoscience and Nanotechnology Commons](#), and the [Toxicology Commons](#)

Recommended Citation

bhardwaj, vinay, "Label-free surface-enhanced Raman spectroscopy-linked immunosensor assay (SLISA) for environmental surveillance" (2015). *FIU Electronic Theses and Dissertations*. 2321.

<https://digitalcommons.fiu.edu/etd/2321>

FLORIDA INTERNATIONAL UNIVERSITY

Miami, Florida

LABEL-FREE SURFACE-ENHANCED RAMAN SPECTROSCOPY-LINKED
IMMUNOSENSOR ASSAY (SLISA) FOR ENVIRONMENTAL SURVEILLANCE

A dissertation submitted in partial fulfillment of

the requirements for the degree of

DOCTOR OF PHILOSOPHY

in

BIOMEDICAL ENGINEERING

by

Vinay Bhardwaj

2015

To: Interim Dean Ranu Jung
College of Engineering and Computing

This dissertation, written by Vinay Bhardwaj, and entitled Label-Free Surface-Enhanced Raman Spectroscopy-Linked ImmunoSensor Assay (SLISA) for Environmental Surveillance, having been approved in respect to style and intellectual content, is referred to you for judgment.

We have read this dissertation and recommend that it be approved.

Chenzhong Li

Wei-Chiang Lin

Helen Tempest

Walter M. Goldberg

Anthony J. McGoron, Major Professor

Date of Defense: October 2, 2015

The dissertation of Vinay Bhardwaj is approved.

Interim Dean Ranu Jung
College of Engineering and Computing

Dean Lakshmi N. Reddi
University Graduate School

Florida International University, 2015

© Copyright 2015 by Vinay Bhardwaj

All rights reserved.

Royal Society of Chemistry, Photon Foundation, SPIE and OMICS Publishing Group kindly provided copyright permission to use material contained in the following publications as part of my dissertation, a copy of their written permission is included in the appendices.

Bhardwaj V., Srinivasan, S., McGoron A. J. (2013). AgNPs-based label-free colloidal SERS nanosensor for the rapid and sensitive detection of stress proteins expressed in response to environmental toxins. *J. Biosens. Bioelectron.* S12:005: pp 7. Permission from OMICS Publishing Group.

Bhardwaj V., McGoron, A. J. (2014). Biosensor technology for chemical and biological toxins: progress and prospects. *Photon J. Biomed. Eng.* 112:380-392. Permission from Photon Foundation

Bhardwaj V., Srinivasan S., McGoron A. J. (2015). Efficient intracellular delivery and improved biocompatibility of colloidal silver nanoparticles towards intracellular SERS immunosensing. *Analyst*, 140: 3929-3934. Permission from Royal Society of Chemistry.

Bhardwaj V., Srinivasan S., McGoron A. J. (2015). On-chip surface-enhanced Raman spectroscopy (SERS)-linked immune-sensor assay (SLISA) for rapid environmental surveillance of chemical toxins. *Proc. SPIE*, 5684 Pages 8. Permission from SPIE Publisher

DEDICATION

I dedicate this thesis to my parents

Ganga Dayal Bhardwaj & Savitri,

Whose shields of love, affection and prayers

Have helped me achieve the success.

ACKNOWLEDGMENTS

First and foremost, I thank my advisor, Professor (Dr.) Anthony J. McGoron for his support during my past six years of research. He is one of the most intellectual and lively people I met. Indeed, his didactic, little-more approach to push me beyond my limits has motivated me to think critical and acquire engineering perspectives. I hope, I could be as fair, lively and sincere as my advisor and someday be able to become an excellent advisor like him. I am also very grateful to the members of my research team, Dr. Joshy F. John, Dr. Romila Manchanda, Supriya Srinivasan and Abhigyan Nagasetti for insightful discussions and suggestions in our lab meet sessions.

I thank my committee members Dr. Goldberg, Dr. Tempest, Dr. Li and Dr. Lin for their advice and recommendations to improve quality of my research work. I will take this opportunity to admire Dr. Goldberg for his active help in teaching me histology skills. I also want to thank Dr. Rosen and his team members for sharing their microbiology experience and resources to help me complete my study with yeast. Also, I thank John Goolcharan, an ARCH fellow, who helped me develop design of the prototype chip. I will always be thankful to my former research advisor, Dr. Abhishek Chanchal for providing continuous advice during my doctorate studies. I often think of my time working in his NanoBiotech Lab. His interesting analogies to teach basics of Nanotechnology are contagious. I also thank Dr. Neera Mehra, Dr. Tanushree Saxena and Dr. Rajni Arora, my undergraduate professors, who are my role models for a teacher.

I thank all my friends, fellow Ph.D. students in Department of Biomedical Engineering at Florida International University, who shared their experiences with me,

acted as peer mentors and accompanied me during my past six year journey towards doctorate degree.

I specially thank my family, including my father, mother, wife, sister and brother. The love, care, prayers and sacrifice of my hard-working parents have helped me pass through the rough-times. I hope I made my parents proud.

I thank my Departmental chairperson, Dr. Ranu Jung, who believed in my work and provided me fiscal support by continuous teaching assistantship from Department of Biomedical Engineering. I acknowledge Florida International University - Library for providing Open Access publication funds towards making my research freely and globally available to scientific community. I thank Dr. Isis Artze, Associate Director of FIU-CATE (Center for the Advancement of Teaching), whose periodic workshops have helped me develop effective teaching skills. At last, I would acknowledge Royal Society of Chemistry, Photon Foundation, SPIE and OMICS Publishing Groups for giving me permissions to use their copyright material (mentioned in copyright page) as part of my dissertation.

In past six years, I found a great advisor, my soul mate and many good friends.

ABSTRACT OF THE DISSERTATION

LABEL-FREE SURFACE-ENHANCED RAMAN SPECTROSCOPY-LINKED
IMMUNOSENSOR ASSAY (SLISA) FOR ENVIRONMENTAL SURVEILLANCE

by

Vinay Bhardwaj

Florida International University, 2015

Miami, Florida

Professor Anthony J. McGoron, Major Professor

The contamination of the environment, accidental or intentional, in particular with chemical toxins such as industrial chemicals and chemical warfare agents has increased public fear. There is a critical requirement for the continuous detection of toxins present at very low levels in the environment. Indeed, some ultra-sensitive analytical techniques already exist, for example chromatography and mass spectroscopy, which are approved by the US Environmental Protection Agency for the detection of toxins. However, these techniques are limited to the detection of known toxins. Cellular expression of genomic and proteomic biomarkers in response to toxins allows monitoring of known as well as unknown toxins using Polymerase Chain Reaction and Enzyme Linked Immunosensor Assays. However, these molecular assays allow only the endpoint (extracellular) detection and use labels such as fluorometric, colorimetric and radioactive, which increase chances of uncertainty in detection. Additionally, they are time, labor and cost intensive. These technical limitations are unfavorable towards the development of a biosensor technology for continuous detection of toxins. Federal agencies including the Departments of

Homeland Security, Agriculture, Defense and others have urged the development of a detect-to-protect class of advanced biosensors, which enable environmental surveillance of toxins in resource-limited settings.

In this study a Surface-Enhanced Raman Spectroscopy (SERS) immunosensor, aka a SERS-linked immunosensor assay (SLISA), has been developed. Colloidal silver nanoparticles (Ag NPs) were used to design a flexible SERS immunosensor. The SLISA proof-of-concept biosensor was validated by the measurement of a dose dependent expression of RAD54 and HSP70 proteins in response to H₂O₂ and UV. A prototype microchip, best suited for SERS acquisition, was fabricated using an on-chip SLISA to detect RAD54 expression in response to H₂O₂. A dose-response relationship between H₂O₂ and RAD54 is established and correlated with EPA databases, which are established for human health risk assessment in the events of chemical exposure. SLISA outperformed ELISA by allowing RISE (rapid, inexpensive, simple and effective) detection of proteins within 2 hours and 3 steps. It did not require any label and provided qualitative information on antigen-antibody binding. SLISA can easily be translated to a portable assay using a handheld Raman spectrometer and it can be used in resource-limited settings. Additionally, this is the first report to deliver Ag NPs using TATHA2, a fusogenic peptide with cell permeability and endosomal rupture release properties, for rapid and high levels of Ag NPs uptake into yeast without significant toxicity, prerequisites for the development of the first intracellular SERS immunosensor.

TABLE OF CONTENTS

CHAPTER	PAGE
CHAPTER 1 INTRODUCTION AND BACKGROUND	1
1.1 SCOPE AND MOTIVATION	1
1.2 SENSOR TECHNIQUES	2
1.3 CELL-BASED BIOSENSORS	8
1.4 LABEL-FREE CELL-BASED BIOSENSORS	11
1.5 RAMAN SPECTROSCOPY AND SURFACE-ENHANCED RAMAN SPECTROSCOPY (RS AND SERS)	13
1.6 SERS SUBSTRATES	17
REFERENCES	25
CHAPTER 2 STATEMENT OF RESEARCH, HYPOTHESES & SPECIFIC AIMS	35
2.1 STATEMENT OF RESEARCH	35
2.2 HYPOTHESES	35
2.3 SPECIFIC AIMS	36
REFERENCES	37
CHAPTER 3 MATERIALS AND METHODS	38
3.1 MATERIALS AND METHODS FOR EXTRACELLULAR DETECTION OF STRESS PROTEINS USING ELISA	38
3.1.1 YEAST GROWTH	38
3.1.2 TOXINS EXPOSURE	38
3.1.3 CELL LYSIS	39
3.1.4 TOTAL PROTEIN ESTIMATION	39
3.1.5 SPECIFIC STRESS PROTEIN ESTIMATION	40
3.2 MATERIALS AND METHODS FOR FABRICATION OF COLLOIDAL SERS SENSOR	41
3.2.1 SYNTHESIS OF COLLOIDAL SERS SUBSTRATES	41
3.2.2 PHYSICAL CHARACTERIZATION OF SERS SUBSTRATES	41
3.2.3 SELECTION OF ACTIVE SERS SUBSTRATE	42
3.2.4 FABRICATION OF SERS SENSOR	42
3.2.5 CHARACTERIZATION OF SERS SENSOR	43
3.2.6 SELECTIVITY TESTING OF SERS SENSOR	44
3.3 MATERIALS AND METHODS FOR EXTRACELLULAR DETECTION OF STRESS PROTEINS USING SERS SENSOR AKA SLISA	44
3.3.1 SERS INSTRUMENTATION AND MEASUREMENT	44
3.3.2 ESTIMATION OF PROTEINS	45
3.3.3 COMPARISON OF TWO SENSORS, ELISA VS. SLISA	45
3.4 MATERIALS AND METHODS FOR INTRACELLULAR DELIVERY AND DETECTION USING SERS SENSOR	45

3.4.1 CELLULAR TOXICITY STUDIES	45
3.4.2 CELLULAR UPTAKE STUDIES	46
3.4.3 SENSOR STABILITY AND INTRACELLULAR DETECTION	47
3.5 MATERIALS AND METHODS FOR A CASE STUDY	47
3.5.1 FABRICATION OF A PROTOTYPE MICROCHIP	47
3.5.2 ON-CHIP SLISA: A CASE STUDY	47
REFERENCES	48
CHAPTER 4 EXTRACELLULAR DETECTION OF STRESS PROTEINS USING ELISA	51
4.1 DETERMINATION OF CELL CONCENTRATION	51
4.2 PURITY ANALYSIS OF PROTEINS IN CELL EXTRACT	52
4.3 ESTIMATION OF TOTAL PROTEIN	52
4.4 ESTIMATION OF STRESS PROTEIN USING ELISA	53
4.5 SUMMARY	57
REFERENCES	57
CHAPTER 5 FABRICATION OF COLLOIDAL SERS SENSOR	59
5.1 SYNTHESIS AND CHARACTERIZATION OF SERS SUBSTRATES	59
5.2 SELECTION OF ACTIVE SERS SUBSTRATE	60
5.3 PHYSICOCHEMICAL CHARACTERIZATION OF SERS SENSOR	61
5.4 SELECTIVITY TESTING OF SERS SENSOR	63
5.5 SUMMARY	64
REFERENCES	65
CHAPTER 6 EXTRACELLULAR DETECTION OF STRESS PROTEINS USING SERS SENSOR AKA SLISA	67
6.1 ESTIMATION OF PROTEINS USING SLISA	67
6.2 COMPARISON OF SENSING ATTRIBUTES, ELISA VS. SLISA	68
6.3 SUMMARY	72
REFERENCES	73
CHAPTER 7 INTRACELLULAR DELIVERY AND DETECTION OF PROTEINS USING SERS SENSOR AKA CBB-SIST	74
7.1 CELLULAR TOXICITY	74
7.2 CELLULAR UPTAKE	77
7.3 INTRACELLULAR DETECTION	80
7.4 SUMMARY	82
REFERENCES	83
CHAPTER 8 A CASE STUDY: ON-CHIP SLISA	85
8.1 FABRICATION OF A PROTOTYPE MICROCHIP	85
8.2 A CASE STUDY	97
8.3 SUMMARY	90
REFERENCES	90

SUMMARY AND FUTURE WORK	92
APPENDICES	96
VITA	117

LIST OF FIGURES

FIGURE	PAGE
Fig 1. Classification of biosensor technologies	3
Fig 2. Schematic of bioreporter technology	10
Fig 3 Mechanisms and examples of commercial label-free cell-based biosensors	13
Fig 4 Schematic of various interactions of a molecule with monochromatic light	15
Fig 5 Raman vs fluorescence spectrum	15
Fig 6 Size dependent Ag NPs properties	19
Fig 7 Three limiting steps in efficient delivery of NPs for intracellular applications	22
Fig. 8 Microchip design	49
Fig 9 Absorption spectra of supernatant after cell lysis	53
Fig 10 BSA standard curve	54
Fig 11 Quantitation of RAD54 expressed by yeast cells exposed to H ₂ O ₂ for 60 minutes and detected by ELISA	55
Fig 12 Quantitation of RAD54 expressed by yeast cells exposed to UV for 15 minutes and detected by ELISA	55
Fig 13 Quantitation of HSP70 expressed by yeast cells exposed to H ₂ O ₂ for 60 minutes and detected by ELISA	56
Fig 14 Quantitation of HSP70 expressed by yeast cells exposed to UV for 15 minutes and detected by ELISA	56
Fig 15 Characterization of colloidal Au (top row) and Ag (bottom row) NPs-based SERS substrates	61
Fig 16 Physical characterization of Ag NPs-based SERS substrate (left column) and sensor for RAD54 detection (right column)	62
Fig 17 Chemical characterization of the SERS sensor for RAD54 detection	64

Fig 18 Selectivity of the RAD54 SERS sensor	65
Fig 19 Schematic representation of the SERS sensor (aka SLISA, left) and characteristic SERS spectra (right)	69
Fig 20 Correspondence of SLISA with ELISA for the extracellular detection of stress proteins	70
Fig 21 Damaging effect of electroporation shown by SEM	76
Fig 22 Ag NPs vaporization (A & B) and shape change (C) on exposure to 200 kV in TEM	77
Fig 23 The growth inhibition effect of Ag	78
Fig 24 SEM images of yeast cells before and after I ₂ /KI etching	79
Fig 25 Kinetics of Ag NPs uptake in yeast via passive and TATHA2-facilitated diffusion	80
Fig 26 In situ TEM images to observe intracellular distribution of Ag NPs into yeast after surface etching	81
Fig 27 Stability of RAD54 SERS sensor	82
Fig 28 Raman spectra of the CBB-SIST	83
Fig 29 Schematic of on-chip SLISA	87
Fig 30 Translation of dose-response relationship to assess environmental risk of toxins	89

ABBREVIATIONS, ACRONYMS AND SYMBOLS

Ag NPs	Silver Nanoparticles
APDS	Autonomous Pathogen Detection System
ATSDR	Agency for Toxic Substances and Disease Registry
Au NPs	Gold Nanoparticles
BCA	Bicinchoninic Acid
BERA	Bioelectronic Recognition Assay
BSA	Bovine Serum Albumin
CANARY	Cellular Analysis & Notification of Antigen Risks & Yields
CBB	Cell-Based Biosensor
CBB-SIST	Cell-Based Biosensor using SERS ImmunoSensor Technology
CBTs	Chemical and Biological Toxins
CDC	Centers for Disease Control and prevention
ECIS	Electric Cell-substrate Impedance Sensor
EF	Enhancement factor
ELISA	Enzyme-Linked ImmunoSorbent Assay
EPA	Environmental Protection Agency
FAFGF	Fatty Acid-Free Globulin-Free
FETs	Field Effect Transistor Sensor
H ₂ O ₂	Hydrogen Peroxide
HPLC	High Performance Liquid Chromatography
HRS	Hyper Raman Scattering/Spectroscopy
ICP-MS	Inductively Coupled Plasma-Mass Spectrometry
IDLHs	Immediately Dangerous to Life and Health Concentrations

LAPS	Light Addressable Potentiometric Sensor
LF	Label-Free
Lk	Linker
LOD	Limit of Detection
MAB	Monoclonal Antibody
MMT	Mercapto Methyl Thiazoleacetate
mPEG-SH	methoxy Poly (Ethylene Glycol) - Thiol
PAb	Polyclonal Antibody
PMBA	P-Mercapto Benzoic Acid
PMNPs	Plasmon Metal Nanoparticles
R6G	Rhodamine-6-G
RISE	Rapid, Inexpensive, Simple and Effective
RRS	Resonant Raman Scattering/Spectroscopy
RS	Raman Scattering/Spectroscopy
RWG	Resonant Waveguide Grafting
SEM	Scanning Electron Microscopy
SERS	Surface-Enhanced Raman Scattering/Spectroscopy
SLISA	SERS-Linked ImmunoSensor Assay
TEM	Tunneling Electron Microscopy
WRT	With Respect To
YPD	Yeast-extract Peptone Dextrose
Y-PER	Yeast-Protein Extraction Reagent

CHAPTER 1 INTRODUCTION AND BACKGROUND

1.1 SCOPE AND MOTIVATION

The threat of intentional or accidental contamination of the environment with chemical and biological toxins (CBTs) persists since ancient times. For example, the poisoning of water by disposing of corpses in wells and the use of toxins for assassination; in the 14th century the Mongols hurled plague-infected bodies into the Crimean city of Kaffa to hasten its fall and the British in 1763 used smallpox-infected blankets in an attempt to kill native Americans allied with France during the French-Indian war (Poupard et al. 1992). During and after the World Wars, leading countries did extensive research on CBTs, particularly chemical warfare agents (CWAs). The use of anthrax in USA, 1984 and 2001, and Sarin in Japan, 1995 and Syria, 2013 are some examples of chemical and biological warfares. The release of toxic industrial chemicals (TICs) is another major concern. For example, Minamata disaster due to mercury release in Japan, 1932-1968; Bhopal tragedy due to methyl isocyanate gas leak in India, 1984; nuclear disaster in Chernobyl- Ukraine, 1986 and more recently in Fukushima Daiichi - Japan, 2011. A contaminated environment has direct severe impact on human health. Indeed, if we need to cure human health we must first decontaminate the polluted environment. It is shocking to know that newborn babies who enter the world are contaminated before birth. According to The Environment Working Group, a research organization based in Washington, D. C., testing the umbilical cord blood of ten newborn infants in US hospitals in 2004 revealed contamination of with 287 toxic chemicals; consumer products, pesticides, waste products and other TICs, 212 of 287 that are banned or severely restricted in US (Hulihan et al. 2005). Of the 287 chemical

toxins, most (180) are listed as causative agents of cancers (217), birth defects and abnormal development (208).

The major problem with attacks and incidents resulting in the release of various toxins is their detection when they are present in very low concentration in the environment. There is a critical need for detection techniques, which can be used for continuous environmental surveillance. The following section discusses the trend in development of detection techniques for CBTs, primarily chemical toxins TICs and CWAs and summarizes their key advantages and inherent limitations.

1.2 SENSOR TECHNIQUES

In response to the global fear and the severe health effects associated with environmental contamination of CBTs, substantial investments have been made to develop sensor/detection techniques. The progress and prospects of the techniques to detect CBTs have been reviewed (Bhardwaj et al. 2014; Lim et al. 2005) and can be broadly categorized as using conventional and advanced biosensors (Fig. 1). The following terms will be used with respect to the types of detection/biosensor approaches throughout the report:

Cell-free and cell-based detection: Biosensor approaches that employ cell lysates for cell-free/ extracellular detection of cellular components or employ intact live cell for cell-based/intracellular detection of cellular components.

Label-free and label-based detection: Biosensor approaches that employ the use of fluorescent, luminescent or radioactive dyes or labels (label-based) or those without dyes or labels (label-free).

Detect-to-protect and detect-to-treat biosensors: Classes of biosensors developed for the detection of environmental contaminants, primarily to give rapid warning signals to protect human health from toxin exposure (detect-to-protect) or identification of toxins to allow health treatment (detect-to-treat).

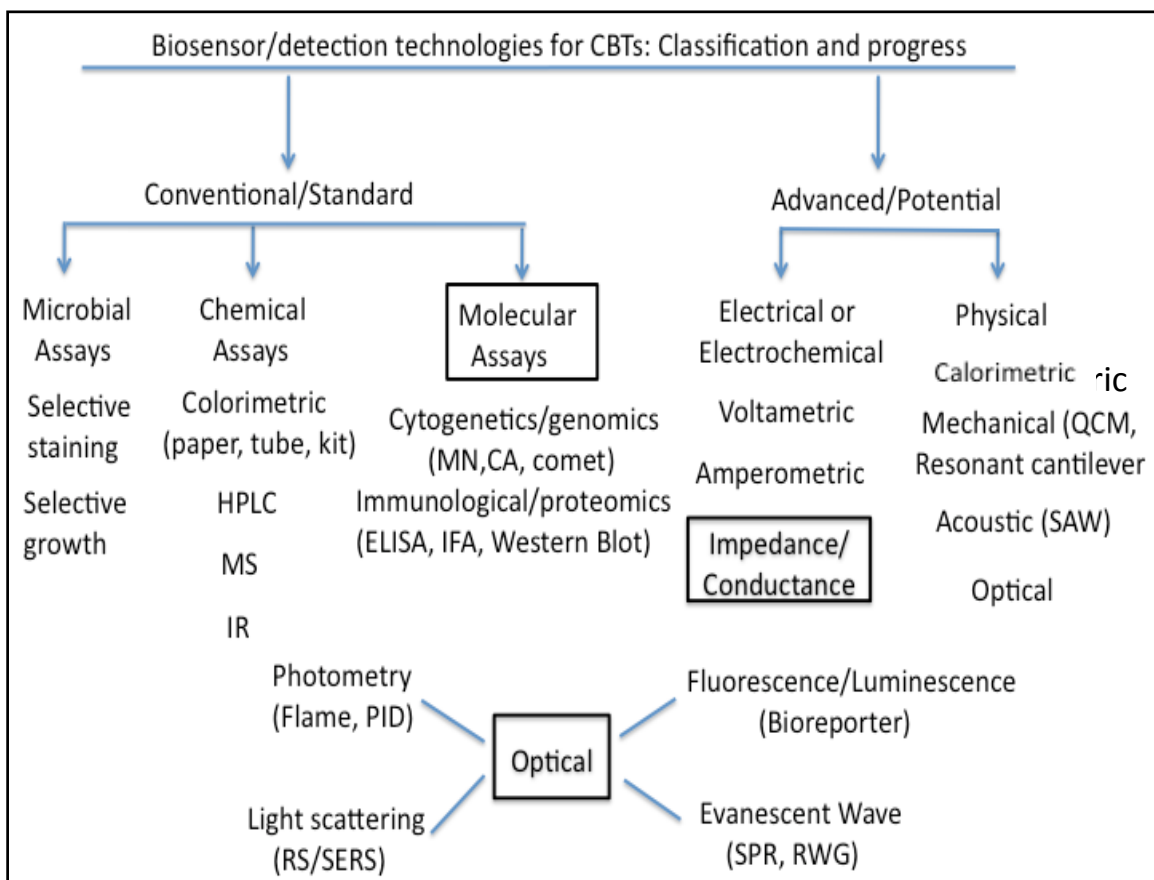


Fig. 1: Classification of biosensor technologies. Acronyms and abbreviations: HPLC: High Performance Liquid Chromatography, MS: Mass Spectroscopy, IR: Infrared Spectroscopy, MN: Micronuclei, CA: Chromosomal Aberrations, ELISA: Enzyme-Linked ImmunoSorbent Assay, IFA: Immuno Fluorescence Assay, SAW: Surface Acoustic Wave, QCM: Quartz Crystal Microbalance, SPR: Surface Plasmon Resonance, RWG: Resonant Wave Grafting and RS/SERS: Raman Spectroscopy/Surface-Enhanced Raman Spectroscopy. Boxes represent the most successful detection/biosensor techniques (after Bhardwaj et al. 2014).

Microbial assays or cultures to identify toxins, primarily biological toxins or pathogens, were first described by Koch et al. (1882) as “Koch’s postulates”, a staple of

microbiological science. Ames (1979) developed a test based on chemical agents that induce bacterial mutagenesis, which is now used as a standard technique to validate the development of advanced biosensor techniques (Terziyaska et al. 2000; Knight et al. 2004; Yang et al. 2005). However, the long incubation and culture time of the toxins (days to weeks) required to produce a response is an inherent limitation of microbial assays. Additionally, such tests are performed manually and require well-established laboratory settings. Automation has shown great progress in the last decade to produce commercial microbial assay systems such as MicroLog by BioLog, USA, VITEK and API series by bioMerieux, USA and the microbial identification system by MIDI Inc., USA. These systems allow rapid detection and high accuracy compared to standard manual assays (Lavalley et al. 2010). The microbes used in commercial assays either produce natural signals or are engineered (bioreporters) to produce signals in response to toxins. The natural microbial systems are limited to *Vibrio fischeri*, a marine organism, e.g. Microtox by Aquatox Research Inc., USA and ToxAlert by Toxalert International Inc., USA. The bioreporter technology using genetically engineered microbes is a promising cell-based biosensor (CBB) technology for environmental surveillance and will be discussed separately in CBB, section 1.3.

As compared to biological toxins, chemicals can be easily produced in large scale and they can be customized for their intent of use (Ganesan et al. 2010). Quimby 2002 and Sferopoulos 2009 reviewed the progress in detection of chemical toxins, particularly CWAs and TICs. Spectroscopy, including mass, infrared, near infrared, and chromatography, including high performance liquid chromatography (HPLC) are sensitive, accurate and are the industry standard to detect chemical toxins. However, these are

sophisticated analytical techniques that are expensive; require technical skills, long turnaround time, sophisticated instrumentation and sample processing such as acid digestion for inductively coupled plasma-mass spectroscopy (ICP-MS), alkyl halides for infrared spectroscopy, and solvent/mobile phase optimization for HPLC. By contrast colorimetric detection, the chemical reaction of toxins with substrate or solution resulting in a specific color change, is relatively inexpensive, portable, rapid and easy-to-use. Commercial examples of such assays include chemical detection papers, and colorimetric kits. However, colorimetric detection is not accurate and correlate poorly with standard spectroscopy and chromatography techniques (Erickson 2003; George et al. 2012). Additionally, they are designed for detection of a single analyte and therefore several chemical kits or reactions are required if multiple analytes are present (Sun et al. 1992).

Almost every living entity is able to adjust to adverse environmental conditions (i.e., stress) by undergoing relevant cellular and molecular changes at the genomic or proteomic level. Stress is broadly referred to as any “disturbance to normal development” affecting structure, function, stability, growth and/or survival. Eukaryotic cells, from yeasts to mammals, respond and adapt to environmental stress by an evolutionary conserved endogenous system through a network of signal transduction pathways expressing stress biomarkers. Biomolecules such as DNA, proteins, carbohydrates and lipids can act as stress biomarkers. Cells activate signaling cascade leading to activation and induction of stress biomarkers in response to stressors, which are either inactive or under expressed during optimal growth conditions. There are numerous environmental stimuli that can act as stressors and can be categorized as biotic (living) or abiotic (non-living). Biological toxins or infectious agents are considered biotic stressors. Abiotic stressors are: hyper/hypo

thermal, hypoxia, reactive oxygen species, radiation, starvation, hypo/hyper osmotic conditions, mutations, heavy metals, toxic agents and exposure to certain drugs.

Although the stress-response is organism-specific and toxin-specific, the general stress response pathways, referred to as damage repair and removal systems, have been found for all organisms (Fulda et al. 2010). Depending on severity and duration of stress, there are three outcomes of cellular response to stress. First, cell damage can be successfully repaired with no genetic alteration. Second, if the cell damage is beyond repair then removal by apoptosis takes place. Third, sometimes DNA repair is not successfully repaired and cells evade apoptosis, they will carry forward the genetic alteration. Second and third outcomes are highly detrimental, demanding cytotoxic and genotoxic assays for their assessment. Current gold-standard cytogenetic assays to test genotoxicity include micronuclei, chromosomal aberration and comet assays. These assays are widely accepted for their accuracy. However, the difference in end-point biological detection can lead to contrary results demanding a battery of tests (Goethem et al. 1997; Kawaguchi et al. 2010). Additionally, the inherent limitation of these cytogenetic assays is the long turnaround time of several hours-days and the requirement of specially trained personnel, which limits their applications to laboratory settings. Therefore these assays are not suitable for applications in resource-limited settings required for environmental surveillance. The advent of microarray and nanotechnology allowed the development of automated assays to develop faster, smaller and easier-to-use biosensor designs for CBTs: such as TIGER (triangular identification for genetic evaluation of risk), APDS (autonomous pathogen detection system), RAPTOR, QTL, BioVERis and Nano-nose (Brown, 2004). Polymerase chain reactions and immunoassays employ cell lysis (examples of cell-free endpoint detection)

and chromophore or fluorophore dye (labels), which limit their potential. The progress in cell-based and label-free detection/biosensor technologies is discussed in the next section. Several studies report involvement of a conserved sequence of elements, called Stress Response Elements (STRE) in yeast, which regulate the expression of genes whose products provide protection against most, if not all, environmental stressors (Jamieson 1998). STRE are proposed to be generally activated in response to diverse classes of stressors and became to be known as “general stress” transcription factors. This general stress response results in altered expression, induction and repression of ~ 900 genes in yeast (Gasch et al. 2000). Among these 900, RAD54 (Walmsley et al. 1997 and Knight et al. 2004), HSP70 (So et al. 2007 and La Terza et al. 2008), CASP3 (Kojio et al. 2006 and Vachova et al. 2007) and NSMase (Jaffrezou et al. 1998 and Matmati et al. 2008) are characterized for their strong induction during cellular stress, such as oxidative, heat, UV, ionizing radiations and chemotherapeutic agents or drugs. Ambiguity in the specificity of CASP3 assay kits (Pozarowski et al. 2003 and Vachova et al. 2007) and the acute and cyclic expression of NSMase in response to toxins (Jaffrezou et al 1998) deter the employment of these two proteins for the development of an environmental biosensor.

HSP70 and RAD54 are highly conserved from yeast to human, and their stress-response mechanisms have been well understood (Richter et al. 2010; Heyer et al. 2006; Jamieson 1998). HSP70s, alias molecular chaperons, are key players in facilitating de novo folding of polypeptide chains produced by ribosomes into functional proteins under normal physiological conditions. Under stress conditions, the HSP70s are involved in correct refolding of proteins, preventing aggregation of unfolding proteins and even degradation of damaged or denatured protein. For all these functions high copy numbers of HSP70s are

required, which are automatically upregulated in response to stress via activation of heat shock factor 1 in eukaryotes. RAD54, alias DNA repair and recombination proteins, were originally identified in yeast with sensitivity to UV radiations. Among different types of DNA damages, double strand breaks are considered the most lethal for cell survival. DNA double strand breaks are repaired by two major pathways, non-homologous end joining (most rapid repair) and homologous recombination (most accurate repair). RAD54 is a core factor in homologous recombination, which serves as a non-mutagenic DNA damage tolerance pathway that is well characterized in response to genotoxins. Proverbially, RAD54 serves like a Swiss Army Knife, required at every stage of homologous recombination, repair and chromatin remodeling in response to DNA damage caused by genotoxins and other classes of toxins. RAD54 is the most studied stress protein biomarker used to develop yeast bioreporters for environmental sensing (Cahill et al. 2004).

1.3 CELL-BASED BIOSENSORS

The information from functioning live cells is clearly more useful and reliable than those from cell-free preparations. The salient feature of a CBB is that it measures the actual amount of an analyte that is available for activity in the target site (bioavailability), not the total concentration of analyte (Bahl et al. 2004). CBB tests also allow dynamic studies, an important attribute for continuous environmental monitoring as compared to endpoint detection by ELISA and polymerase chain reaction. Since the year 2000, many efforts have been made to develop CBB technologies (Pancrazio et al. 2001; Stenger et al. 2001; Gu et al. 2004; Van der Meer et al. 2008; Banerjee et al 2009 and 2010; Xu et al. 2013). No doubt, mammalian CBB produces human-like functional response and prove an excellent

choice for developing screening device for environmental surveillance (Banerjee et al. 2009). However, mammalian cells are fragile, as they have no cell wall and demand stringent growth conditions and maintenance. These characteristics are unfavorable for developing a robust environmental CBB, which is required in a field application, requiring long-term stability and an extended shelf life. Additionally, most mammalian CBB technologies are based on cellular electrical properties such as the electrical cell-substrate impedance sensor (ECIS), bioelectric recognition assay (BERA), field effect transistor sensor (FETs), or light addressable potentiometric sensor (LAPS) etc. CANARY (Cellular Analysis and Notification of Antigen Risks and Yields) is an ECIS-based biosensor technique that can detect < 50 pathogen particles in < 3 minutes (Rider, 2003; Brown 2004). While CANARY was the first and true “detect to protect” class of biosensors, its shelf life is normally limited to two days at room-temperature, although that can be extended to 2 weeks with additional genetic engineering to over-express certain protective genes in the cells (Petrovick et al. 2010). Unlike mammalian cells and electric detection, the use of microbial cells and the optical detection technique to measure the functional response to toxins has great potential to be developed into a specific, robust and portable design for environmental application.

Microbes are robust, easy to grow and modify genetically for use in the detection of toxins. Such cells contain two essential elements; a promoter gene that is turned on (transcribed) when a toxin is present, and a reporter gene that then produce a visible signal (Fig. 2).

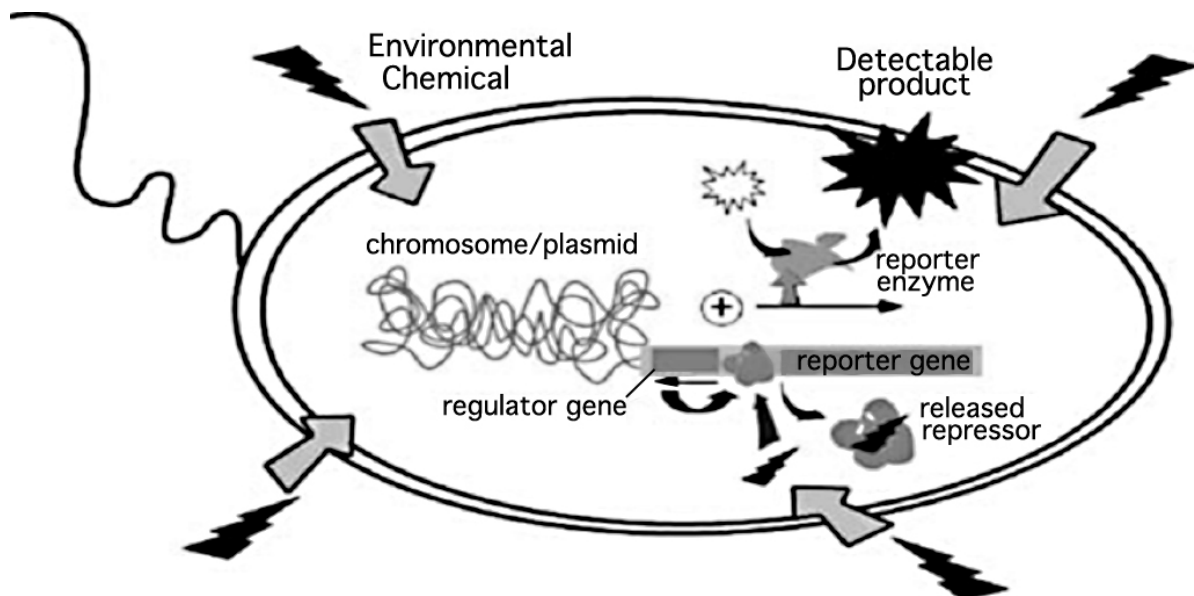


Fig. 2: Schematic of bioreporter technology. A promoter/regulator gene responds to stress, which in turn results in transcription of a reporter gene that is then translated into visible reporter protein/enzyme. The accumulation of visible reporter enzyme is directly related to the stress levels (after Harms et al. 2006).

Naturally occurring biomolecules such as DNA, protein, lipid and carbohydrates are thought to adapt to, or combat stress. These molecules are linked to genes that can be engineered and replaced with a label or marker. The engineered microbial cell is called a bioreporter, which is one of the most successful CBB technologies for environmental monitoring (Gu et al. 2004; Harms et al. 2006; Van der Meer et al. 2008; Xu et al. 2013). Since the first bioreporter employed prokaryotes (Bahl et al. 2004), bacteria have been the primary choice for this technology (Van der Meer et al. 2010), despite the considerable differences between compared to eukaryotes.

Yeast, a single-celled eukaryote, is a better choice among microbes to develop a CBB (Baronian, 2004). The stress response elements (STRE)-regulated induction of proteins in response to stress is a well characterized mechanism, which is particularly well studied for oxidative stress conditions (Jamieson et al. 1998). Generation of reactive oxygen species

(ROS) by organisms in response to oxidants, such as peroxide (H_2O_2) and photochemical damage by UV radiation (when UV acts on O_2 converting it to highly unstable O_3 molecules, ozone) are major stress and toxicity mechanisms. Several yeast bioreporters have been developed to study stress response (Terziyska et al. 2000; Afanassiev et al. 2000; Knight et al. 2002; Leskisen et al. 2005; Bovee et al. 2007; Alonso et al. 2009). Bioreporters for intracellular detection of HSP70 and RAD54 stress proteins have been developed as portable sensors for environmental applications (La Terza et al. 2008 and Knight et al. 2004). A commercially developed assay, Green Screen Assay (Cahill et al. 2004) uses a RAD54 promoter green fluorescent protein (GFP) reporter gene to measure cytotoxicity and genotoxicity (Jia et al. 2002), and to improve high throughput screening (Knight et al. 2002) and portability (Knight et al. 2004). The Green Screen Assay has been used for environmental and pharmaceutical applications. However, although, the yeast model has shown promising results and potential in academia, it is not widely accepted for commercial applications because of the required prolonged incubation with toxins (Harms et al. 2006). This is the major limitation towards the development of a rapid detect-to-protect biosensor for environmental surveillance.

1.4 LABEL-FREE CELL-BASED BIOSENSORS

Label-free cell-based biosensor (LF-CBB) technologies have been developed and commercialized since 1990, when Biacore (now GE Healthcare) first introduced their surface plasmon resonance (SPR)-based instrument. There has been a lot of progress in LF-CBBs since then. Depending on the nature of the transducers, the successful LF-CBBs can be broadly divided into two categories, optical and electrical (Comley 2008; Harigan

et al. 2010; Fang 2011). Commercially available LF-optical CBB technologies including SPR and resonant waveguide grafting (RWG) and LF-electrical CBB are impedance-based detection systems (Fig. 3).

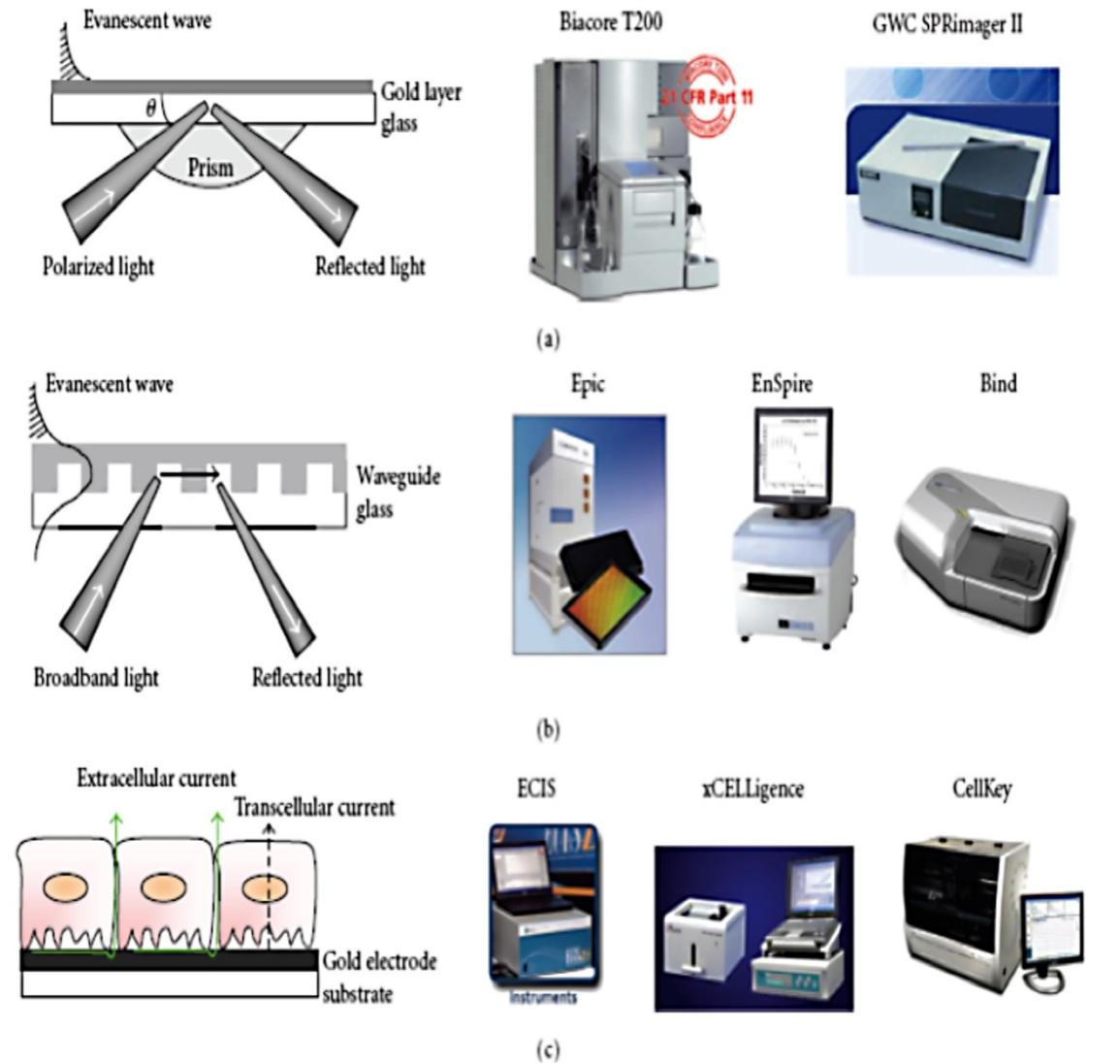


Fig. 3: Mechanisms and examples of commercial label-free cell-based biosensors. Surface plasmon resonance (SPR) (a) and resonant waveguide grafting (RWG) (b) are optical sensors that use surface bound evanescent wave to characterize the alteration in refractive index (θ) generated by metal surfaces and leaky nano-grafting structures, respectively. Electrical cell-impedance sensors (ECIS) (c) are based on the impedance of the cell to current flow between and within the cell. The change in refractive index and the current is directly related to stress in the environment (after Fang 2011).

SPR and RWG use surface bound evanescent waves to characterize the alteration in the local refractive index at a sensor surface. Electromagnetic waves in SPR are generated by a metallic surface made of gold or silver (plasmonic metal nanoparticles, PMNPs) through plasmon resonance. In RWG, the electromagnetic waves are developed by the diffraction of broadband light through a leaky nano-grating structure. The change in refractive index in the case of optical sensors, and current in the case of electrical ones is directly related to the stress conditions in the environment that act on the cells. However, these sensors have not found widespread commercial success as compared to ELISA detection because of the several problems that are described by Comely (2008) and Hartigan (2010), which are listed below:

1. Low sensitivity and selectivity
2. High cost of the instruments and plates, which prohibit their applications for continuous environmental surveillance and primary screening
3. Stringent growth conditions of mammalian cells do not allow the development of portable and/or wearable designs.

These limitations have led to the continued search of new types of LF-CBB techniques that are ultra-sensitive, accurate, multiplex, portable and continuous.

1.5 RAMAN SPECTROSCOPY AND SURFACE-ENHANCED RAMAN SPECTROSCOPY (RS AND SERS)

Raman spectroscopy (RS) is an optical-based sensing technology, which is used to observe light scattering from the sample with energy different from the incident light (Fig.4).

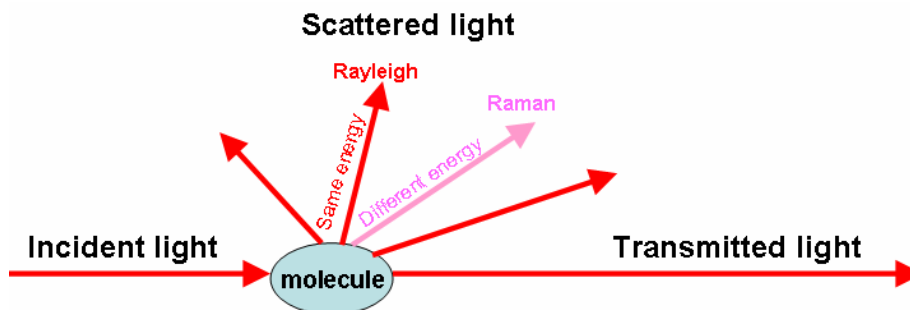


Fig. 4: Schematic of various interactions of a molecule with monochromatic light. Unlabeled arrows indicate other types of scattering, known such as Thompson scattering and Compton scattering, and unknown (after Ansari 2008).

Most of the incident photons are transmitted, although some of the photons are absorbed or scattered in different directions. The majority of the scattered light has the same energy as the incident light (elastic scattering). However, a small amount (1 photon per 10^8 - 10^{10} incident photons) is in-elastically scattered, which is the basis of RS. RS produces rich and narrow spectral peaks as compared to fluorescence spectroscopy, which are based on light absorption and produces few and broad peaks (Fig. 5).

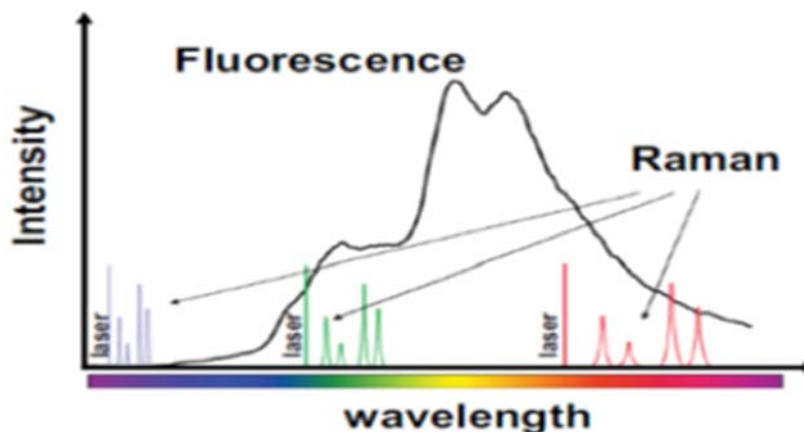


Fig. 5: Raman vs. fluorescence spectrum (after Ansari 2008).

Raman signals are often weaker and accompanied by fluorescence, which interfere with the desired Raman signals. To address this limitation, several modified techniques have been developed to enhance Raman signals, such as resonance Raman scattering (RRS), hyper Raman scattering (HRS) and surface-enhanced Raman scattering (SERS). The cross-section area of different types of spectroscopy is directly related to its sensitivity. SERS has the highest cross section area among all RS types, comparable to fluorescence spectroscopy (Table 1).

Table 1: Raman cross-section areas of different types of Raman spectroscopy (RS) compared to fluorescence spectroscopy (Kneipp et al. 2002).

Type of Spectroscopy	Raman Cross Section (cm²/molecule)
Normal/ Spontaneous RS	$10^{-31} - 10^{-29}$
Resonant RS	$10^{-27} - 10^{-25}$
Surface Enhanced RS	10^{-16}
Fluorescence	$10^{-16} - 10^{-17}$

In the mid-1970s, it was first reported that the intensity of the Raman scattering for a molecule might be dramatically increased when the analyte is in close proximity to colloidal metal NPs or rough metal surfaces with SPR properties, a phenomenon called Surface-Enhanced Raman Scattering or SERS (Fleischm et al. 1974; Jeanmaire et al. 1977). The enhancement factor in SERS can be on the order of 10^{14} – 10^{15} , allowing the detection of a single molecule, once considered unthinkable (Kneipp et al. 1997; Doering et al. 2002). The sensitivity of RS in the presence of plasmonic metal nanoparticles can equal or exceed

fluorescence sensitivity (Rossi et al. 2005; Lutz et al. 2008). SERS can be performed without labels (label-free) as well as by employing labels (label-based), using Raman reporters such as crystal violet, cresyl violet, Rose Bengal, rhodamine6G and p-mercaptobenzoic acid. These Raman reporters are non-fluorescent and when attached to SERS NPs gives sharper Raman spectral peaks. Several researchers have decorated pH-sensitive Raman reporters on SERS substrates to create cellular maps with a pH range of 2-8 (Kneipp et al. 2007; Wang et al. 2008). Such information can be very useful to study the cellular response to various environmental stressors. Undoubtedly, Raman reporters can facilitate SERS detection of multiple analytes (Maltzahn et al. 2009). However, SERS signal intensity of Raman reporters or dyes is significantly attenuated in protein/dye mixtures and conjugates, a major limitation of label-based SERS immunosensing (Zhang et al. 2009). In label-free detection the analyte is either directly applied to the SERS substrate (Au/Ag) or is captured and immobilized by specific interactions with antibodies, aptamers or related molecules. Much research has been devoted to develop label-free SERS sensors (Pal et al. 2006; Qi et al. 2007; Stokes et al. 2008; Lin et al. 2008).

The application of RS/SERS towards development of CBB (Notingher et al. 2006, Notingher 2007; Chan et al. 2008; Han et al. 2009) and detection of cellular components such as nucleic acids (Cao et al. 2002; Pal et a. 2006; Vo-Dinh et al. 2002; Culha et al. 2003; Wabuyele et al. 2005; Fabris et al. 2007) proteins and amino acids (Grubisha et al. 2003; Tuma 2005; Jun et al. 2007; Li et al. 2008; Lutz et al. 2008; Culha 2012) and lipids (Nan et al. 2006; Wang et al. 2008) has been reviewed. DNA and protein arrays for simultaneous detection of multiple analytes also have been reported (Cao et al. 2002; Jun

et al. 2007). However, there is no CBB for the detection of specific proteins using intracellular SERS immunosensing.

1.6 SERS SUBSTRATES

Plasmonic metal nanoparticles (PMNPs) such as Au and Ag exhibit strong scattering and robust photo stability to generate intense and stable Raman signals compared to QDs and fluorescence dyes/materials (Ansari 2008). Scattering of a single 80 nm PMNP can be as bright as the fluorescence of 10^5 QDs or 10^3 dye-doped beads of 100-nm diameter (Ansari 2008; Schultz et al. 2000). Like QDs, PMNPs can also be size-tuned for emission of specific color wavelengths (Fig. 6a, Stamplecoskie et al. 2011,). Their optical properties strongly depend on type of material, size, shape and other physio-chemical properties (Fig. 6b, Mulvaney 1996; Oldenberg et al. 1998; Lazarides et al. 2000; Mock et al. 2002; Lee et al. 2006 and Prathna et al. 2011). Spherical NP of 50-60 nm diameter is the optimal size for high SERS intensity (Fig. 6c, Stamplecoskie et al. 2011) and cell uptake (Fig. 6d, Chithrani et al. 2006). Interestingly, Ag NP exhibits much higher scattering property than Au NP of similar shape and size, which makes Ag NP a better SERS substrate over Au NP (Kerker 1987 and Lee et al. 2006).

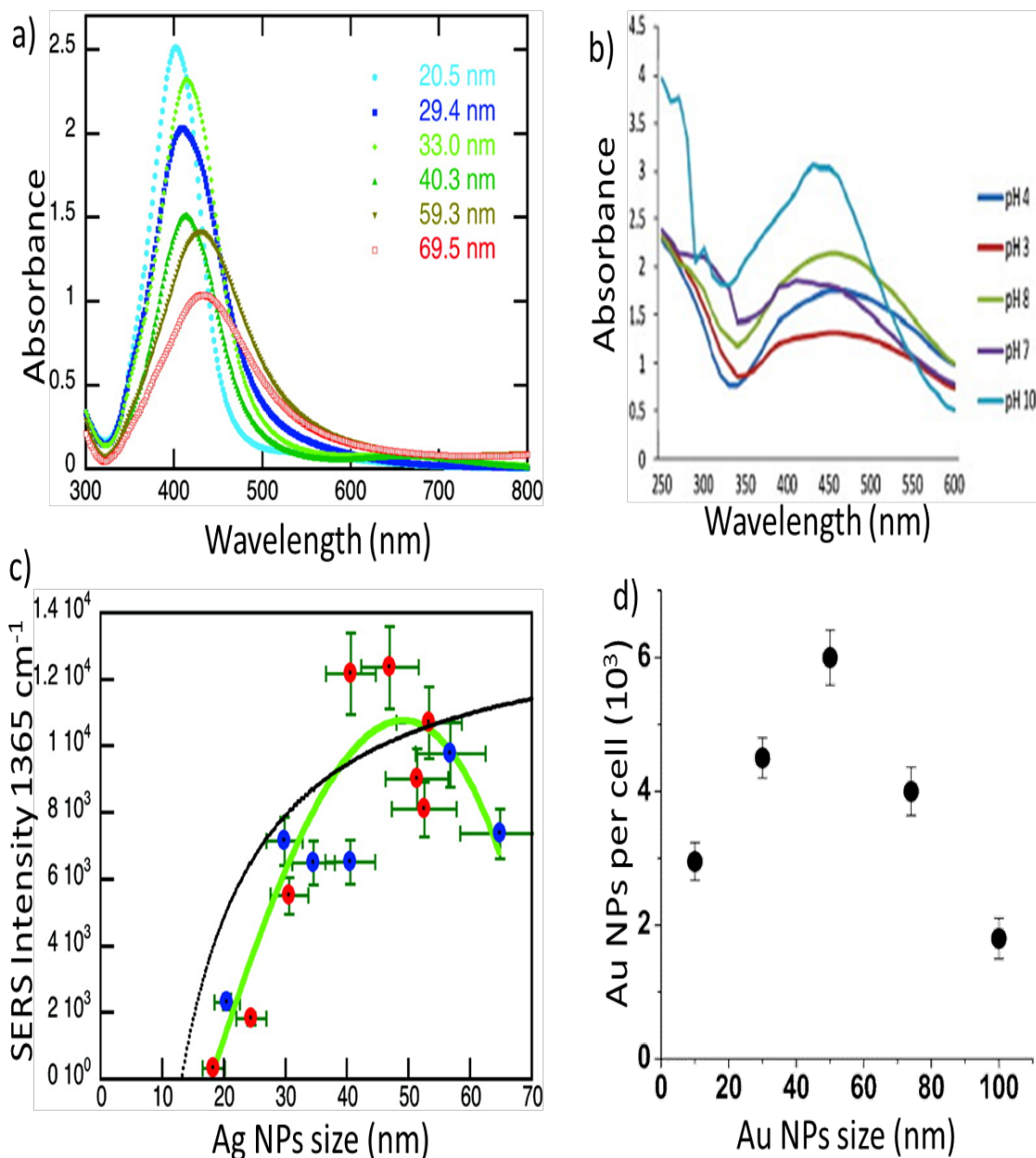


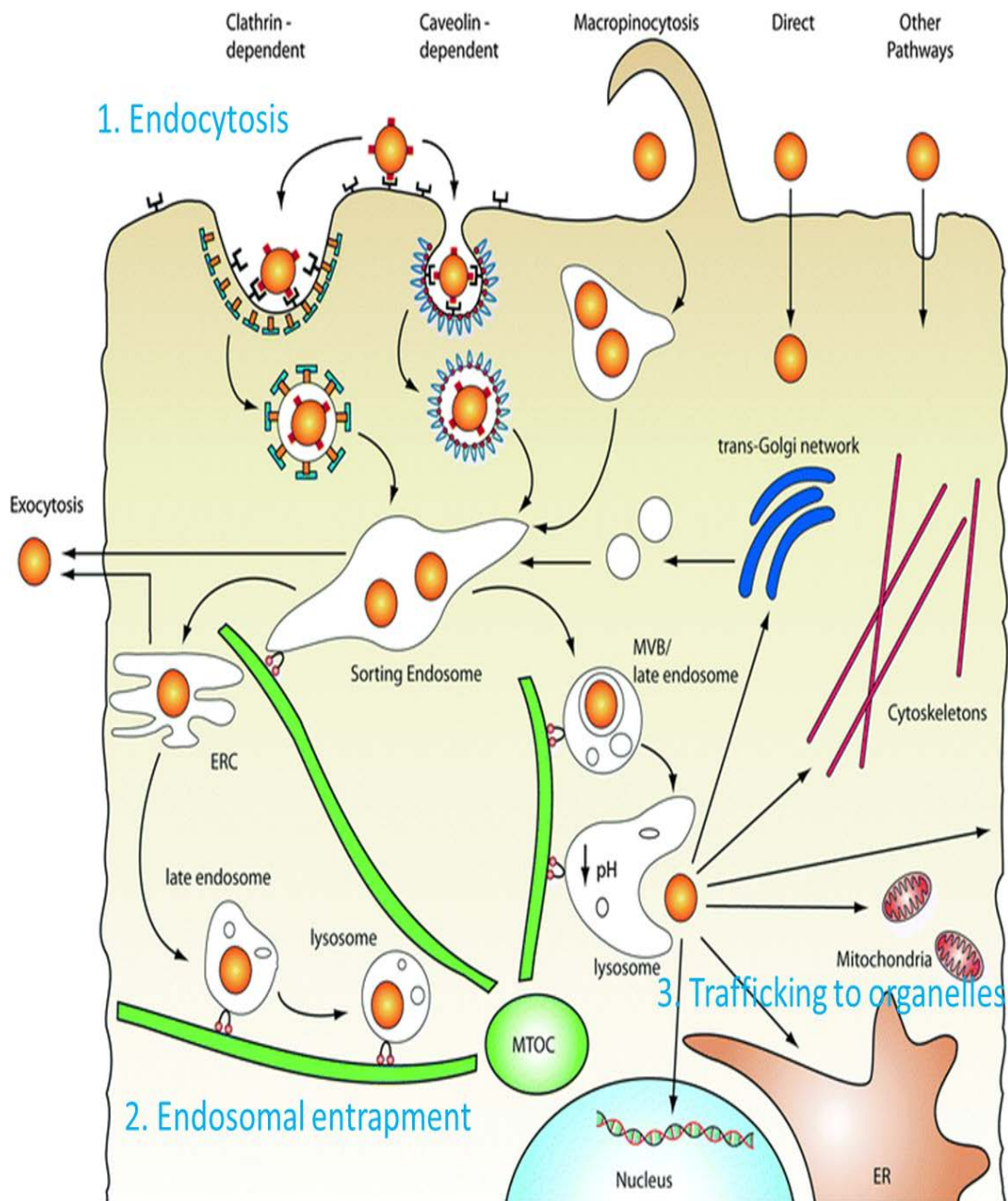
Fig. 6: Size dependent Ag NPs properties. Ag NPs UV-Vis absorbance maximum shifts to higher wavelength, with increasing size (a) and increasing pH (b). SERS signal intensity of rhodamine 6G at 1365 cm^{-1} as a function of Ag NPs size (c) and cell uptake as a function of Au NPs size (d). Black line indicates best curve fit and the green line is the polynomial fit to the data points (c), to guide readers' eyes to easily observe the trend in SERS intensity w.r.t. Ag NPs size. Red and blue data points (c) correspond to two completely different batches of Ag NPs measured one year apart. 50-60 nm is the optimal size for high SERS

sensitivity and cell uptake (a and c are after Stamplecoskie et al. 2011; b after Prathna et al. 2011 and d after Chithrani et al. 2006).

Au and Ag NPs are used as PMNPs because they can induce SPR at visible excitation wavelengths (400-700 nm), which are commonly used for biological detection and imaging (Lee et al. 2006). Since the discovery of the SERS technology, researchers have been attempting to develop a SERS substrate that is biologically compatible and can be used within a single cell. Although the methods of synthesizing Au and Ag NPs are well known, their toxicity and rapid aggregation in buffer and culture media is a concern (Turkevich et al. 1951; Frens 1973; Lee et al. 1982; Ansari, 2008). Therefore, they must be coated with nontoxic organic compounds (Yu, 2001; Su, 2005; Wei, 2007; Kumar, 2008; Liu, 2010; Li, 2012; Potara, 2012) with little or no Raman background. Each metallic SERS substrate has its own advantages and disadvantages in developing biosensors. However, Au is reported to be more compatible for biological applications compared to Ag, but to have less SERS potential (Kerker 1987; Lee et al. 2006). Different shapes/architectures of Au and Ag have been developed to increase compatibility and/or SERS signals (Pande et al. 2007; Kumar, 2012).

Advances in nanotechnology have generated many nanomaterials that are being engineered for diagnosis and therapeutic applications. To fully realize their potential in physiological systems they must reach their sub-cellular targets with high efficiency and specificity. Indeed, such intracellular delivery of SERS sensors to live cells is necessary for continuous and dynamic monitoring of their responses to environmental toxins. Physical and chemical properties including surface charge, polarization and other functionalities at the surface primarily govern the delivery efficiency, while the inclusion of targeting ligands such as

antibodies, aptamers and DNA strands confer specificity. The ideal composition of the sensor depends on the application. For intracellular applications of NPs, efficient delivery to the site of interest (mostly intracellular organelles) is a prerequisite. Any cell, microbial or animal, expresses a very large number of specific protein molecules in response to stress, toxin or disease conditions. The most widely studied biomarkers include CASP, HSP, RAD and several others, are in range of 10^3 to 10^6 molecules per cell (yeast to animal cell, respectively) as baseline levels. A typical charge-driven passive diffusion has three limiting steps including slow endocytosis, entrapment in endosomes and little or no movement through dense cytoplasm into target organelles. Therefore, passive diffusion technically fails to efficiently deliver high payload with uniform intracellular distribution of sensor molecules required for intracellular immunosensing. Most charge-driven uptake of NP is through receptor-mediated endocytosis, which is slow but can be increased by ligands attached to the NP (Wadia et al. 2004; Ye et al. 2012). After internalization, depending on the different modes of endocytosis, NPs can be exocytosed or the endosome can undergo internal rupture and release of cargo to organelles (Fig. 7).



Abbreviations: ERC, endocytic recycling compartment; ER, endoplasmic reticulum; MTOC, microtubule-organizing centre; MVB, multivesicular bodies;

Fig. 7: Three limiting steps in efficient delivery of NPs for intracellular applications. First, endocytosis of NPs through cellular membrane occurs by different mechanisms based on the property of the cell and the NPs. Second, encasing of internalized NPs in small endosomal vesicles, which grow and fuse with lysosome (endocytic pathway), followed by sorting of the NPs and their exocytosis or entrapment. Third, rupture release of NPs from endo-lysosomes results in their passage to cellular organelles (after Chou et al. 2011).

The presence of the cell-wall in yeast and other microbial cells as compared to mammalian cells represents an additional barrier that makes the intracellular delivery of cargo very challenging. Several techniques that ameliorate this problem involve active, facilitated and passive delivery. Active techniques include electroporation, bombardment using microprojectiles, and microinjection (Hashimoto et al. 1985; Johnston et al. 1988; Riveline et al. 2009). However, these techniques are primarily designed and tested to deliver DNA (transformation). Facilitated uptake by conjugation of cationic polymers (Yezhelyev et al. 2008; Kievit et al. 2009), cell permeability peptides (Stewart et al. 2008; Heitz et al. 2009), or ligands, including transferrin (Choi et al. 2010), RGD (Oba et al. 2008) and folic acid (Bharali et al. 2005) have all been reported to increase NP uptake.

TATHA2, a combination of two viral peptides, has emerged to be one of the best ligand-facilitated approaches to confer efficient delivery of NPs into cells (Wadia et al. 2004; Kumar et al. 2007; Kumar et al. 2008; Ye et al. 2012). TAT stands for “trans-activator of transcription”, a regulatory protein encoded by TAT gene in HIV-1 virus, and the HA stands for “hemagglutinin”, a glycoprotein present on influenza virus’s surface. The mechanism of internalization (macropinocytosis) and lack of toxicity of TATHA2 have been established (Wadia et al. 2004; Ye et al. 2012). TATHA2-mediated intracellular delivery is a lipid raft-dependent form of micropinocytosis that facilitates uptake of NPs by a receptor- and energy-independent mechanism (Wadia et al. 2004; Ye et al. 2012; Herce et al. 2014). By contrast, receptor- and energy-dependent endocytosis is slow and typical of charge-driven cellular uptake of NPs (Chithrani et al. 2006; Yen et al. 2009; Cho et al. 2010). The fundamental mechanism of TATHA2-mediated uptake of NPs is proposed to be universal among cells from different species and kingdoms (Herce et al. 2014; Wadia

et al. 2004). Briefly, cellular internalization is facilitated by a TAT moiety, which is a very rapid process (an hour or less), while endosomal rupture release is controlled by the HA2 moiety, a rate limiting step that can take up to several hours (Wadia et al. 2004). Like any other cell penetrating peptides, TAT is rich in highly cationic arginine molecules, which have a high binding affinity to deprotonated fatty acid chains that are abundant in plasma membrane. The TAT-fatty acid complex inserts and nucleates a channel in the plasma membrane leading to cellular internalization of NPs and concurrent protonation of fatty acid chains, which are available to repeat the next cycle. Besides the plasma membrane, the endosome plays a vital role in cellular uptake because most NPs, including those that are TAT functionalized, are entrapped by this structure. However, HA2 moieties are able to protonate the endosome (macropinosome) in TATHA2-mediated delivery. This results in conformational changes in the α -helix of the HA2 hydrophobic face to increase the lateral pressure and surface tension, resulting in endosomal rupture release of the NPs (Ye et al. 2012).

There are very few reports on delivery of Au and Ag NPs in living cells by TATHA2 facilitated delivery and electroporation, respectively (Kumar 2008; Lin et al. 2009; Yu et al. 2011; Yuan et al. 2012). Single 18-nm Au NP is functionalized with ~ nine MAbs for targeting and TATHA2 delivery peptides towards intracellular sensing (Sonia et al. 2008). The relationship between size of NP and the number of MAbs can be extrapolated to estimate the number of 60-nm SERS substrate required to detect a given number of protein molecules expressed by a single cell, protein to MAb ratio is 1:1. Accordingly, for intracellular detection of 5×10^4 protein molecules inside yeast, roughly 4000 60-nm SERS sensor molecules with preferentially uniform intracellular distribution are estimated to be

required. Additionally, proteins such as RAD54, which are abundant in the cytosol and nucleus, ~7000 molecules in yeast (Mazin et al 2010) will require at least 4000 sensor molecules to be internalized into a single yeast cell. To estimate the number of Au NPs, a mild iodine/potassium iodide (I₂/KI) solution can be used to selectively etch the Au NPs, removing Au NPs exclusively from the cell surface and not the internalized, without leading to any significant toxicity and change in cell morphology (Cho et al. 2009). Advantages and disadvantages of intracellular delivery techniques in the context to development of a SERS CBB are tabulated (Table 2).

Table 2: Comparison of three types of strategies to deliver NPs inside cells.

Property	Passive	Active	Facilitated
Basis	Uptake relies on inherent physicochemical properties of SERS substrate without any cell alteration	Direct manipulation of cell by making holes or creating pores using physical methods including microinjection or electroporation	Decorating the SERS substrate with functional molecules; biological or chemicals) without cell manipulation
Damage	Little/none	High as the techniques involve cell manipulation	Little/none
Time needed for delivery	Several hours (12-24 hours)	1-60 min depending on type and number of repetitions	1-6 hrs
Number of cells treated per expt.	Billions	Thousands	Billions

Extra cost and labor	None	\$Thousands one-time investment to buy instrument, and some labor	Higher cost of proteins and more labor required for conjugation of ligand.
Intracellular distribution	Endosomal entrapment	Primarily in cytosol, may or may not reach organelles	Uniformly distributed within cell to cytosol and organelles

REFERNCES

Afanassiev A., Sefton M. et al. (2000). Applications of yeast cells transformed with GFP expression constructs containing the RAD54 and RNR2 promoters as attest for the genotoxic potential of chemical substances. *Mutat. Res.*, 464: 297-308

Alonso J. G., Greenway G. M., et al. (2009) A prototype microfluidic chip using fluorescent yeast for detection of toxic compounds. *Biosens. Bioelectron.*, 24(5): 1508-1511

Ames, B. N. (1979). Identifying environmental chemicals causing mutations and cancer. *Science*, 204(4393): 587–593

Ansari D. O. (2008). Raman encoded nanoparticles for biomolecular detection and cancer diagnostics. PhD Dissertation Thesis, Georgia Inst. Technol., Pages 1-139

Bahl M. I., Hestbjerg H. L., et al. (2004). In –vitro detection and quantification of tetracycline by use of a whole-cell biosensor in the rat intestine. *Antimicrob. Agents Chemother.*, 48: 112-117

Banerjee P., Bhunia A. K. (2009). Mammalian cell-based biosensors for pathogens and toxins. *Trends Biotechnol.*, 27(3): 179-188

Banerjee P., Bhunia A. K. (2010). Cell-based biosensor for rapid screening of pathogens and toxins. *Biosens. Bioelectron.*, 26: 99-106

- Baronian K. H. (2004). The use of yeast and moulds as sensing elements in biosensors. *Biosens. Bioelectron.*, 19(9): 953-962
- Bharali D. J., Lucey D. W. (2005). Folate receptor mediates delivery of quantum dots for bioimaging using confocal and two-photon microscopy. *J. Am. Chem. Soc.*, 127: 11364-71
- Bhardwaj V., McGoron A. J. (2014). Biosensor technology for chemical and biological toxins: progress and prospects. *P. J. Biomed. Eng.*, 112: 380-392
- Bovee T. F. H., Helsdingen R. J. R., et al. (2007). A new highly specific and robust yeast estrogen bioassay for the detection of agonists and antagonists. *Anal. Bioanal. Chem.*, 389: 1549-1558
- Brown K. (2004). Up in the air. *Science*, 305(5688): 1228-1229
- Cahill P. A., Knight A. W., et al. (2004). The Green Screen toxicity assay: a screening validation programme. *Mutagenesis*, 19: 105-119
- Cao Y. C., Jin R. et al. (2002). Nanoparticles with Raman spectroscopic fingerprints for DNA and RNA detection. *Science*, 297(5586): 1536-1540
- Chan J., Fore S., et al. (2008). Raman spectroscopy and microscopy of individual cells and cellular components. *Laser Photonics Rev.*, 2(5): 325-349
- Chithrani B. D., Ghazani A. A., et al. (2006). Determining the size and shape dependence of gold nanoparticle uptake into mammalian cells. *Nano Lett.*, 6(4): 662-668
- Cho E. C., Xie J. et al. (2009). Understanding the role of surface charges in cellular adsorption versus internalization by selectively removing gold nanoparticles on the cell surface with a I2/KI etchant. *Nano Lett.*, 9(3): 1080-1084
- Choi C. H., Alabi C. A., et al. (2010). Mechanism of active targeting in solid tumor with transferring containing gold nanoparticles. *Proc. Natl. Acad. Sci. USA*, 107: 1235-40
- Chou L. Y., Ming K., et al. (2011). Strategies for intracellular delivery of nanoparticles. *Chem. Soc. Rev.*, 40(1): 233-245
- Comley J. (2008). Progress in the implementation of label-free detection. *Drug Discovery World, Part II, Fall 2008*: 28-49
- Culha M., Cullum B., et al. (2012). SERS as an emerging characterization and detection technique. *J. Nanotechnol.*, Pages 15
- Doering W. E., Nie S. M. (2002). Single molecule and single nanoparticle SERS: examining the roles of surface active sites and chemical enhancement. *J. Phys. Chem.*, 106(2): 311-317

- Erickson, B. E. (2003). Field kits fail to provide accurate measure of arsenic in groundwater. *Environ. Sci. Technol.*, pages 35A-38A
- Fabris, L., Dante M., et al. (2007). A heterogenous PNA-based SERS method for DNA detection. *J. Am. Chem. Soc.*, 129(19): 6086-6087
- Fang Y. (2011). Label-free biosensors for cell biology. *Int. J. Biochem.*, pages 1-16
- Fleischm M., Hendra P. J. et al. (1974). Raman spectra of pyridine adsorbed at a silver electrode. *Chem. Phys. Lett.*, 26(2): 163-166
- Frens G. (1973). Controlled nucleation for regulation of particle size in monodisperse gold suspension. *Nature Phys. Sci.*, 241(105): 20-22
- Fulda S., Gorman A. M., et al. (2010). Cellular stress responses: cell survival and cell death. *Int. J. Cell Biol.*, Pages 23
- Ganesan K., Raza S. K., et al. (2010). Chemical warfare agents. *J. Pharm Bioallied Sci.*, 2: 166-178
- Gasch A. P., Spellman P. T., et al. (2000) Genomic expression programs in the response of yeast cells to environmental changes. *Molecular Biology of the Cell*, 11: 4241-4257
- George C. M., Zheng, Y. et al. (2012) Evaluation of an arsenic test kit for rapid well screening in Bangladesh. *Environ. Sci. Technol.*, 46:11213-11219
- Goethem E., Lison D., et al. (1997). Comparative evaluation of the in vitro micronucleus test and the alkaline single cell gel electrophoresis assay for the detection of DNA damaging agents: genotoxic effects of cobalt powder, tungsten carbide and cobalt-tungsten carbide. *Mutation Res.*, 392(1-2):31-43
- Grubisha D. S., Lipert R. J. et al. (2003). Femtomolar detection of PSA: an immunoassay based on SERS and immunogold labels. *Anal. Chem.*, 75(61): 5936-5943
- Gu M. B., Mitchell R. J.; et al. (2004). Whole-cell-based biosensors for environmental biomonitoring and application. *Adv. Biochem. Eng./Biotechnol.*, 87: 269-305
- Han X. X., Zhao B., et al. (2009). SERS for protein detection. *Anal Bioanal. Chem.*, 395: 1719-1727
- Harms H., Wells M., et al. (2006). Whole-cell living biosensors: Are they ready for environmental application? *Appl. Microbiol. Biotechnol.*, 70: 273-280
- Hartigan J., Liu C., et al. (2010). Moving forward with label-free technology. *Drug Discovery World*, Winter 2010/2011: 41-48

- Hashimoto H., Morikawa H., et al. (1985). A novel method for transformation of intact yeast cells by electroinjection of plasmid DNA. *Appl. Microbiol. Biotechnol.*, 21: 336-339
- Hatmann A., Elhajauji A., et al. (2001). Use of the alkaline comet assay for industrial genotoxicity screening: comparative investigation with the micronucleus test. *Food Chem. Toxicol.*, 39(8): 843-858
- Heitz F., Morris M. C., et al. (2009). Twenty years of cell penetrating peptide: from molecular mechanism to therapeutics. *Br. J Pharmacol.* 157: 195-206
- Herce H. D., Garcia A. E., et al. (2014). Fundamental molecular mechanism for the cellular uptake of guanidinium-rich molecules. *J. Am. Chem. Soc.* 136: 17449-17467
- Heyer W. D., Li X., et al. (2006). Rad54: The Swiss Army Knife of homologous recombination? *Nucleic Acid Research*, 34(15): 4115-4125
- Houlihan J., Kropp T., et al. (2005). Body burden: The pollution in newborns. <http://www.ewg.org/research/body-burden-pollution-newborns>
- Jaffrezou J. P., Maestre N., et al. (1998). Positive feedback control of neutral sphingomyelinase by ceramide. *FASEB*, 12: 999-1006
- Jamieson D. J. (1998). Oxidative stress responses of the yeast *Saccharomyces cerevisiae*. *Yeast*, 14: 1511-1527
- Jeanmaire D. L., Van Duyne R. P. (1977). Surface Raman spectroelectrochemistry I: heterocyclic, aromatic and aliphatic amines adsorbed on anodized silver electrode. *J Electroanaly. Chem.*, 84(1): 1-20
- Johnston S. A., Anziano P. Q., et al. (1988). Mitochondrial transformation in yeast by bombardment with microprojectiles. *Science*, 240(4858): 1538-1541
- Jun B. H., Kim J. H. et al. (2007). SERS encoded beads for multiplex immunoassay. *J. Comb. Chem.*, 9(2): 237-244
- Kawaguchi S., Nakamura T., et al. (2010). Is the comet assay a sensitive procedure for detecting genotoxicity? *J. Nucleic Acids*, pages 1-8
- Kerker M. (1987). Estimation of SERS from surface-averaged electromagnetic intensities. *J Colloid Interf. Sci.*, 102: 493-497
- Kievit F. M., Veiseh O., et al. (2009). PEI-PEG-Chitosan copolymer coated iron-oxide nanoparticles for safe gene delivery: synthesis, complexation and transfection. *Adv. Funct. Mater.*, 19: 2244-2251

- Kneipp K., Wang Y. et al. (1997). Single molecule detection using SERS. *Phys. Rev. Lett.*, 78(9): 1667-1670
- Kneipp K., Kneipp H. et al. (1998). Extremely large enhancement factors in SERS for molecules on colloidal gold clusters. *Appl. Spectrosc.*, 52: 1493-1497
- Kneipp K., Kneipp H., et al. (2002). Surface-enhanced Raman scattering and biophysics. *J. Phys. Condens. Matter*, 14: R597-R624
- Kneipp K., Kneipp H., et al. (2006). SERS in local optical fields of silver and gold nanoaggregates - from single molecule Raman spectroscopy to ultrasensitive probing in live cells. *Acc. Chem. Res.*, 39: 443-450
- Kneipp K. (2007). Surface-enhanced Raman spectroscopy. *Phys. Today*, 60: 40-46
- Kneipp J., Kneipp H. et al. (2007). One-and-two-photon excited optical pH probing for cells using surface enhanced Raman and hyper Raman nanosensors. *Nano Lett.*, 7: 2819-2823
- Knight A. W., Goddard N. J., et al. (2002). Fluorescent polarization discriminates GFP from interfering autofluorescence in a microplate assay for genotoxicity. *J. Biochem. Biophys. Methods*, 51: 165-177
- Knight A. W. Keenan P. O. et al. (2004). A yeast-based cytotoxicity and genotoxicity assay for environmental monitoring using novel portable instrumentation. *J. Environ. Monit.*, 6: 71-79
- Koch R. (1882). The etiology of tuberculosis. *Berl. Klin. Wochenschr.*, 15: 109-115
- Kojio S., Zhang H. M., et al. (2006). Caspase-3 activation and apoptosis induction coupled with retrograde transport of shiga toxin: inhibition by brefeldin A. *FEMS Immunol. Med. Microbiol.*, 29: 275-281
- Kumar S., Harrison N., et al. (2007). Plasmonic nanosensors for imaging intracellular biomarkers in living cells. *Nano Lett.*, 7(7): 1338-43
- Kumar S., Aaron J., et al. (2008). Directional conjugation of antibodies to nanoparticles for synthesis of multiplexed optical contrast agents with both delivery and targeting moieties. *Nat. Protoc.*, 3(2): 314-320
- Kumar P. (2012). Plasmonic nanoarchitectures for SERS: a review. *J. Nanophotonics*, 6: 1-20
- La Terza A., Barchetta S., et al. (2008). The protozoan ciliate tetrahymena thermophila as biosensor for sublethal levels of toxicants in the soil. *FEB*, 17: 1144-1150

- Lavallee C., Rouleau D., et al. (2010). Performance of an agar dilution method and a Vitek Z card for detection of inducible clindamycin resistance in *staphylococcus* spp. *J. Clin. Microbiol.*, 48(4): 1354-1357
- Lazarides A. A., Lance K. K., et al. (2000). Optical properties of metal nanoparticles and aggregates important in biosensors. *J. Mol. Str.: Theochem* 529 (1-3) 59-63
- Lee K. S., El-Sayed M. A. (2006). Gold and silver nanoparticles in sensing and imaging: sensitivity of Plasmon resonance to size, shape and metal composition. *J. Phy. Chem. B.* 110(39): 19220-25
- Lee P. C., Meisel D. (1982). Adsorption and Surface Enhanced Raman of dyes on silver and gold sols. *J Phy Chem.*, 86(17): 3391-95
- Leskinsen P., Michelini E. et al. (2005). Bioluminescent yeast assays for detecting estrogenic and androgenic activity in different matrices. *Chemosphere*, 61: 259-266
- Li T., Guo L., et al. (2008). Gold nanoparticle based SERS spectroscopic assay for the detection of protein-protein interaction. *Anal. Sci.*, 24(7): 178-183
- Li X., Lenhart J. J., et al. (2012). Aggregation kinetics and dissolution of coated silver nanoparticles. *Langmuir* 28(2): 1095-1104
- Lim D., Simpson J. et al. (2005). Current and developing technologies for monitoring agents of bioterrorism and biowarfare. *Clin. Microbiol. Rev.*, 18(4): 583-607
- Lin J., Chen R., et al. (2009). Rapid delivery of silver nanoparticles into living cells by electroporation for SERS. *Biosens. Bioelectron.*, 25: 388-94
- Lin M., He L., et al. (2008). Detection of melamine in gluten, chicken feed and processed foods using SERS and HPLC. *J. Food Sci.*, 73: T129-T134
- Liu F., Cao Z., et al. (2010). Ultrathin diamond like carbon film coated silver nanoparticles-based substrate for SERS. *ACS Nano*, 4(5): 2643-48
- Lutz B., Dentinger C., et al. (2008). Raman nanoparticle probes for antibody based protein detection in tissues. *J. Histochem. Cytochem.*, 56(4): 371-379
- Matmati N., Hannun Y. A. (2008). Thematic review series: Sphingolipids. ISC1 (Inositol Phosphosphingolipid Phospholipase C) , the yeast homologue of neutral sphingomyelinases. *J. Lipid Res.*, 49(5): 922-928
- Mock J., Barbic M., et al. (2002). Shape effects in Plasmon resonance of individual colloidal silver nanoparticles. *J Chem. Phys.*, 116 (15): 6755-59

- Mulvaney P. (1996). Surface Plasmon spectroscopy of nanosized metal particles. *Langmuir* 12(3): 788-800
- Nottingham I., Hench L L. (2006). Raman spectroscopy: a non-invasive tool for studies of individual living cells and cellular components. *Expert Rev. Med. Devices*, 3(2): 215-234
- Nottingham I. (2007). Raman spectroscopy cell-based biosensors. *Sensors*, 7: 1343-1358
- Oba M., Aoyagi K., et al. (2008). Polyplex micelles with cyclic RGD peptide ligands and disulfide cross-links directing to the enhanced transformation via controlled intracellular trafficking. *Mol. Pharm.*, 5(6): 1080-1092
- Oldenberg S. J., Averitt R. D., et al. (1998). Nanoengineering of optical resonances. *Chem. Phys. Lett.*, 288(2-4): 243-47
- Pal A., Isola N. R., et al. (2006). Synthesis and characterization of SERS gene probe for BRCA-1 (breast cancer). *Faraday Discuss.*, 132: 293-301
- Pancrazio J. J., Whelan J. P., et al. (1999). Development and application of cell based biosensor. *Ann. of Biomed. Eng.*, 27: 697-711
- Pande S., Ghosh S. K., et al. (2007). Synthesis of normal and inverted gold silver core-shell architectures in β cyclodextrin and their applications in SERS. *J. Phys. Chem. C*, 11: 10806-13
- Petrovick M. S., Nargi F. E., et al. (2010). Improving the long-term storage of a mammalian biosensor cell line via genetic engineering. *Biotechnol. Bioeng.*, 106(3): 474-481
- Potara M., Baia M., et al. (2012). Chitosan-coated anisotropic silver nanoparticles as a SERS substrate for single molecule detection. *Nanotechnology*, 23: 55501-55510
- Poupard J., Miller L. (1992). History of biological warfare: catapults to capsomeres. *Ann. N. Y. Acad. Sci.*, 666: 9-20
- Pozarowski P., Huang X., et al. (2003). Interaction of Fluorochrome-labeled caspase inhibitors with apoptotic cells: a caution in data interpretation. *Cytometry A*, 55: 50-60
- Prathna T. C., Chandrasekaran N., et al. (2011). Studies on aggregation behavior of silver nanoparticles in aqueous matrices: Effect of surface functionalization and matrix composition. *Colloids Surf. A*, 390(1-3): 216-224
- Qi D. H., Berger A. J. (2007). Chemical concentration measurement in blood serum and urine samples using liquid core optical fiber Raman spectroscopy. *Appl. Opt.*, 46: 1726-1734
- Quimby B. (2002). Detection of toxic industrial compounds: A guide to analytical techniques. Agilent Technologies, Inc. pages 9

- Richter K., Haslbeck M., Buchner J. (2010). The heat shock response: Life on the verge of death. *Molecular Cell*, 40: 253-266
- Rider T. H., Petrovick M. S., et al (2003). A B cell-based sensor for rapid identification of pathogens. *Science* 301(5630): 213-215
- Riveline D., Nurse P. (2009). Injecting yeast. *Nat. Methods*, 6: 513-514
- Rossi N. L. (2005). Nanostructures in biodiagnostics. *Chem. Rev.*, 105: 1547-1562
- Schultz S., Smith D. R., et al. (2000). Single target molecule detection with nonbleaching multicolor optical immunolabels. *Proc. Natl. Acad. Sci. USA*, 97(3): 996-1001
- Sferopoulos R. (2009). A review of chemical warfare agent (CWA) detection technologies and commercial-of-the-shelf items. Defence Science and technology organization (DSTO) pages 1-98
- So A., Hada S. B., et al. (2007). The role of stress proteins in prostate cancer. *Curr. Genomics*, 8:252-261
- Stamplecoskie K. G., Scaiano J. C., et al. (2011). Optimal size of silver nanoparticles for surface-enhanced Raman spectroscopy. *J. Phys. Chem. C*, 115(5): 1403-1409
- Stenger D. A., Gross G. W., et al. (2001). Detection of physiologically active compounds using cell-based biosensors. *Trends Biotechnol.*, 19(8): 304-309
- Stewart K. M., Horton K. L., et al. Cell penetrating peptide as delivery vehicles for biology and medicine. *Org. Biomol. Chem.*, 6: 2242-55
- Stokes R. J., McBride E., et al. (2008). SERS spectroscopy as a sensitive and selective technique for the detection of folic acid in water and human serum. *Appl. Spectrosc.*, 62: 371-376
- Su X. Zhang J. et al. (2005). Composite Organic-inorganic nanoparticles (COINS) with chemically encoded optical signatures. *Nano Lett.* 5(1): 49-54
- Sun Y., Ong K. (1992). Detection technologies for chemical warfare agents and toxic vapors. 1st ed. Boca Raton, Florida: CRC Press
- Terziyska A., Waltschewa L., et al. (2000). A new sensitive test based on yeast cells for studying environmental pollution. *Environ. Pollut.*, 109(1): 43-52
- Tuma R. (2005). Raman spectroscopy of proteins: from peptides to large assemblies. *J. Raman Spectrosc.*, 36: 307-319

- Turkevich J., Stevenson P. C., et al. (1951). A study of the nucleation and growth processes in the synthesis of colloidal gold. *Discuss. Faraday Soc.*, 11: 55-57
- Vachova L., Palkova Z. (2007). Caspases in yeast apoptosis-like death: facts and artefacts. *FEMS Yeast Res.*, 7: 12-21
- Van der Meer J., Belkin S. (2010). Where microbiology meets microengineering: Design and applications of reporter bacteria. *Nat. Rev. Microbiol.*, 8: 511-522
- Van Dyk T. K., De Rose E. J., et al. (2001). Lux array, a high-density genomewide transcription analysis of *E. coli* using bioluminescent bioreporter strains. *J. Bacteriol.*, 183: 5496-5505
- Vo-Dinh T., Allain L. R. (2002). Cancer gene detection using SERS. *J. Raman Spectrosc.*, 33(7): 511-516
- Wabuyele M. B., Vo-Dinh T. (2005). Detection of human immunodeficiency virus type I DNA sequence using plasmonics nanoprobe. *Anal. Chem.*, 77(9): 7810-7815
- Wadia J. S., Stan R. V., et al. (2004). Transducible TAT-HA fusogenic peptide enhances escape of TAT-fusion protein after lipid raft macropinocytosis. *Nat. Med.*, 10(3): 310-15
- Walmsley R. M., Billinton N., et al. (1997). GFP as a reporter for the DNA damage-induced gene RAD54 in *Saccharomyces cerevisiae*. *Yeast*, 13: 1535-1345
- Wang H., Lee T. T. et al. (2008). Label-free imaging of arterial cells and extracellular matrix using a multimodal CARS microscope. *Opt. Commun.*, 281: 1813-1822
- Wang P. (2009). Cell-based biosensors- Principles and applications. In: Lin Q., ed. *Norwood, MA-USA, Artech House*, pages 286
- Wang Z., Bonoiu A. et al. (2008). Biological pH sensing based on SERS through a 2-aminothiophenol-silver probe. *Biosens. Bioelectron.*, 23: 886-891
- Wei H., Li J., et al. (2007). Silver nanoparticles coated with adenine: Preparation, self-assembly and application in SERS. *Nanotechnology*, 26(1): 83-90
- Xu T., Close D. M., et al. (2013). Genetically modified whole-cell bioreporters for environmental assessment. *Ecol. Indic.*, 28: 125-141
- Yang H., Kim B., et al. (2005). In vitro assessment of biocompatibility of biomaterials by using yeast biosensor. *Curr. Appl. Phys.*, 5(5): 444-448
- Ye S. F., Tian M. M. et al. (2012). Synergistic effect of cell-penetrating peptide Tat and fusogenic peptide HA2-enhanced cellular internalization and gene transduction of organosilica nanoparticles. *Nanomedicine* 8(6): 833-841

Yen H. J. Hsu S. H., et al. (2009) Cytotoxicity and immunological response of gold and silver nanoparticles of different sizes. *Small* 5(13): 1553-1561

Yezhelyev M. V., Qi L., et al. (2008). Proton-sponge coated Quantum dots for JSiRNA delivery and intracellular imaging. *ACS Nano*, 130: 2006-2012

Yu S. F., Lee S. B., et al. (2001). Size-based protein separations in PEG derivatized gold nanotubule membranes. *Nano Lett.*, 1(9): 495-98

Yu Y., Lin J., et al. (2011). Improved electroporation parameters of delivering silver nanoparticles into living C666 cells for SERS. *J Phys.: Conf. Ser.*, 277: 012045

Zhang D., Ansari S. M., et al. (2009). Protein adsorption drastically reduces SERS of dye molecules. *J. Raman Spectrosc.*, Pages 1-6

Zhang Z. M., Chen S., et al. (2009). An intelligent background correction algorithm for highly fluorescent samples in Raman spectroscopy. *J. Raman Spectrosc.*, Pages 1-11

CHAPTER 2 STATEMENT OF RESEARCH, OBJECTIVE, HYPOTHESES & SPECIFIC AIMS

2.1 STATEMENT OF RESEARCH

Almost all current biosensor technologies detect the molecule of interest using exogenous or endogenous labels. Those inside the cell include bioreporters, whereas the typical extracellular technique is ELISA. However, these techniques present several limitations, discussed in chapter one. Most noteworthy, the label-based design introduces uncertainty in detection due to indirect measurement of the signals from the label-conjugated analyte, wherein the intensity of the label is measured and not the analyte. In addition, a cell-free detection has inherent limitation of end-point measurement, which requires lysing the cell to extract analyte concentration

To overcome these limitations, I developed a SERS immunosensor for extracellular detection of proteins expressed by yeast in response to potential TICs and CWAs. The SERS immunosensor fulfilled the critical attributes of a RISE detect-to-protect class of biosensor for environmental surveillance that can be used in resource-limited settings.

2.2 OBJECTIVE AND HYPOTHESES

The objective of the project was to design a SERS immunosensor, compare its sensing attributes with industry-standard ELISA technique, and develop a proof-of-concept prototype microchip design for applications in environmental surveillance. The following hypotheses were tested to meet the objective:

H1: The SERS immunosensor prepared using Ag NPs will outperform ELISA in the extracellular detection of the stress proteins, RAD54 and HSP70 by allowing label-free detection with sensitivity \geq ELISA and turnaround time < 2 hours.

H2: The SERS sensor will be efficiently delivered intracellularly with uptake of > 4000 sensor molecules/cell within 12 hours towards development of a SERS immunosensor for intracellular detection.

2.3 SPECIFIC AIMS

Below is a list of specific aims to test the two hypotheses. Please refer to chapter 3 for details on methodology and the subsequent chapters for the results and summary of each. Almost all results on the specific aims have been published (Bhardwaj et al. 2013, Bhardwaj et al. Analyst 2015; Bhardwaj et al. SPIE 2015). Written permissions have been obtained from the journal editors to use the content of my publications. Please see appendices for the permission emails.

2.3.1. Specific aim#1: Extracellular detection of stress proteins using ELISA

2.3.2. Specific aim#2: Fabrication of colloidal SERS sensor

2.3.3. Specific aim#3: Extracellular detection of stress protein using SERS sensor aka SLISA

2.3.4. Specific aim#4: Efficient intracellular delivery and detection using SERS sensor

2.3.5. Specific aim#5: A case study: on-chip SLISA.

REFERENCES

Bhardwaj V., Srinivasan S., et al. (2013). AgNPs-based label-free colloidal SERS nanosensor for the rapid and sensitive detection of stress proteins expressed in response to environmental toxins. *Biosens. Bioelectron.*, S12: 005 pages 7

Bhardwaj V., Srinivasan S., et al. (2015). Efficient intracellular delivery and improved biocompatibility of colloidal silver nanoparticles towards intracellular SERS immunosensing. *Analyst*, 140: 3929-3934

Bhardwaj V., Srinivasan S., et al. (2015). On-chip surface-enhanced Raman spectroscopy (SERS)-linked immunosensor assay (SLISA) for rapid environmental surveillance of chemical toxins. *Proc. SPIE 9486*, pages 8.

CHAPTER 3 MATERIALS AND METHODS

3.1 MATERIALS AND METYHODS FOR EXTRACELLULAR DETECTION OF STRESS PROTEINS USING ELISA

3.1.1 YEAST GROWTH

The culturing and handling of yeast was adapted from standard protocols (Clontech 2009; MacDonald et al. 2001). Briefly, the dehydrated YPD broth and YPD Agar (Sigma Aldrich USA) were dissolved in de-ionized (DI) water, 50 g/l and 65 g/l, respectively and sterilized using Barnstead SterileMax Sterilizer for 15 minutes at 1 bar and 121 °C. The 20 µl inoculum/10 ml YPD broth were added and incubated for ~ 3 days in shaker incubator (VWR USA) 30 °C and 150-200 rpm. For growth on solid YPD agar media the cell inoculum was spread over the solidified agar plates using a sterilized loop (Sigma Aldrich USA). The plates were inverted and incubated at 30 °C for 3-5 days to allow full development of colonies. The stock liquid and solid cultures were stored at 4 °C, and remained good for a few months. The number of cells in the culture was determined using absorbance at 600 nm measured using a CaryWinUV spectrophotometer (Varian/Agilent Technologies, Switzerland). Cell density was calculated by the Beer-Lambert equation (Von der Haar 2007) and confirmed using a hemocytometer and agar colony counts. The log phase densities of yeast culture is typically 10^6 - 10^8 cells/ml; early log phase ($< 10^7$), mid log phase (1 to 5×10^7) and late log phase ($> 5 \times 10^7$).

3.1.2 TOXINS EXPOSURE

The cells in log phase (10^7 cells/ml) were harvested and exposed to UV radiation using a handheld UV lamp (UVP LLC USA), and hydrogen peroxide (H_2O_2) (Sigma Aldrich

USA). One ml culture of yeast was exposed to 3 incremental doses of each toxin and H₂O₂ at concentrations of 5, 50 and 500 mM for 60 minutes and UV A, B and C (365, 302 and 254 nm, respectively) for 15 minutes.

3.1.3 CELL LYSIS

The cells exposed to toxins and those not exposed (controls) were washed twice with phosphate buffer saline (PBS) and lysed using a yeast-protein extraction reagent (Y-PER) (Thermo Fisher Scientific USA), in a mild lysing buffer, following manufacturer's instructions (appendix I). Briefly, the cell pellet was incubated with 1 ml. Y-PER in the presence of 10 µl protease inhibitor cocktail (Sigma Aldrich USA) for 20 minutes at room temperature with intermittent agitation, followed by collection of supernatant after centrifugation at 14,000 g for 10 minutes (model 5415C, Eppendorf USA). The quality of protein extraction was validated by scanning for maximum UV absorption in range 200-400 nm (Marenchino et al. 2009).

3.1.4 TOTAL PROTEIN ESTIMATION

The quantity of total protein in the extract was estimated using a commercial BCA kit (Thermo Fisher Scientific USA), following manufacturer's instructions. Briefly, 25 µl of standard (BSA), sample (cell-extract) and blanks (the diluent and lysing buffer) were loaded in duplicate in 96 well-plates. The 200 µl of the BCA reagent was added, mixed, and incubated for 30 minutes at 30°C in an Enviro-Genei (Thomas Scientific, USA). A micro plate reader (Synergy HT from BioTek USA) was employed to determine absorbance at 562 nm, followed by average blank subtraction, standard curve preparation, and subsequent determination of protein concentration. Please see chapter 4, section 4.3

for brief information and the instruction manual in the appendix II for detailed information on principle of the BCA assay.

3.1.5 SPECIFIC STRESS PROTEIN ESTIMATION

The specific proteins, RAD54 (Cedarlane Laboratories, Inc. USA) and HSP70 (Thermo Fisher Scientific Inc. USA) were quantified in yeast extract using commercial ELISA assay kits, following manufacturer's instructions. Brief information on the general principles of all ELISA kits used in the study is reported below. Please see the instructional manual for detailed information on the individual ELISA kits, appendix IIIa for RAD54 and appendix IIIb for HSP70.

ELISA

Proteins were detected using the standard sandwich ELISA kit/technique. Briefly, 100 µl of standard, sample and blank were loaded in duplicate in the micro titre plate supplied in the kit with wells pre-coated with monoclonal antibody (MAb) specific to the protein being detected, and incubated for 2 hours at 37°C. The preparation was then aspirated and several detection reagents were added: biotin-conjugated polyclonal antibody (PAb) for 1 hour, avidin-conjugated horseradish peroxidase for 30 minutes, chromogen substrate solution for 20 minutes, and finally a stop solution, usually sulphuric acid. The absorbance was measured at 450 nm using a Bio Tek micro plate reader, followed by the determination of specific protein concentration from a standard curve. ELISA assay required ~ 6 hours.

* Please refer to the instruction manuals, appendix I-III, of the commercial kits used in the study for details on principles and protocols. Certificates of Analysis of the products are available online.

3.2 MATERIALS AND METHODS FOR FABRICATION OF COLLOIDAL SERS SENSOR

3.2.1 SYNTHESIS OF COLLOIDAL SERS SUBSTRATES

Two widely used SERS substrates, colloidal Au and Ag NPs were prepared by the single-step citrate reduction of their salts, gold (III) chloride trihydrate or silver nitrate, respectively (Sigma Aldrich USA) (Lee et al. 1982) with some modifications to mitigate particle-specific toxicity (Xiu et al. 2012; Levard et al. 2012; Bondarenko et al. 2013). Briefly, 1% trisodium citrate dehydrate (Sigma Aldrich USA) was added rapidly while stirring to a boiling solution of either 1 mM Au or Ag salt solution that was cooled to room temperature after reaching wine-red (Au) or yellow-greenish (Ag) color. The parameters affecting transformation of NPs to ions by oxidation and dissolution were controlled at the time of synthesis and storage to mitigate NP-specific toxicity. All glass materials were washed with aqua regia prepared by mixing hydrochloric acid and nitric acid (Sigma Aldrich USA) in three parts to one, followed by DI water and were then oven-dried. Ultrapure DI water was used for preparing all solutions. Exposure of NPs to light, cold temperature and centrifugation was minimized.

3.2.2 PHYSICAL CHARACTERIZATION OF SERS SUBSTRATES

The size, shape, distribution, surface charge and concentration of colloids was determined using state-of-the-art analytical instruments; a UV-Vis spectrophotometer (Cary Varian,

Agilent Technologies, USA) a laser Doppler micro-electrophoretic analyzer (Zetasizer nano-ZS, Malvern, UK), a transmission electron microscope (TEM CM200, Philips, Netherlands) and an inductively coupled plasma mass spectrometer (ICP-MS ELAN DRC-II, PerkinElmer, USA).

3.2.3 SELECTION OF ACTIVE SERS SUBSTRATE

The SERS potential/activity of Au and Ag NPs was evaluated using Rhodamine 6G (R6G) (Sigma Aldrich USA) as a probe molecule. The average SERS enhancement factor (EF) was calculated using a simple equation (Payne et al. 2005):

$$EF = (N_{vol}/I_{surf}).(N_{surf}/I_{vol})$$

N_{vol} and N_{surf} indicate the number of probe molecules in the aqueous sample volume and on the surface of the SERS substrate, respectively. I_{vol} and I_{surf} are the corresponding Raman and SERS intensities. The R6G characteristic peak at 1503cm^{-1} and the footprint area \AA was considered for the calculation of EF. Ag NPs showed significantly higher activity than Au NPs and therefore, Ag NP substrate was used for the fabrication of SERS immunosensors as described in the following section.

3.2.4 FABRICATION OF SERS SENSOR

The MAbs for RAD54 and HSP70 (Abcam Plc USA) were conjugated to Ag NPs via a bifunctional mercapto-methyl-thiazoleacetic acid linker (MMT Lk) from Sigma Aldrich USA using standard carbodiimide chemistry using a protocol adapted from a previous report (Li et al. 2006). The reported protocol was modified to increase yield and stability by following a reported MAbs-to-MMT-to-Ag NPs conjugation methodology (Kumar et al. 2007). Briefly, the MMT Lk (10 μl , 10 mM prepared in 15% ethanol) activated with a

carbodiimide-N-hydroxysuccinimide reagent was mixed with 10 μg MAbs for 1 hr at room temperature with intermittent mixing. The MMT-MAbs solution was passed through an Amico ultracentrifugal filter units of molecular weight cut off 10 KDa (Sigma Aldrich USA) by centrifugation. The conjugate was mixed with 1 ml Ag NP colloids (roughly 7×10^{10} NPs per ml) for 1 hr. Two blocking agents from Sigma Aldrich USA, mPEGSH (methoxy-poly-ethylene-glycol-sulphydryl) for primary blocking and BSA's FAFGF (bovine serum albumin fatty-acid free and globulin-free) preparation for secondary blocking were sequentially added and incubated for 20 minutes each, followed by a single centrifugation at 2500g for 20 minutes. This produced the MAbs-Ag NP immunosensor. Sensors with targeting MAbs for RAD54 and HSP70 is expected to diffuse passively and exhibit slow and poor cell uptake. Therefore, to achieve efficient intracellular uptake, a fusogenic delivery peptide with cell permeability and endosomal rupture-release properties, TATHA2 from AnaSpec Eurogentec USA, was conjugated to the Ag NPs. For synthesis of the SERS immunosensor with targeting as well as delivery peptides, an equal ratio of MAbs for targeting and delivery was used, and TATHA2 was added prior to the blocking agents.

3.2.5 CHARACTERIZATION OF SERS SENSOR

Besides physical characterization, similar to the SERS substrate mentioned in 3.2.4, the immunosensor was also chemically characterized for the conjugation at each step using a Raman spectro-microscope. A drop of sample at each conjugation step was air-dried on a microscope slide and the Raman spectra were acquired. The methodology for Raman instrumentation and analysis is reported separately in section 3.3.2.

3.2.6 SELECTIVITY TESTING OF SERS SENSOR

The selectivity of the SERS immunosensor was tested by measuring standard proteins in pure solution (direct SERS by adsorbing proteins on the Ag NPs) and in mixture with R6G. Clearly delineated peak/s characteristic of proteins were used for their quantification.

3.3 MATERIALS AND METHODS FOR EXTRACELLULAR DETECTION OF STRESS PROTEINS USING SERS SENSOR AKA SLISA

3.3.1 SERS INSTRUMENTATION AND MEASUREMENT

The RamanStation 400F uses an excitation laser source of 785 nm wavelength, average power of 100 mW at the sample and a spot size of 100 microns under Raman spectroscopy. Built-in Spectrum software was used for processing the spectra, including baseline correction, normalization, background subtraction, peak assignment and resolution. All spectra were acquired using a laser exposure time of 5-10 seconds (5 acquisitions of 1-2 seconds each). The Raman microscope was used for low sample volumes and chemical characterization of the SERS sensor. A drop of sample was placed on a pre-cleaned glass slide and manually focused under a 20x objective, scanning the sample from center to the edge. The Raman spectroscopy was used for high throughput screening of the sample. 200 μ l of sample volume was loaded in a glass bottom well plate in duplicate and analyzed at three different spots per sample (2x3 spectra for each sample) to obtain a mean intensity of the Raman peaks. The experiment was repeated three times (n=3). The intra- and inter-batch variation in intensity of the Raman peaks was reported as the mean \pm S.D. to assess reproducibility (Malvaney et al. 2003).

3.3.2 ESTIMATION OF PROTEINS

Yeast was grown to 10^7 cells/ml and exposed to incremental doses of stress toxins, H_2O_2 at 5, 50 and 500 mM for 60 minutes, and UV A, B and C for 15 minutes. The cells were then lysed using mild Y-PER, reported in section 3.1.3. To detect RAD54 and HSP70 proteins, 10 μ l cell lysate was incubated with SERS immunosensor for 90 minutes to allow ample time for interaction between antigen and antibody, followed by SERS measurement. The yield of specific proteins was calculated from the SERS calibration curves of standard proteins.

3.3.3 COMPARISON OF TWO SENSORS, ELISA VS. SLISA

The performance of SLISA was compared to industry-standard ELISA in terms of RISE detection. Other sensor attributes, including the limit of detection (LOD), correlation coefficient (R^2), reproducibility etc. were also compared.

3.4 MATERIALS AND METHODS FOR INTRACELLULAR DELIVERY AND DETECTION USING SERS SENSOR

3.4.1 CELLULAR TOXICITY STUDIES

SERS substrates and sensors were incubated with yeast normalized to 10^5 Ag NPs per cell. The growth inhibition effect of Ag NPs was studied using nanoparticle concentrations of 1, 10 and 100 ppm for 3, 6 and 12 hours. The cell mortality was determined by agar plating, and growth inhibition was assessed by optical density at 600 nm and dye exclusion assay using trypan blue from Sigma Aldrich USA (Almeida et al. 2008; Xiu et al. 2012). The silver ions (Ag^+) and chitosan nanoparticles (80-200 nm, prepared using ionic gelation

method reported by Janes et al. 2001) were included in the study as positive and negative controls, as they are well characterized for their cytotoxicity and biocompatibility properties, respectively. Electroporation apparatus and the cuvettes from Bio RAD USA, designed especially for yeast was used to test the cytotoxicity effect of active/electroporation-mediated intracellular delivery of Ag NPs (Lin et al. 2009; Yu et al. 2011). Almost every possible parameter (electric field strength, pulse duration and pattern, temperature and electroporation media) was investigated to identify the least toxic electroporation settings. Cellular morphological damage in response to electroporation was assessed using SEM and toxicity by colony formation assay. Electroporation exhibited high toxicity even at the lowest achievable electric field strength (E) and time (1 ms) and was therefore determined to not be a good choice towards development of a SERS immunosensor for intracellular detection, and was not investigated for cell uptake.

3.4.2 CELLULAR UPTAKE STUDIES

The number of Ag NPs and their localization after intracellular delivery via passive and TATHA2-facilitated diffusion was estimated by ICP-MS and *in situ* by TEM, respectively (Cho et al. 2009; 2010; Zhu et al. 2008; Sen et al. 2011). The cells were lysed to release the Ag NPs, and were then dissolved by acid digestion to Ag⁺ and measured using ICP-MS. The cells were thin-sectioned (25-50 nm thick) using a Porter-Blum MT-1 Ultramicrotome (DuPont-Sorvall USA) and a diamond knife (DDK USA) to observe the intracellular distribution of Ag NPs using TEM. The intracellular Ag NPs localization and yield was estimated after selective removal of Ag NPs from the cell surface using a mild I₂/KI etching procedure and validated by SEM 6330F (Jeol USA) (Cho et al. 2009; 2010).

The TATHA2 mediated delivery method was able to efficiently deliver Ag NPs into yeast cells and was therefore considered further for intracellular detection to test the feasibility of CBB-SIST.

3.4.3 SENSOR STABILITY AND INTRACELLULAR DETECTION

SERS immunosensor with targeting and delivery peptides were incubated with cells (CBB) for 3, 6 and 12 hrs at room temperature, followed by three washings with PBS using centrifugation (Kumar et al. 2007 and 2008). The SERS immunosensor and CBB were tested for stability and the intracellular signals of the nano-bioconjugate using a Raman spectro-microscope.

3.5 MATERIALS AND METHODS FOR A CASE STUDY

3.5.1 FABRICATION OF A PROTOTYPE MICROCHIP

Polymethyl methacrylate, common name plexiglass, from McMaster-Carr, Inc., Atlanta, GA, USA, was used to fabricate the microchip (2x3 wells). The dimensions of the microchip were 30.5x25.5x1 mm (LxWxH) with a 3 mm step around the perimeter of the top to fit a lid and a 1 mm step at the bottom to accommodate a commercial microscope coverslip (30x25 mm).

3.5.2 ON-CHIP SLISA: A CASE STUDY

Yeast cells grown in YPD were harvested in early saturation phase of growth and distributed into the first row of the microchip (A1 through A3, Figure 8), covered with a plexiglass lid, and stored as slurries of 10^7 cells at 4°C until use.

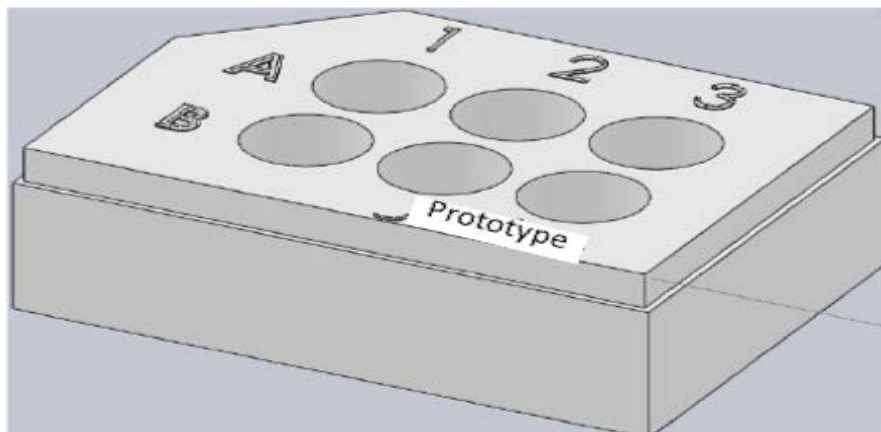


Fig. 8: Microchip Design.

H₂O₂ was added to experimental wells and DI water to the control well. A single-time multiple-dose study employed peroxide concentrations of 5, 50 and 500 mM for 60 minutes. Y-PER supplemented with protease inhibitor cocktail was added to the cells and incubated for 20 minutes at RT. The supernatant (cell extract) was transferred using an ultrafine pipette tip into the second row of wells (B1 through B3) and incubated with the colloidal SERS immunosensor for RAD54 SERS detection by incubating for 90 minutes at RT. The H₂O₂-RAD54 dose-response relationship was translated to a three-tiered scheme of toxicity established by the US EPA (<http://www.epa.gov/oppt/aegl/pubs/humanhealth.htm>), Immediately Dangerous to Life and Health concentrations (IDLHs). Three-tiered toxicity guideline levels are intended to describe the risk of chemical toxins to human health.

REFERENCES

Almeida T., Marques M., et al. (2008). Isc1p plays a key role in hydrogen peroxide resistance and chronological lifespan through modulation of iron levels and apoptosis. *Mol.*

Biol. Cell, 19: 865-876

Bondarenko O., Juganson K., et al. (2013). Toxicity of Ag, CuO and ZnO nanoparticles to selected environmentally relevant test organisms and mammalian cells in vitro: a critical review. Arch. Toxicol., 87(7): 1181-1200

Cho E. C., Xie J. et al. (2009). Understanding the role of surface charges in cellular adsorption versus internalization by selectively removing gold nanoparticles on the cell surface with a I2/KI etchant. Nano Lett., 9(3): 1080-1084

Cho E. C., Au L., et al. (2010). The effects of size, shape, and surface functional group of gold nanostructures on their adsorption and internalization by cells. Small, 6(4): 517-522

Clontech Laboratories, Inc. (2009). Yeast protocols handbook. Pages 64

Janes K. A., Fresneau M. P., et al. (2001). Chitosan nanoparticles as delivery systems for doxorubicin. J. Controlled Release, 73(2): 255-267

Kumar S., Harrison N., et al. (2007). Plasmonic nanosensors for imaging intracellular biomarkers in living cells. Nano Lett., 7(7): 1338-1343

Kumar S., Aaron J., et al. (2008). Directional conjugation of antibodies to nanoparticles for synthesis of multiplexed optical contrast agents with both delivery and targeting moieties. Nat. Protoc., 3(2): 314-320

Lee P. C., Meisel D. (1982). Adsorption and surface enhanced Raman of dyes on silver and gold sols. J. Phys. Chem., 86: 3391-3395

Levard C., Hotze E. M., et al. (2012). Environmental transformations of silver nanoparticles: impact on stability and toxicity. Environ. Sci. Technol., 46: 6900-6914

Li H., Sun J. et al. (2006). Label-free detection of proteins using SERS-based immunonanosenors. NanoBiotechnology., 2: 17-28

Lin J., Chen R., et al. (2009). Rapid delivery of silver nanoparticles into living cells by electroporation for surface-enhanced Raman spectroscopy. Biosens. Bioelectron., 25(2): 388-394

MacDonald P. N., Paul N. (2001). Two-hybrid systems methods and protocols. Methods Mol. Biol., 177: pages 9-14

Malvaney S. P., He L. et al. (2003). Three-layer substrates for SERS: Preparation and preliminary evaluation. J. Raman Spectrosc., 34: 163-171

Marenchino M., Armbruster D. W., et al. (2009). Rapid and efficient purification of RNA-binding proteins: Application to HIV-1 Rev. Protein Expr. Purif., 63(2): 112-119

- Payne E. K., Rosi N. L., et al. (2005). Sacrificial biological templates for the formation of nanostructured metallic microshells. *Angew Chem. Int. Ed. Engl.*, 44: 5064-5067
- Sen K., Sinha P., et al. (2011). Time dependent formation of gold nanoparticles in yeast cells: A comparative study. *J. Biomed. Eng.*, 55(1): 1-6
- Von der Harr T. (2007). Optimized protein extraction for quantitative proteomics of yeasts. *PLoS One*, 2(10) e1078, pages 8
- Xiu Z. M., Zhang Q. bo, et al. (2012). Negligible particle-specific antibacterial activity of silver nanoparticles. *Nano Lett.*, 12(8): 4271-4275
- Yu Y., Lin J., et al. (2011). Optimizing electroporation assisted silver nanoparticle delivery into living C666 cells for surface-enhanced Raman spectroscopy. *Spectroscopy*, 25(1): 13-21
- Yu Y., Lin J., et al. (2011). Improved electroporation parameters of delivering silver nanoparticles into living C666 cells for surface-enhanced Raman spectroscopy. *J. Phys. Conf. Ser.*, 277: 012045, pages 5
- Zhu Z. J., Ghosh P. S., et al. (2008). Multiplexed screening of cellular uptake of gold nanoparticles using laser desorption/ionization mass spectrometry. *J. Am. Chem. Soc.*, 130(43): 14139-14143

CHAPTER 4 EXTRACELLULAR DETECTION OF STRESS PROTEINS USING ELISA

The purpose of this chapter is to determine levels of stress biomarker proteins, normalized to yeast cell number and total protein concentration, in response to toxins using industry-standard techniques/kits (specific aim 1). Total protein concentration was determined using BCA (Bicinchoninic acid) followed by ELISA for the detection of specific proteins. This work has been published in a full-length research article in Journal of Biosensor & Bioelectronics (Bhardwaj et al. 2013). Written permission (e-mail) to use publication content in my dissertation has been obtained from the editor of the journal and a copy of the e-mail is incorporated in the appendix IV.

Materials and methods for this specific aim#1 are discussed in chapter III, section 3.1.

4.1 DETERMINATION OF CELL CONCENTRATION

The concentration of yeast growing in cell culture media was estimated by three standard microbiological methods:

- (i) Indirect spectrophotometric/turbid-metric method: absorbance ($A_{600 \text{ nm}}$), converted to cell number/volume using the Beer-Lambert equation:
- (ii) Direct method (cell counting in hemocytometer chamber):
- (iii) Direct method (colony count using agar plating):

Method iii gives the concentration of viable cells as they form colonies, but such cell clusters take 3-4 days to develop, and therefore was not used for regular practice unless otherwise mentioned.. Spectrophotometric and hemocytometric methods on the other hand

rapidly determine concentration and were employed for regular cell concentration determination.

4.2 PURITY ANALYSIS OF PROTEINS IN CELL EXTRACT

The yeast cell extract had pure proteins, as evident from maximum absorption ~ 280 nm and the absorbance ratio $260/280 = 0.64$ (Fig. 9), which is comparable to previous work (Marenchino et al. 2009).

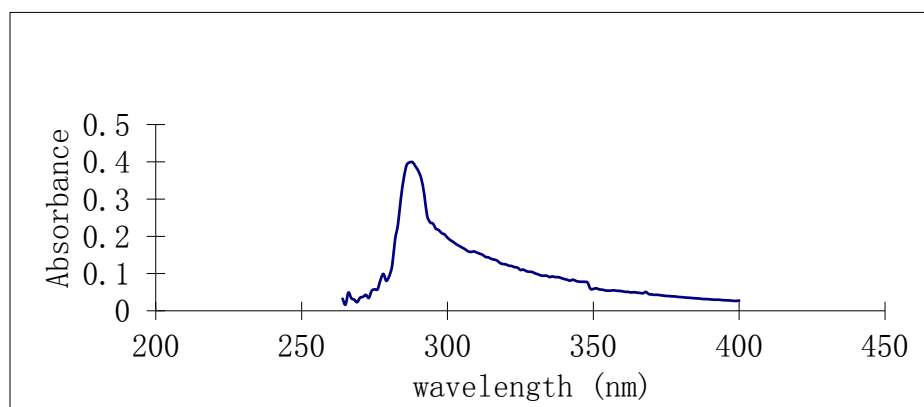


Fig. 9: Absorption spectra of supernatant after cell lysis. Protein characteristic peak maxima around 280 nm and absorption ratio $260/280 \text{ nm} = 0.5503/0.8534 = 0.64$.

4.3 ESTIMATION OF TOTAL PROTEIN

The bicinchoninic acid (BCA) assay is a biochemical colorimetric assay to determine total protein concentration in a solution, including cell lysates. The mechanism of the BCA assay is primarily dependent on two reactions. First, the peptide bonds in the proteins reduce copper (II) sulfate present in the BCA solution (Cu^{2+} to Cu^{+}). This is a temperature-dependent step. Second, each Cu^{+} ion chelates two molecules of BCA forming a purple colored product that is quantified by $A_{595 \text{ nm}}$ and shows a linear response to increasing protein concentration. Accordingly, the protein concentration in cell lysate or in other

samples is typically determined by using a BSA protein standard to develop a calibration curve.

The BSA calibration curve was linear in the range 20-200 $\mu\text{g/ml}$ (Fig. 10). The estimated yield of total protein was 60 μg per ml of yeast culture (10^7 cells), which is comparable to previous work (von der Haar 2007).

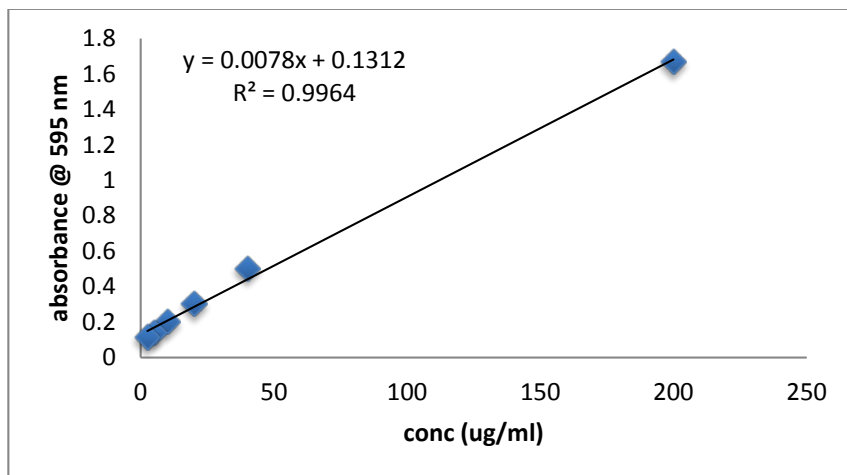


Fig. 10: BSA standard curve. A useful linear range of protein concentration up to 200 $\mu\text{g/ml}$ is achieved.

4.4 ESTIMATION OF SPECIFIC STRESS PROTEINS USING ELISA

The batch of 10^7 cell ml^{-1} yielded $60 \mu\text{g ml}^{-1}$ protein and was analyzed for specific stress proteins using a standard commercial ELISA technique. Stress-biomarker proteins, RAD54 and HSP70, were measured when yeast cells were exposed to H_2O_2 at 5mM, 50mM and 500 mM concentrations for 60 minutes each, and when cells were exposed to UV A, B and C at 365 nm, 302 and 254 nm, respectively for 15 minutes each. The experiments were repeated three times ($n=3$) loading the samples in duplicate each time, and were graphically represented along with mean \pm SD. Detection of stress-biomarker proteins, RAD54 and HSP70 is reported below.

An increase in expression of RAD54 protein (Fig. 11 and Fig. 12) and HSP70 (Fig. 13 and Fig. 14) occurred in response to H₂O₂ and UV.

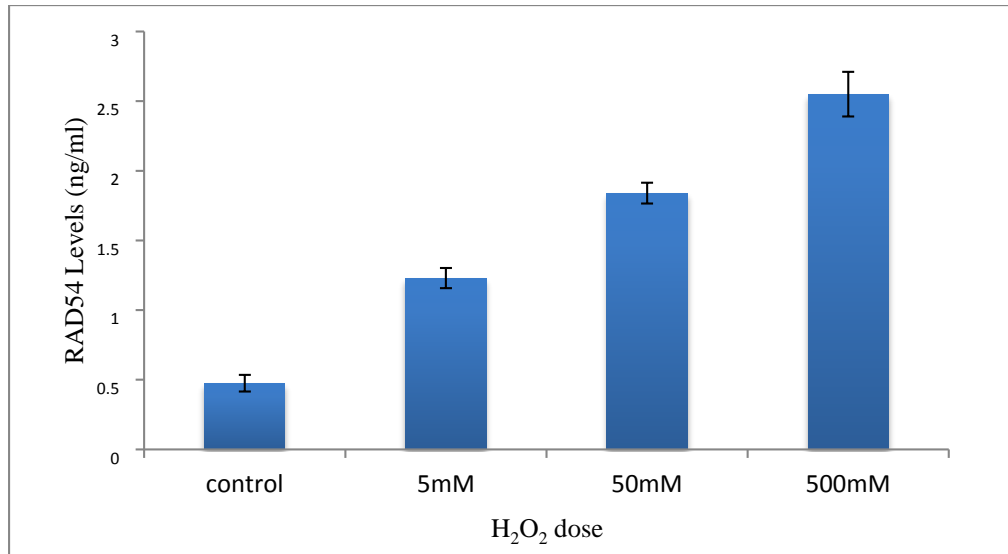


Fig. 11: Quantitation of RAD54 expressed by yeast cells exposed to H₂O₂ for 60 minutes and detected by ELISA. Control: baseline levels expressed by cells, without exposure to H₂O₂. Significant difference was observed between treatments groups as well as wrt control ($P < 0.05$, $n = 3$).

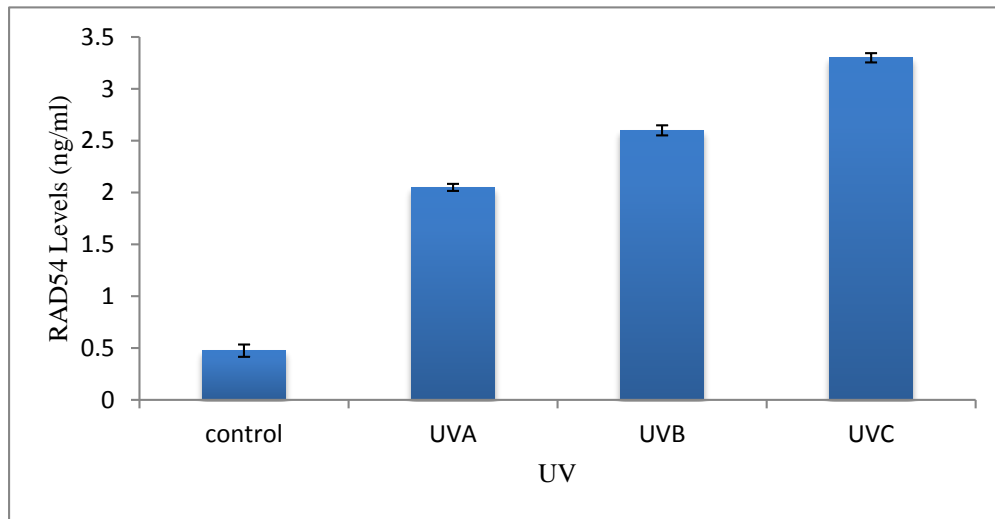


Fig. 12: Quantitation of RAD54 expressed by yeast cells exposed to UV for 15 minutes and detected by ELISA. Control: baseline levels expressed by cells, no UV exposure. Significant difference was observed between treatment groups as well as wrt control ($P < 0.05$, $n = 3$).

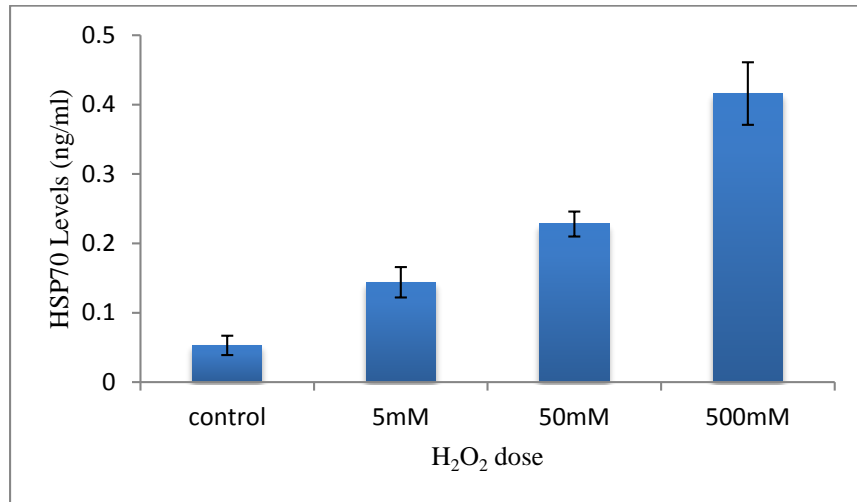


Fig. 13: Quantitation of HSP70 expressed by yeast cells exposed to H₂O₂ for 60 minutes and detected by ELISA. Control: baseline levels, no H₂O₂ treatment. Significant difference was observed between treatment groups as well as wrt control ($P < 0.05$, $n = 3$).

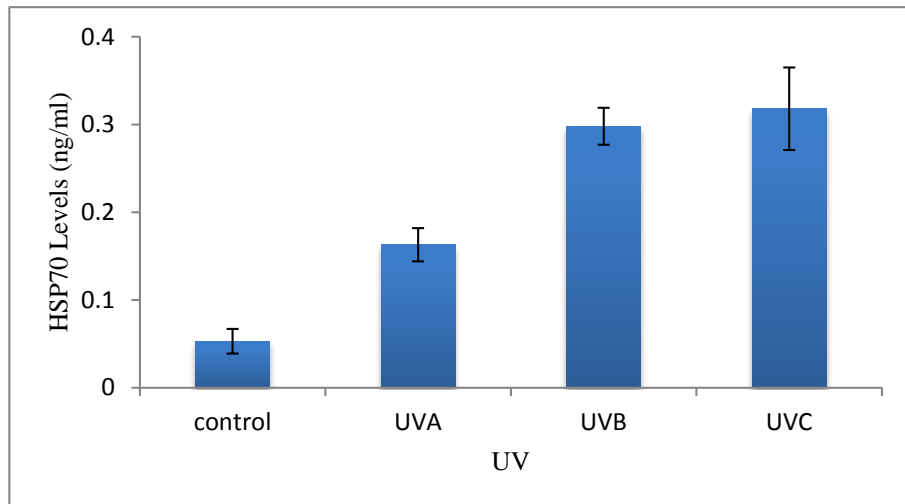


Fig. 14: Quantitation of HSP70 expressed by yeast cells exposed to UV for 15 minutes and detected by ELISA. Control: baseline levels, no UV treatment. Significant difference was observed between treatment groups, except UVC compared to UVB, as well as wrt control ($P < 0.05$, $n = 3$).

When yeast cells were exposed to H₂O₂ for 20-60 min, and to UVA and UVB for 5-15 minutes a continuous increase in levels of stress-proteins RAD54 and HSP70 was observed

for up to 60 minutes (Figs. 11-14). Baseline or constitutive levels of RAD54 and HSP70 were roughly 400 and 50 pg per ml culture, respectively. The induction of RAD54 in response to UV (Fig. 12) is rapid and higher compared to H₂O₂ (Fig. 11). RAD54 induction in response to the two toxins was 5-6 folds wrt baseline levels, control. Although, HSP70 cellular expression levels were low compared to RAD54, HSP70 (inductive isoform) showed an ~8-fold higher induction in response to toxins (Fig. 12 and Fig. 13). In contrast to HSP70, which did not show any significant increase in response to UVC as compared to UVB, RAD54 induction in response to different doses of UV was incremental. RAD54 and HSP70 induction levels in response to toxins are in agreement with previous reports (Cole et al. 1987; Scott et al. 2003 and Wang et al. 2012).

All aerobic organisms, including yeast, suffer exposure to oxidative stress caused by reactive oxygen species (ROS), which is a major pathway in stress tolerance and toxicity mechanisms (Jamieson et al. 1998). ROS is ubiquitous in nature and has numerous sources including H₂O₂ and UV. Radiation acts on the stable form of elemental oxygen (O₂) to form highly unstable ozone molecules (O₃), which are sources of ROS. Undoubtedly, besides oxidative stress there are several other pathways of stress including those due to carbonyl groups, glyoxals, and methylglyoxals, among other chemical agents. However, none of them are well characterized because of the intricate interplay between these numerous pathways. However, the difference between induction of RAD54 and HSP70 in response to UV may be explainable. RAD54 nomenclature is derived from being RADiAtion sensitive, which supports the finding of a continuous increase in levels of RAD54 in response to UV as compared to HSP70. UV is reported to cause photochemical damage to cellular DNA, which is repaired by DNA enzyme (RAD54) and hence, UV

induction of RAD54 is more significant than that of HSP70. Although heat was not included in the study, interestingly, RAD54 is not responsive to heat stress (Cole et al. 1987). On the other hand, Heat Shock Protein (HSP) can be speculated to express higher sensitivity to heat, similar to higher RADiAtion sensitivity of RAD54, as observed in this study.

4.5 SUMMARY

Stress proteins, RAD54 and HSP70 were tested for their expression in response to incremental doses of H₂O₂ at 5, 50 and 500 mM concentrations for up to 60 minutes and to UV, A, B and C for 15 minutes. HSP70 and RAD54 showed 4 to 8 fold induction in response to both peroxide toxins and UV light exposure.

REFERENCES

- Bhardwaj V., Srinivasna S., et al. (2013). AgNPs-based label-free colloidal SERS nanosensor for the rapid and sensitive detection of stress proteins expressed in response to environmental toxins. *Biosens. Bioelectron.*, S12: 005, pages 7
- Cole G. M., Schild D., et al. (1987). Regulation of RAD54- and RAD52-lacZ gene fusions in *Saccharomyces cerevisiae* in response to DNA damage. *Mol. Cell Biol.*, 7: 1078-1084
- Jamieson D. J. (1998). Oxidative stress responses of the yeast *Saccharomyces cerevisiae*. *Yeast*, 14: 1511-1527
- Marenchino M., Armbruster D. W., et al. (2009). Rapid and efficient purification of RNA-binding proteins: Application to HIV-1 Rev. *Protein Expr. Purif.*, 63(2): 112-119
- Scott M. A., Locke M., et al. (2003). Tissue-specific expression of inducible and constitutive Hsp70 isoforms in the western painted turtle. *J. Exp. Biol.*, 206: 303-311
- Von der Harr T. (2007). Optimized protein extraction for quantitative proteomics of yeasts. *PLoS One*, 2(10) e1078, pages 8
- Wang Y., Gibney P. A., et al. (2012). The yeast Hsp70 ssa1 is a sensor for activation of the heat shock response by thiol-reactive compounds. *Mol. Bio Cell*, 23: 3290-3298

CHAPTER 5 FABRICATION OF COLLOIDAL SERS SENSOR

The purpose of this chapter is to select the best active SERS substrate between Au and Ag NPs and use it for the synthesis of the SERS immunosensor (specific aim 2). This work has been published in a full-length research article in *Journal of Biosensor & Bioelectronics* (Bhardwaj et al. 2013). Written permission (e-mail) to use this publication content in my dissertation has been obtained from the editor of the journal and a copy of the e-mail is incorporated in the appendix IV.

Materials and methods for this chapter, consistent with specific aim #2, are discussed in chapter III, section 3.2.

5.1 SYNTHESIS AND CHARACTERIZATION OF SERS SUBSTRATES

Almost spherical Au and Ag NPs were synthesized using a conventional citrate reduction method (Lee et al. 1982). They were ~60-nm diameter and displayed a narrow size distribution (polydispersity index < 0.15) as well as the expected characteristic color and absorption peak (Fig. 15). Roughly 50-60 nm spherical NP is the best size to achieve high SERS activity and cell uptake (Stamplecoskie et al. 2011; Chithrani et al. 2006). The substrates were highly negatively charged (-40 mV) due to citrate groups. Citrate is the most commonly used carboxylic acid because it acts as a reducing agent as well as a capping (coating) agent for Au and Ag NPs. The citrate-cap is significant for two reasons. First, the oxy (O^-) and hydroxyl (OH^-) groups of the citrate offer a high repulsive force that provides stability to the NPs. Second, these groups are easily replaced by other more reactive functional groups such as thiol (SH), thereby, allowing facile conjugation of biomolecules to the NPs. The concentration of the two substrates, estimated using ICP-

MS, was 100 ppm (0.1 mg/ml), which is roughly equivalent to 7×10^{10} NPs/ml. The shape, size, charge and concentration of the Ag NPs are in good agreement with other groups that used a similar citrate reduction process (Emory et al. 1998; Kahraman et al. 2010).

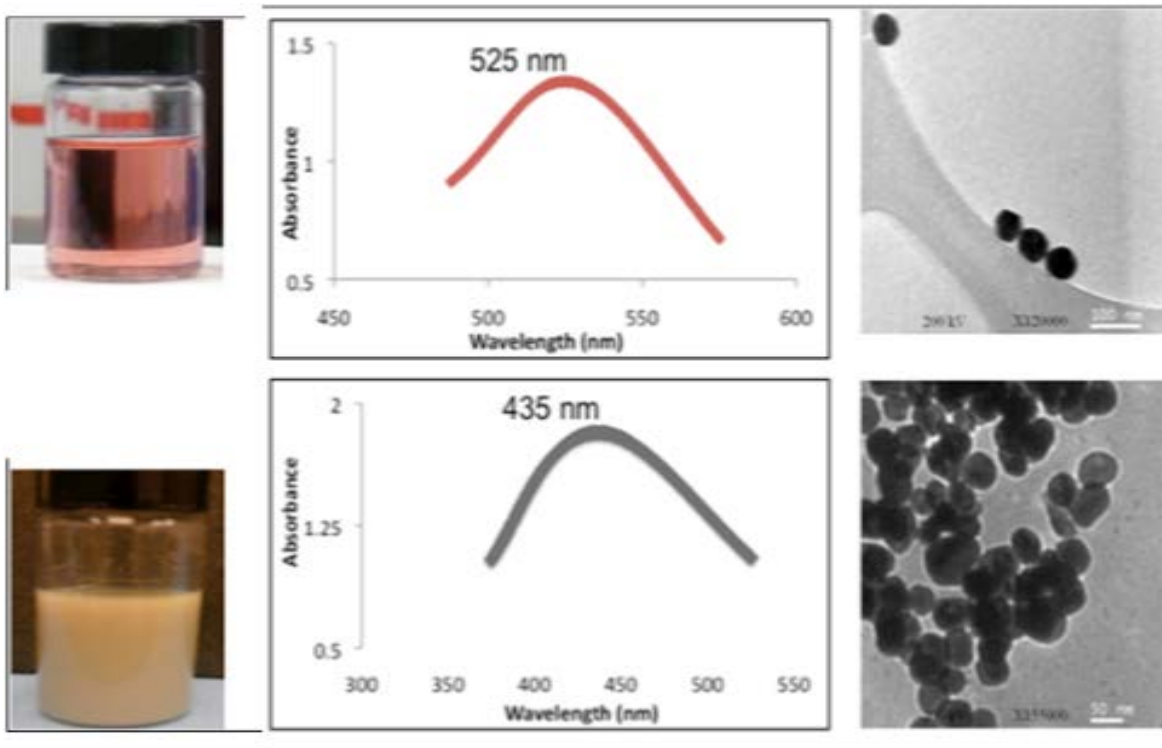


Fig. 15: Characterization of colloidal Au (top row) and Ag (bottom row) NPs-based SERS substrates. Characteristic red color of Au and yellow-greenish Ag (left) with absorption peak at 525 and 435 nm, respectively (middle) indicates the formation of NPs. TEM image (right) indicates the NPs are almost spherical with ~ 50 - 60 nm size.

5.2 SELECTION OF ACTIVE SERS SUBSTRATE

The prominent peak of R6G at 1503 cm^{-1} and the footprint area 20 \AA^2 was considered for the calculation of SERS EF using the equation given in section 3.2.3. The N_{surf} is estimated to be 4.87×10^{11} and the N_{vol} to be 2.47×10^{14} . The ratio of I_{surf} to I_{vol} for AgNPs is estimated to be 8.92×10^2 and therefore the EF is calculated as 4.52×10^5 . However, the Au NPs resulted in lower SERS intensity (I_{surf}) and therefore the lower EF of 2×10^3 .

Theoretical calculations indicate that single Au and Ag NPs can reach the maximum EF to 10^3 - 10^4 and 10^6 - 10^7 , respectively (Kerker 1987). The EF of the colloidal Ag NPs is comparable to 3D silver shells (Payne et al. 2005), which is an improvement over other conventional geometries such as colloids and films (Malvaney et al. 2003). Considering more than 200x difference in SERS activity of the Ag NPs as compared to Au NPs, Ag NPs colloids were used for the fabrication of SERS sensor.

5.3 PHYSICO-CHEMICAL CHARACTERIZATION OF SERS SENSOR

The size of the Ag NPs after conjugation of MAbs for stress proteins increased from 60 to 98 nm, polydispersity increased from 0.12 to 0.16, the charge decreased from -40 to -18 mV and their characteristic yellow-greenish color changed to light grey due to slight aggregation, which is typically observed during sensor fabrication (Fig. 16).

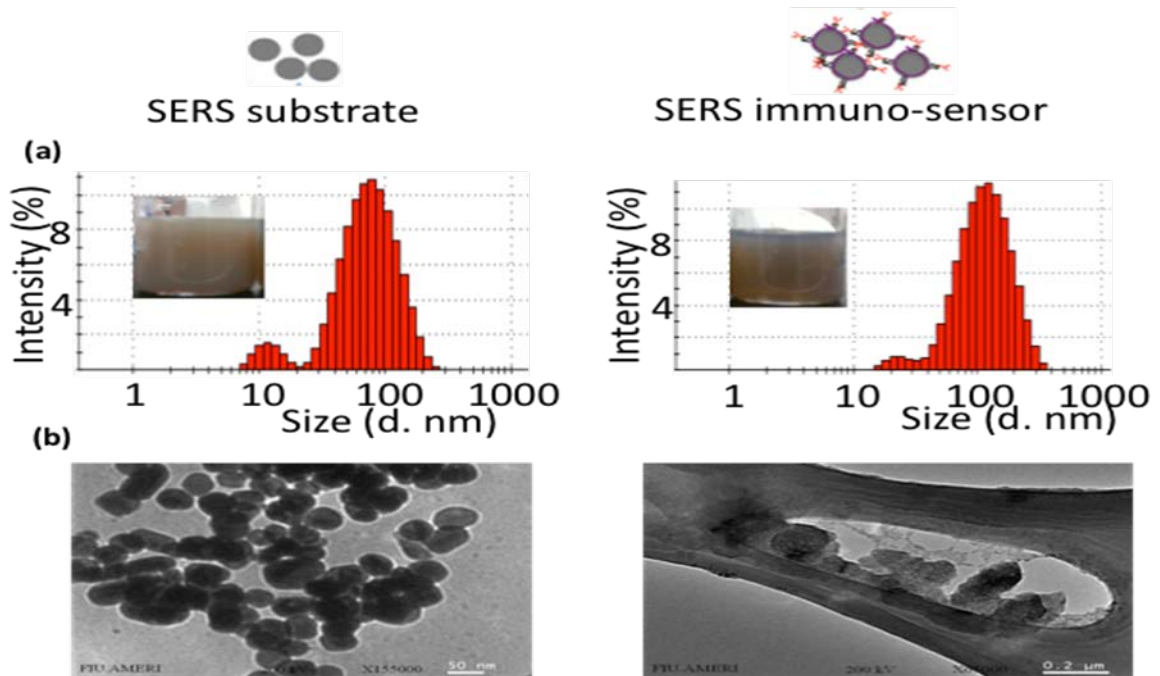


Fig. 16: Physical characterization of Ag NPs-based SERS substrate (left column) and sensor for RAD54 detection (right column). Negligible color change, characteristic of

immunosensor fabrication (inset images) and increase in average size (histogram) of SERS substrate after antibody conjugation (immuno-sensor) is observed (a). TEM images of bare AgNPs (SERS substrate, left) and RAD54 antibody (white dots and filaments, right) conjugated AgNPs (immunosensor).

The SERS immunosensor was chemically characterized by acquiring Raman spectra at each step of sensor fabrication as shown in Fig. 17: a) Preparation of Ag NPs b) Conjugation of MMT cross linker to Ag NPs (Ag NPs-MMT) and c) conjugation of MAbs to Ag NPs-MMT solution (SERS immunosensor). The noticeable bands around 1060 cm^{-1} and 245 cm^{-1} are assigned to nitrate (NO_3^-) stretching and are used to monitor the conjugation process. The successive decrease in this band confirms the replacement of nitrate groups by the functional groups of the linker and the MAbs. Previous work has employed the nitrate band for characterization of Ag NPs, and as an internal standard during sensor fabrication (He et al. 2011; Kora et al. 2012). Likewise, the decrease in intensity of the nitrate peaks and the addition of two main bands around 1300 cm^{-1} characteristic of the MMT linker have been reported (Li et al. 2006). Three Raman active aromatic amino acids, tryptophan (W), Phenylalanine (F) and tyrosine (Y) contributed to the Raman signals with peaks around 1390 and 712 (W), 1005 and 600 (F), 1133 and 853 (Y). The successive conjugation of MAbs to the linker via amide bonds (CO-NH) is validated by the weak peaks originating from amide I (C=O around 1240 and 1290), amide II (out-of-phase C-N stretching around 1454 and 1494) and amide III (in-phase C-N stretching between 1560 to 1660). The Raman peaks of proteins are in good agreement with the literature (Tuma 2005; Han et al. 2008).

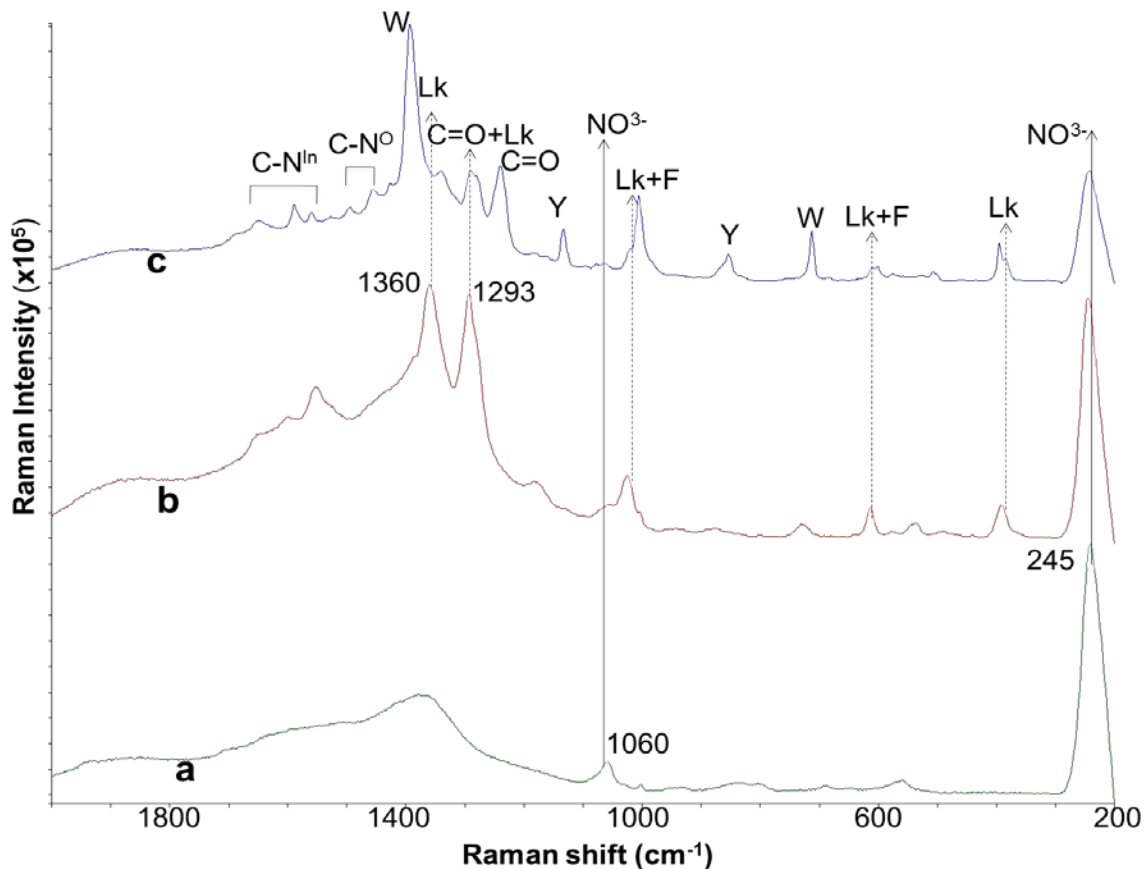


Fig. 17: Chemical characterization of the SERS sensor for RAD54 detection. Weak nitrate (NO_3^-) peaks characteristic to Ag NPs (a) and strong peaks of MMT Lk (b) are replaced by peaks associated with proteins or MAbs (c). The solid and the dotted arrows represent decrease in characteristic peaks of Ag NPs (NO_3^-) and the MMT Lk, respectively. Protein bands are assigned to aromatic amino acids (W: Tryptophan, Y: Tyrosine and F: Phenylalanine) and amide bonds (I: C=O, II: C-N^o, III: C-N^{In} where O is out-of-phase and In for in-phase, after Bhardwaj et al. 2013).

5.4 SELECTIVITY TESTING OF SERS SENSOR

Bovine serum albumin (BSA) has traditionally been used as a blocking agent to avoid non-specific binding. However, all BSAs are not alike in their preparation and therefore differ in their non-specific blocking resistance (Xiao et al. 2012). Crude BSA and other ionic blocking agents such as casein, gelatin and dry milk have high globulin content and fatty

acids, which have high affinity to biomolecules circulating in a real environment (Buchwalow et al. 2011). Therefore, a fatty-acid-free and globulin-free (FAFGF) preparation of BSA (Sigma#A7030) was used. The selectivity of the SERS immunosensor coated with FAFGF-BSA and mPEGSH blocking agents was tested by detection of standard protein mixed with R6G. There was no R6G characteristic peak at 1503 cm^{-1} , but the distinct characteristic protein peak at 1390 cm^{-1} was observed (Fig. 18), which indicates selectivity of the SERS immunosensor for RAD54 detection.

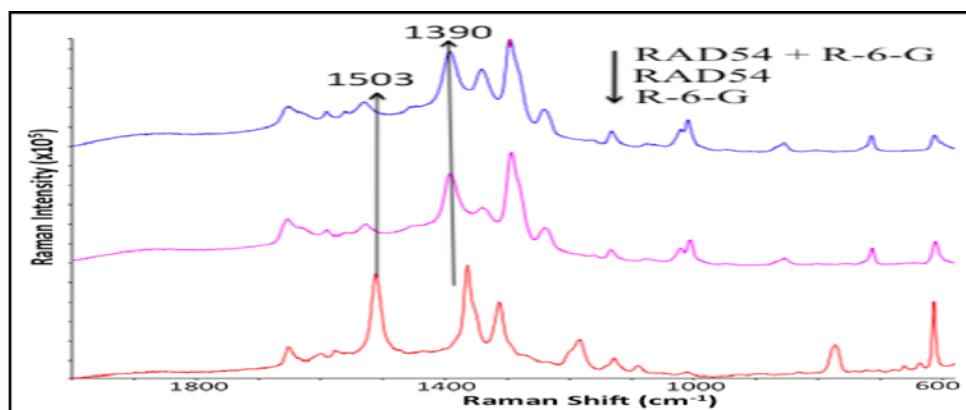


Fig. 18: Selectivity of the RAD54 SERS sensor. The Raman spectrum of the RAD54 SERS sensor showing a peak at 1390 cm^{-1} (top and middle) due to carboxylic groups in the protein. Note that while the characteristic peak of R6G at 1503 cm^{-1} is present in the Raman spectrum of R6G (bottom), it is missing in the Raman spectrum of RAD54 mixed with R6G (top), which indicates the sensor's selectivity. Each spectrum is background subtracted using a spectral calculator (after Bhardwaj et al. 2013).

5.5 SUMMARY

Colloidal spherical SERS substrates, Au and Ag NPs of $\sim 60\text{-nm}$ size were prepared. Ag NPs exhibited $\sim 200\text{x}$ increased activity as compared to Au NPs. Therefore; to achieve higher sensitivity, the SERS immunosensor was fabricated using the Ag NPs SERS substrate. The sensor was fully characterized for their physical and chemical properties

including shape, size, charge, concentration, polydispersity and chemical conjugation. The SERS sensor did not exhibit non-specific binding, as evident from selectivity testing of SERS sensor in presence of R6G.

REFERENCES

- Bhardwaj V., Srinivasan S., et al. (2013). AgNPs-based label-free colloidal SERS nanosensor for the rapid and sensitive detection of stress proteins expressed in response to environmental toxins. *Biosens. Bioelectron.*, 4(5): pages 1-7
- Buchwalow I., Samoilova V., et al. (2011). Non-specific binding of antibodies in immunohistochemistry: fallacies and facts. *Science rep.*, 1: 28
- Chithrani B. D., Ghazani A. A., et al. (2006). Determining the size and shape dependence of gold nanoparticle uptake into mammalian cells. *Nano Lett.*, 6: 662-668
- Emory S. R., Nie S. (1998). Screening and enrichment of metal nanoparticles with novel optical properties. *J. Phys. Chem.*, 102: 493-497
- Han X. X., Jiao H. Y., et al. (2008). Analytical technique for label-free multi-protein detection based on western blot and surface-enhanced Raman scattering. *Anal. Chem.*, 80: 2799-2804
- He L., Rodda T. et al. (2011). Detection of a foreign protein in milk using surface-enhanced Raman spectroscopy coupled with antibody-modified silver dendrites. *Anal. Chem.*, 83: 1510-1513
- Kahraman M., Sur I., et al. (2010). Label-free detection of proteins from self-assembled protein-silver nanoparticle structures using surface-enhanced Raman scattering. *Anal. Chem.*, 82: 7596-7602
- Kerker M. (1987). Estimation of SERS from surface-averaged electromagnetic intensities. *J. Colloid Interf. Sci.*, 118: 417-421
- Kora A. J., Beedu S. R., et al. (2012). Size-controlled green synthesis of silver nanoparticles mediated by gum ghatti (*Anogeissus latifolia*) and its biological activity. *Org. Med. Chem. Lett.*, 2: 17.
- Lee P. C., Meisel D. (1982). Adsorption and surface-enhanced Raman of dyes on silver and gold sols. *J. Phys. Chem.*, 86: 3391-3395
- Li H., Sun J., et al. (2006). Label-free detection of proteins using SERS-based immunonanosenors. *NanoBiotechnology*, 2: 17-28

Malvaney S. P., He L., et al. (2003). Three-layer substrates for SERS: preparation and preliminary evaluation. *J. Raman Spectrosc.*, 34: 163-171

Payne E. K., Rosi N. L., et al. (2005). Sacrificial biological templates for the formation of nanostructured metallic microshells. *Angew Chem. Int. Ed. Engl.*, 44: 5064-5067

Stamplecoskie K. G., Scaiano J. C. (2011). Optimal size of silver nanoparticles for surface-enhanced Raman spectroscopy. *J. Phys. Chem. C* 115(5): 1403-1409

Tuma R. (2005). Raman spectroscopy of proteins: From peptides to large assemblies. *J. Raman Spectrosc.*, 36: 307-319

Xiao Y., Isaacs S. N. (2012). Enzyme-linked immunosorbent assay (ELISA) and blocking with bovine serum albumin (BSA) – Not all BSAs are alike. *J. Immunol. Methods*, 384: 148-151

CHAPTER 6 EXTRACELLULAR DETECTION OF PROTEINS USING SERS SENSOR AKA SLISA

This chapter focuses on the quantification of RAD54 and HSP70 proteins expressed in response to H₂O₂ and UV using a SERS-Linked ImmunoSensor Assay (SLISA) (specific aim 3). The sensing attributes include correlation in accuracy of detection and performance of SLISA compared to ELISA. This work has been published in a full-length research article in *Journal of Biosensor & Bioelectronics* (Bhardwaj et al. 2013) and *SPIE Defense, Security and Sensing* proceedings (Bhardwaj et al. 2015). Written permission (e-mail) to use publication content in my dissertation has been obtained from the editor of the journal and a copy of the e-mail is incorporated in the appendix IV.

Materials and methods for specific aim #3 are discussed in chapter III, section 3.3.

6.1 ESTIMATION OF PROTEINS USING SLISA

The carboxylic (COO⁻) band at $\sim 1390\text{ cm}^{-1}$ is qualitatively as well as quantitatively distinct in the SERS immunosensor (Fig. 18 and Fig. 19), suggesting ionic interactions between antigen and the antibody. Therefore, the levels of proteins expressed in response to toxins were quantified using COO⁻ band. The schematic and qualitative information on SERS immunosensor is shown (Fig. 19). The bifunctional MMT linker (Lk with SH and COOH groups at the end) covalently binds to the Ag NP via a metal-sulphur (M-S) bond and to the antibody via a peptide bond (CO-NH). The spectrum characteristic of ring-containing aromatic amino acids is dominant in direct SERS of the RAD54 protein, but disappears in the immunosensor, perhaps because the agglutination of antibody with antigenic determinant region, epitope occurs via aliphatic-rich region. The Lk band at $\sim 1280\text{ cm}^{-1}$ serves as an internal standard.

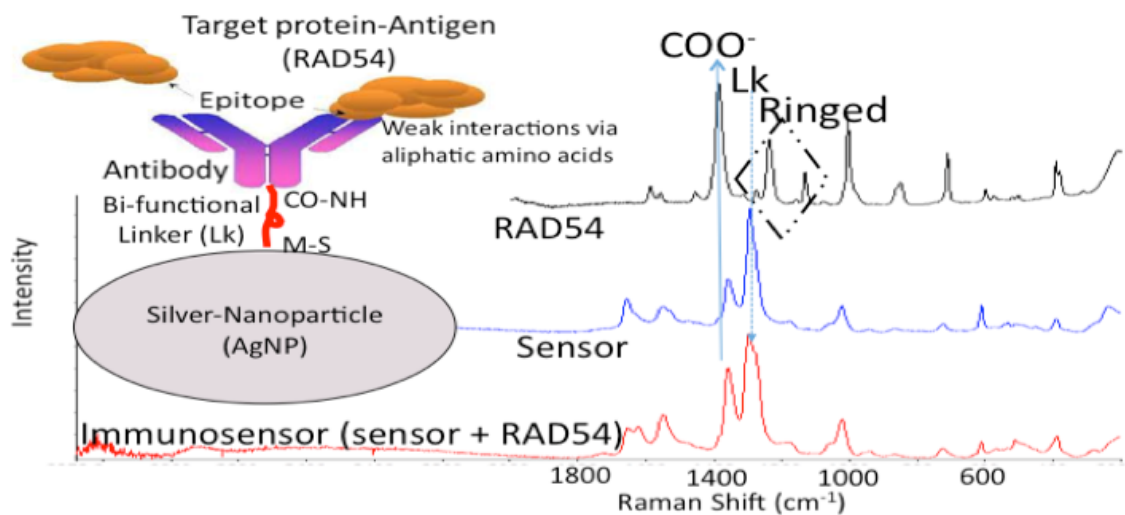


Fig. 19: Schematic representation of the SERS sensor (aka SLISA, left) and the characteristic SERS spectra (right). SLISA gives qualitative information on chemical conjugation of the sensor and the interaction of antigen with antibody (after Bhardwaj et al. 2015).

6.2 COMPARISON OF SENSING ATTRIBUTES, ELISA VS. SLISA

Label-free SLISA showed good correlation in accuracy with the traditional label-based ELISA assay for the extracellular detection of HSP70 and RAD54 expression to H₂O₂ and UV toxins (Fig. 20A and Fig. 20B). A several fold increase in the levels of RAD54 (~5x) and HSP70 (~8x) was observed in agreement with previous reports (Cole et al. 1987; Wang et al. 2012).

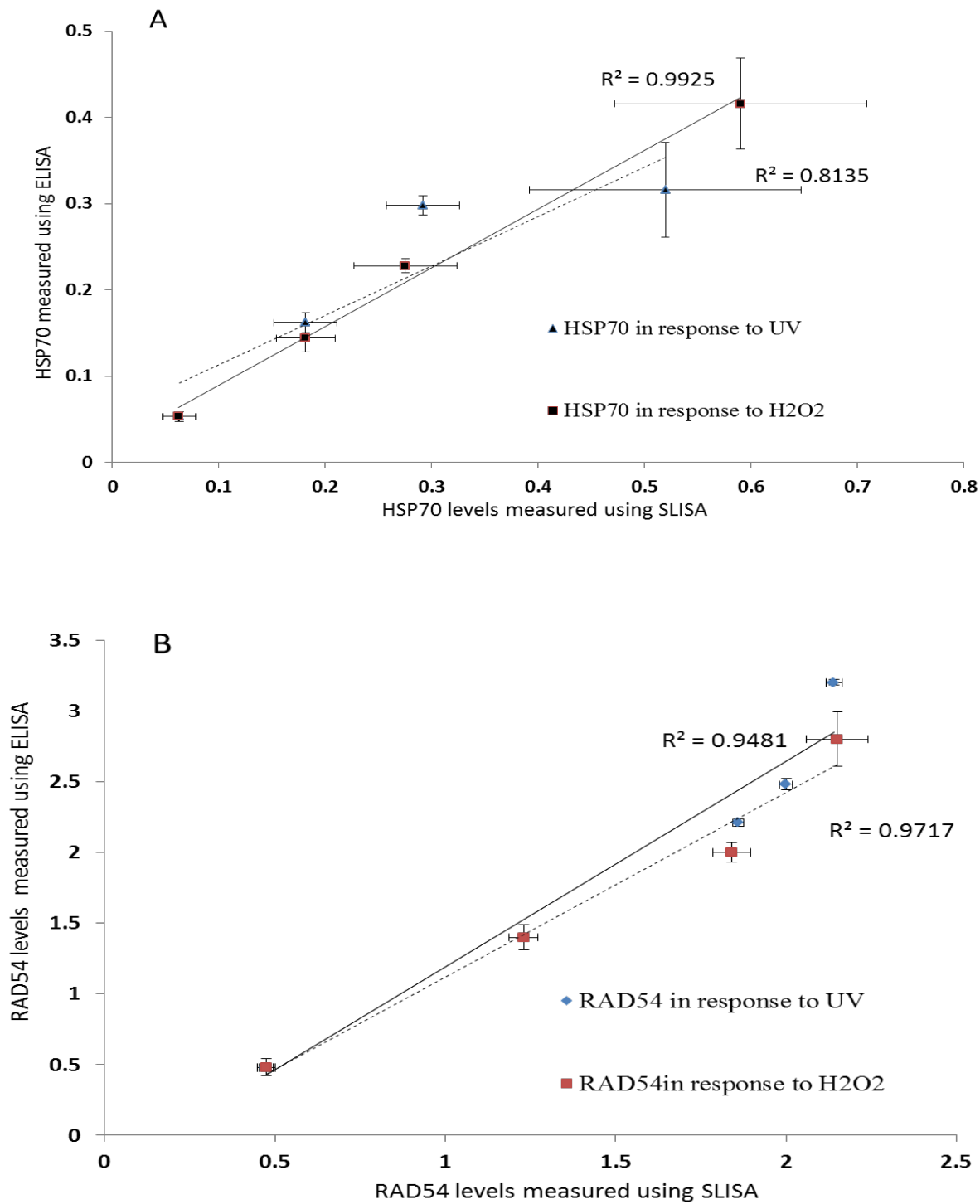


Fig. 20: Correspondence of SLISA with ELISA for the extracellular detection of stress proteins. Both techniques show good correlation (R^2) in the detection of proteins, HSP70 (A) and RAD54 (B), from yeast cells after UV and H₂O₂ exposure. SERS intensity (x10⁶)

is measured at 1390 cm^{-1} and the ELISA intensity is measured at 450 nm. The error bars represent SD of $n=3$ (after Bhardwaj et al. 2013).

SLISA and ELISA detect HSP70 at LOD 50 pg/ml and thus have the same sensitivity. However, SLISA was more sensitive than ELISA for RAD54 detection, 10 vs 50 pg/ml. The increased sensitivity of the SLISA for RAD54 detection is due to its higher Raman activity, possibly because of a stronger interaction of RAD54 with the SERS sensor compared to HSP70. RAD54 is a fairly large protein relative to HSP70 (84KD with 738 amino acids vs. 70 KD with 642 amino acids) with more repeated SERS active aromatic amino acids. Nonetheless, their low electron density renders them poor scattering molecules that are dependent on their adsorption or interaction with the sensor, which in turn depends on protein aggregation, surface charge, and the ionic species present in the suspension. Considering that no aggregating agent/ions were used in the study, the interaction is likely governed by surface charges on both the proteins and the SERS immunosensor. The RAD54 protein has a higher isoelectric point (pI) than HSP70, 8.85 vs 5.48. Hence, RAD54 appears to show high affinity towards the negatively charged colloidal SERS sensor that has pH 7-8. A similar effect of charge on the interaction of proteins to the Ag NPs is reported (Kahraman et al. 2010).

Although SLISA is simple and sensitive as compared to ELISA, the latter is more reproducible. The reproducibility of SLISA is particularly decreased with increasing protein concentration, as reported previously (Kahraman et al. 2010). SERS is an aggregation-based phenomenon that leads to an increase in optical scattering area. However, aggregation is a random process, hence, the decrease in SERS signals. The

reproducibility (< 20% deviation in SERS signal intensity), sensitivity (LOD \leq 0.05 ng/ml) and detection range (LRD 0.05-2.5 ng/ml) of the colloidal SERS sensor to measure proteins is comparable to that achieved by the more labor-intensive, time-consuming and costly lithography approach to array Au and Ag NPs on solid substrates (Malvaney et al. 2003; Lee et al. 2011). SERS assays technically fail to accurately quantitate proteins, which is a major inherent limitation of SERS immunoassay designs (He et al. 2011, Anal. Chem.). This may be due to the following two reasons. First, failure to effectively discriminate between Raman signals of antigen from antibody conjugated SERS substrate (background) at practically relevant pico-levels (He et al. 2011, J. Raman Spectrosc.). Second, antibody is a large protein molecule that leads to binding of antigen outside the zone of electromagnetic enhancement from the SERS substrate (He et al. 2011, Anal. Chem.). Therefore, the distance-dependent and aggregation-based nature of signal enhancement limits the SERS quantitation potential. Use of aptamers to replace the SERS immunosensor with an aptasensor to decrease the distance between SERS substrate and the antigen, as well as a different Raman signature of aptamer from antigen helps improve quantification by SERS (He et al. 2011, Chemical Sci.). Compared to several other Raman instruments, the PerkinElmer RamanStation 400F offers some technical advantages, including high power (100mW), which offers higher sensitivity. In addition, a large spot size (100 μ m) allows better averaging and reproducibility of signals analyzed from a large scanning area (Zheng et al. 2014). Further, scanning in mapping mode over conventional point focus further improves reproducibility (Lee et al. 2011).

SLISA offers direct detection of proteins based on the chemical signatures characteristic of specific proteins. However, because ELISA employs an indirect approach of detection

employing label-conjugated analytes, there is an increased chance of interference. Additionally, SLISA is rapid and simple, allowing measurement of proteins in two hours and requires no mandatory washing, secondary antibody binding, enzyme-substrate reaction, additional reagents and expense, characteristics of ELISA. Most noteworthy, SLISA gives qualitative information on SERS immunosensor's fabrication, stability and antigen-antibody binding, which ELISA fails to do without the addition of western blotting. In short, SLISA outperforms the traditional ELISA assay in allowing RISE detection (Table 3). The RISE properties of SLISA allow its applications in resource-limited settings.

Table 3: Performance comparison (RISE): ELISA vs. SLISA

	Rapid	Inexpensive	Simple	Effective		
	<u>Time (hrs.)</u>	<u>Well-plate</u>	<u>Reagents</u>	<u>#Steps</u>	<u>Qualitative</u>	<u>Quantitative</u>
ELISA	≥ 6	Not reusable Wells pre-coated with antibodies	Primary & secondary Ab Enzyme, Substrate & Label #1 each	≥ 7 Several washings	Label-Based Indirect Detection	LOD: 50 pg/ml R ² : 0.99
SLISA	≤ 2	Reusable	Primary MAb No need of Enzyme, Substrate & Label	≤ 3 No Washing	Label-Free Direct Detection	LOD: 10 pg/ml R ² : 0.97

6.3 SUMMARY

The SLISA is able to quantify induced levels of RAD54 and HSP70 expression in response to toxins. The SLISA has good correspondence with ELISA in extracellular detection of proteins. Most noteworthy, SLISA has an edge over ELISA by allowing label-free detection and giving qualitative information on immunosensing. Additionally, SLISA

allows RISE detection as compared to ELISA and hence it has potential for applications in resource-limited settings.

REFERENCES

Bhardwaj V., Srinivasan S., et al. (2013). AgNPs-based label-free colloidal SERS nanosensor for the rapid and sensitive detection of stress proteins expressed in response to environmental toxins. *Biosens. Bioelectron.*, 4(5): pages 1-7

Bhardwaj V., Srinivasan S., et al. (2015). On-chip surface-enhanced Raman spectroscopy (SERS)-linked immunosensor assay (SLISA) for rapid environmental surveillance of chemical toxins. *Proc. SPIE 9486*, Pages 8

Cole G. M., Schild D., et al. (1987). Regulation of RAD54- and RAD54-lacZ gene fusions in *Saccharomyces cerevisiae* in response to DNA damage. *Mol. Cell Biol.*, 7: 1078-1084

He L., Rodda T., et al. (2011). Detection of a foreign protein in milk using surface-enhanced Raman spectroscopy coupled with antibody-modified silver dendrites. *Anal. Chem.*, 83: 1510-1513

He L., Haynes C. L., et al. (2011). Rapid detection of a foreign protein in milk using IMS – SERS. *J. Raman Spectrosc.*, 42: 1428-1434

He L., Lamont E., et al. (2011). Aptamer-based surface-enhanced Raman spectroscopy detection of ricin in liquid food. *Chemical Sci.*, 2: 1579-1582

Kahraman M., Sur I., et al. (2010). Label-free detection of proteins from self-assembled protein-silver nanoparticle structures using surface-enhanced Raman scattering. *Anal. Chem.*, 82: 7596-7602

Lee M., Lee S., et al. (2011). Highly reproducible immunoassay of cancer markers on a gold-patterned microarray chip using surface-enhanced Raman scattering imaging. *Biosens. Bioelectron.*, 26: 2135-2141.

Malvaney S. P., He L., et al. (2003). Three-layer substrates for SERS: preparation and preliminary evaluation. *J. Raman Spectrosc.*, 34: 163-171

Wang. Y., Gibney P. A., et al. (2012). The yeast Hsp70 Ssa1 is a sensor for activation of the heat shock response by thiol-reactive compounds. *Mol. Biol. Cell*, 23: 3290-3298

Zheng J., Pang S., et al. (2014). Evaluation of surface-enhanced Raman scattering detection using a handheld and a benchtop Raman spectrometer: a comparative study. *Talanta*, 129: 79-85.

CHAPTER 7 INTRACELLULAR DELIVERY AND DETECTION OF PROTEINS USING SERS SENSOR AKA CBB-SIST

The purpose of this chapter is to describe a method for the efficient delivery of colloidal Ag NPs into yeast cells and to describe the development of the first CBB-SIST, consistent with specific aim #4 described in Chapter 2. For intracellular detection of proteins, $\sim 5 \times 10^4$ protein molecules in yeast, roughly 4000 60-nm SERS sensor molecules are required. The nanoparticles should display a uniform intracellular distribution with no significant cytotoxicity. Three intracellular delivery strategies were investigated to achieve the goal, passive and TATHA2-facilitated diffusion, and electroporation. TATHA2 is a fusogenic peptide, which allows rapid and high uptake of NPs across cell membrane/s via macropinocytosis, without any endosomal entrapment and cytotoxicity (Wadia et al. 2004; Ye et al. 2012). Additional emphasis was placed on the development of a high throughput and portable CBB-SIST. This work has been published as a communication research article in the journal *Analyst* (Bhardwaj et al. 2015). Written permission (e-mail) to use the content of this publication in my dissertation has been obtained from the editor of the journal and a copy of the e-mail is incorporated in the appendix IV.

Materials and methods for this specific aim #4 are discussed in chapter III, section 3.4.

7.1 CELLULAR TOXICITY

A Bio RAD MicroPulser Electroporation Apparatus was used to test electric field strength, $E = 0.875$ kV/cm, optimized for rapid intracellular delivery of Ag NPs for SERS detection without any significant cytotoxicity (Yu et al. 2011). However, severe physical damage (Fig. 21) and toxicity to yeast was observed even at lowest electroporation dose, $E = 0.5$ kV/cm for single pulse of 1 ms, inconsistent with previous observation in animal cells (Yu

et al. 2011). Results suggest that electroporation of yeast cells to deliver plasmonic metal NPs are not a suitable strategy for intracellular SERS immunosensing.

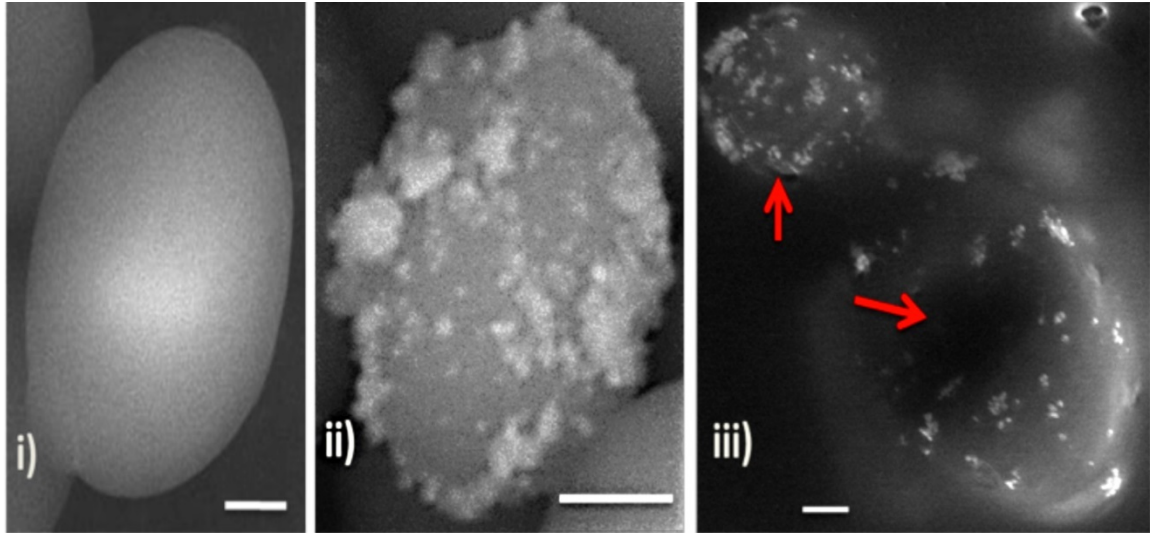


Fig. 21: Damaging effect of electroporation shown by SEM. i): cell with no AgNPs, but electroporation ii): cells with Ag NPs, but no electroporation and iii): cells with Ag NPs as well as after electroporation, cell damage indicated by arrows (after Bhardwaj et al. 2015).

The damaging effect of electroporation to cells in the presence of Ag NPs could be attributed to heat generation, a characteristic phenomenon of metal NPs in the presence of electric field/laser (Govorov et al. 2007). The accelerating voltage of 200 kV from TEM lead to Ag NPs melting, changing shape or vaporization (Fig. 22), consistent with previous reports (Takami et al. 1999).

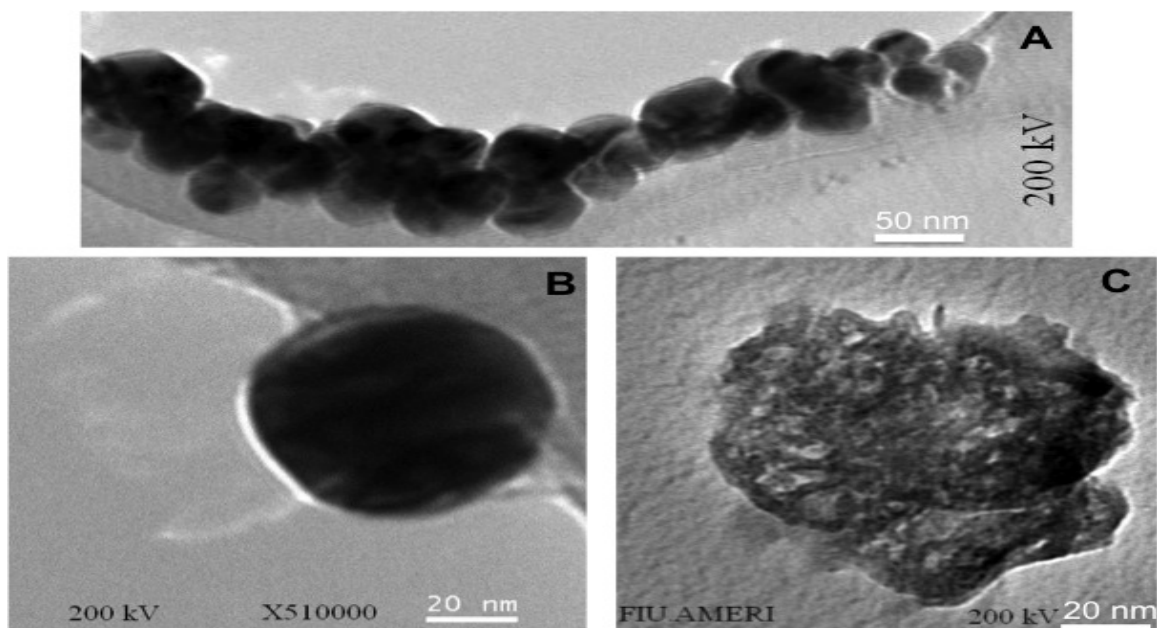


Fig. 22: Ag NPs vaporization (A & B) and shape change (C) on exposure to 200 kV in TEM.

The use of Ag NPs for passive diffusion and TATHA2-functionalized Ag NPs for facilitated diffusion, both induced dose- and time-dependent growth inhibition. At 1 and 10 ppm for up to 12 hr Ag NPs exhibited cell mortality of <5% and 15%, respectively. At the highest dose, 100 ppm for 12 hours, the Ag NPs exhibited < 30% cell mortality and Ag^+ resulted in almost 100% mortality (Fig. 23). Sixty-nm chitosan NPs were used as a negative control in the cytotoxicity study, as the chitosan polymer is considered non-toxic and safe for applications in drug delivery. The suspending solution was non-toxic. Among silver-treated groups, Ag^+ was used as a positive control and showed a significant difference ($P < 0.05$) in cell mortality, but no significant difference ($P > 0.05$) was observed between the cells exposed to bare (BR-) Ag NPs vs TATHA2-functionalized Ag NPs. A similar lack of toxicity of Ag NP in microbial cells has been reported (Xiu et al. 2012) by using a coating of thiol-PEG around Ag NPs to block Ag^+ dissolution.

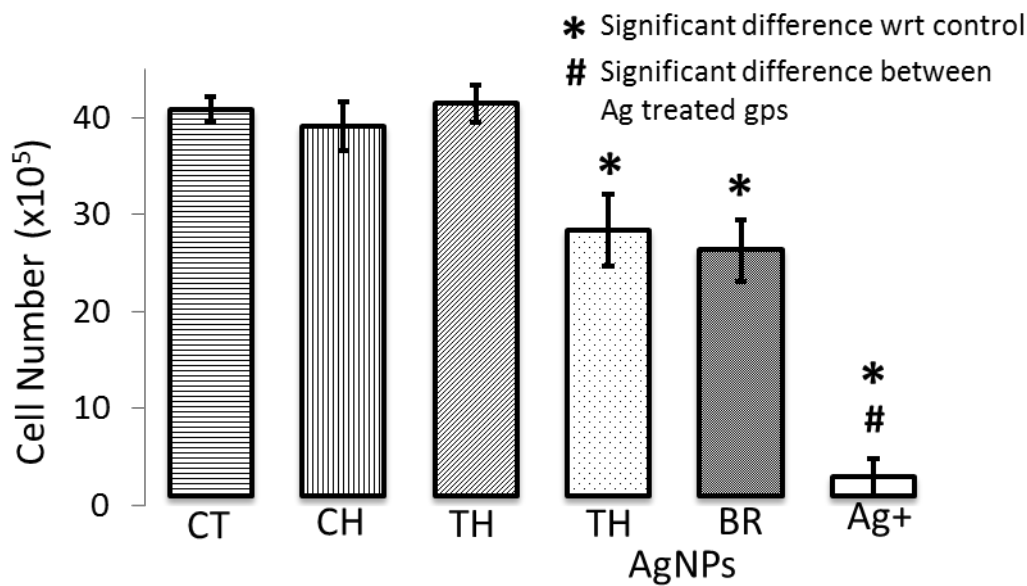


Fig. 23: The growth inhibition effect of Ag. The growth inhibition (toxicity) of non-functionalized or bare- (BR-) and TATHA2- (TH-) functionalized Ag NPs as compared to control (CT), chitosan (CH), TH and Ag⁺. Significant difference is P<0.05 (after Bhardwaj et al. 2015).

In agreement with previous reports on Ag NP toxicity, two major points can be deduced. First, the dissolution of Ag NPs to Ag⁺ is the major cause of toxicity (Xiu et al. 2012). Second, the degree of cell uptake of Ag NPs (bioavailable dose) influences the Ag NPs cell toxicity (Yen et al. 2009). The significant difference in bioavailability of Ag NPs delivered via passive and facilitated diffusion is definitely another critical factor controlling toxicity, as discussed in the next section.

7.2 CELLULAR UPTAKE

The cell uptake (adsorption + internalization) of Ag NPs into yeast was studied following a mild 5 min I₂/KI etching procedure, reported previously (Cho et al. 2010). This process effectively removed the Ag NPs from the yeast surface (Fig. 24).

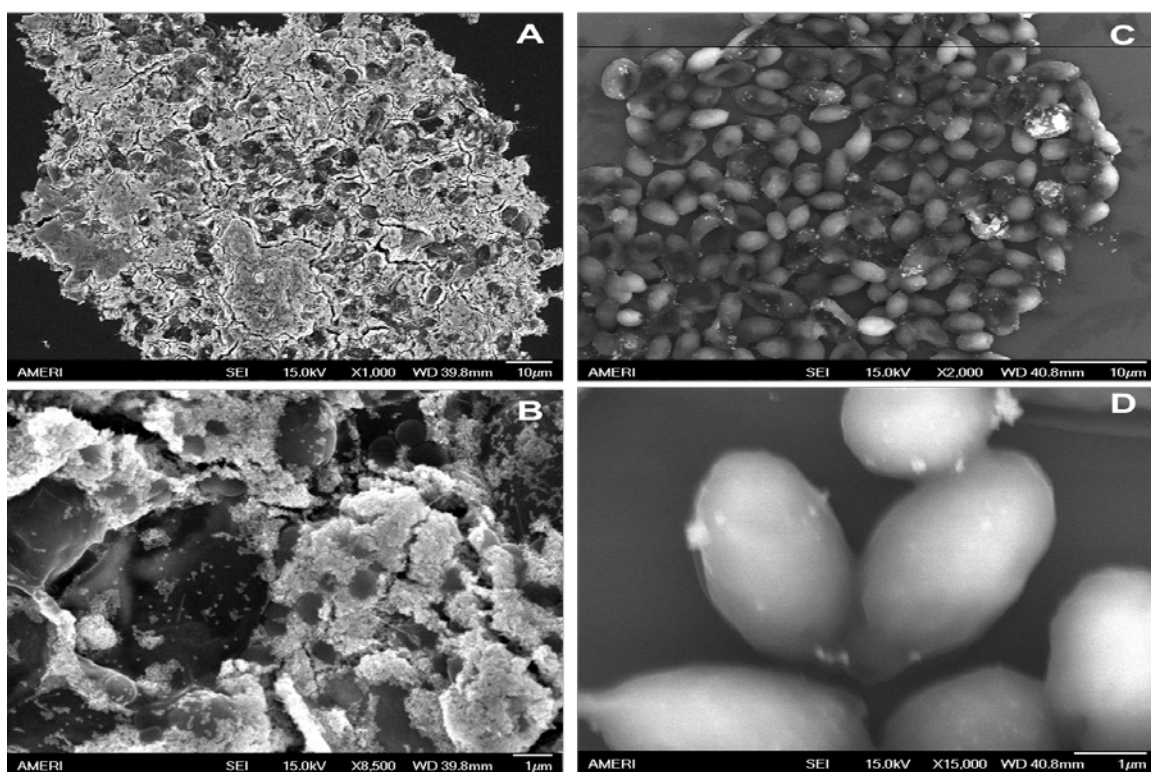


Fig. 24: SEM images of yeast cells before and after I₂/KI etching. A and B are cell masses, though not clearly visible due to their complete coverage by Ag NPs. C and D have been etched using I₂/KI solution, a process that removes the Ag NPs and reveals the cell surfaces (after Bhardwaj et al. 2015).

TATHA2 facilitated delivery resulted in rapid (within 3 hours) and high internalization (~15 fold, > 4000 Ag NPs per cell) of TATHA2-Ag NPs compared to bare-Ag NPs (Fig. 25). A several fold difference in internalization of Ag NPs by the two strategies seems to be due to the difference in endocytic pathways. TATHA2-mediated delivery is due to macropinocytosis, a rapid receptor-independent form of endocytosis in which the transport vesicle is composed of membrane-lipid drafts (Wadia et al. 2004; Ye et al. 2012). This is in contrast to the relatively slow, receptor-mediated endocytosis, which is typical of inward budding of plasma membrane vesicles that contain proteins and specific receptors. The charge-driven cellular uptake of NPs, for example, is controlled by this receptor-mediated process (Chithrani et al. 2006; Zhu et al. 2008; Cho et al. 2010; Yen et al. 2009).

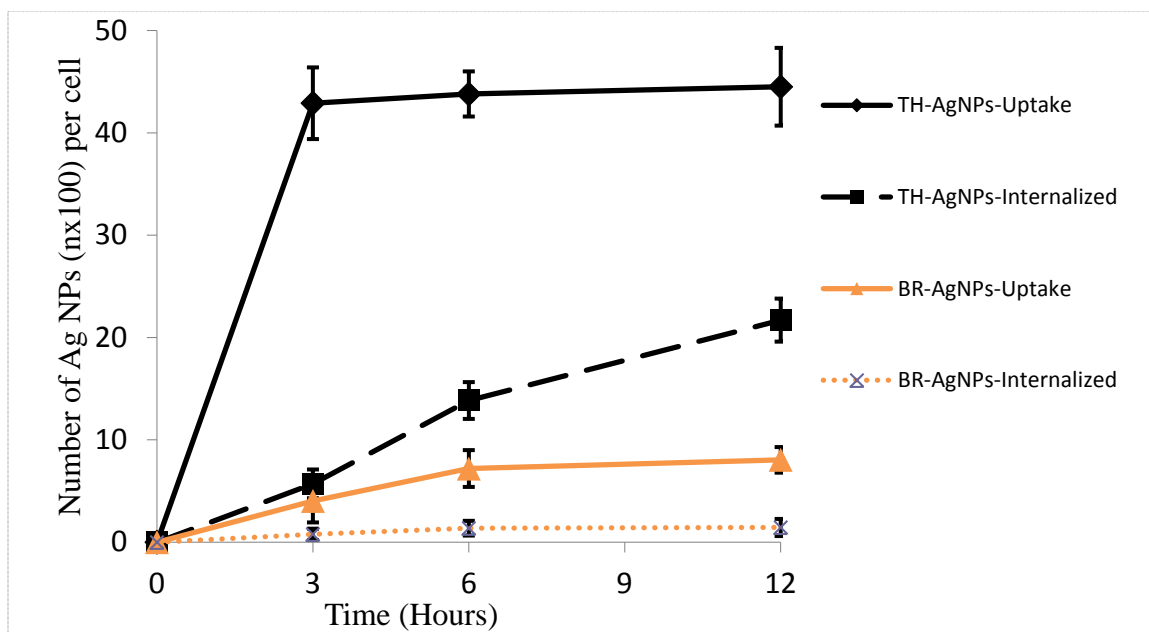


Fig. 25: Kinetics of Ag NPs uptake in yeast via passive and TATHA2-facilitated diffusion. Ag NPs are quantified using ICP-MS. Total uptake is adsorption + internalization. BR: bare and TH: TATHA2-functionalized. Significant increase in number of Ag NPs cell uptake is observed upto 12 hours in TH-Ag NPs-internalized group, while other groups show Ag NPs uptake saturation in 3-6 hours (after Bhardwaj et al. 2015).

Passively diffusing Ag NPs reach internal saturation by 6 hours, while TATHA2-Ag NPs show significant increases even at 12 hours (Fig. 26). The rapid and preferentially uniform intracellular distribution of TATHA2-Ag NPs, (i.e., no compartmentalization), was observed within 3 hours (Fig. 26, A). However, the bare-Ag NPs were primarily found adsorbed to the cell surface, with little/no internalization. Where the passively diffusing bare-Ag NPs were internalized, they were entrapped in endosomes and failed to become uniformly distributed (Fig. 26, B).

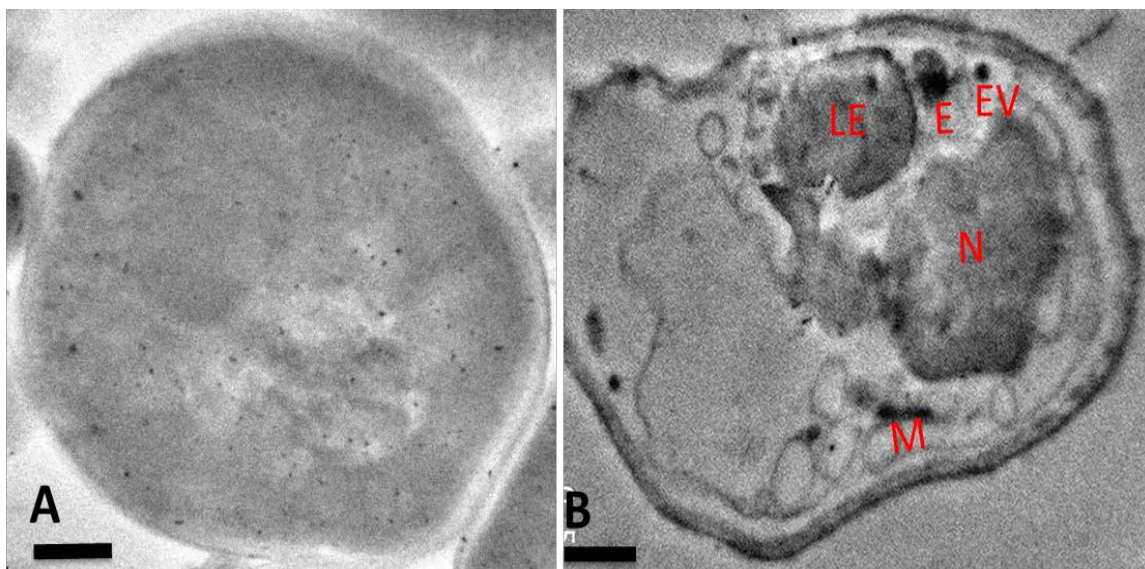


Fig. 26: *In situ* TEM images to observe intracellular distribution of Ag NPs into yeast after surface etching. Ag NPs are observed after 3 hours of TATHA2-facilitated diffusion (A) and 12 hours of passive diffusion (B). AgNPs aggregates appear as dark spots. Endocytic pathway: Endocytic Vesicle (EV), Endosome (E) and Late Endosome (LE); Nucleus (N) and Mitochondrion (M). Scale bar is 0.5 μm (after Bhardwaj et al. 2015).

The high cellular uptake/internalization of Ag NPs by TATHA2-mediated diffusion over passive diffusion exposes the cells to a much higher dose of Ag NPs (~ 15 fold difference in bioavailable dose). The degree of Au and Ag NPs uptake, the bioavailable dose, directly impacts the cell toxicity (Yen et al. 2009). Therefore, TATHA2-facilitated strategy was selected for the efficient delivery of Ag NPs for the intracellular SERS detection of proteins.

7.3 INTRACELLULAR DETECTION

Development of the CBB-SIST requires stability and reproducibility of the sensor and its intracellular signals. The SERS sensor developed by delivering Ag NPs using the TATHA2 peptides was stable for at least 3 hours (Fig. 27), which is the time required to deliver \geq 4000 sensor molecules into yeast towards detection of RAD54 and HSP70 proteins.

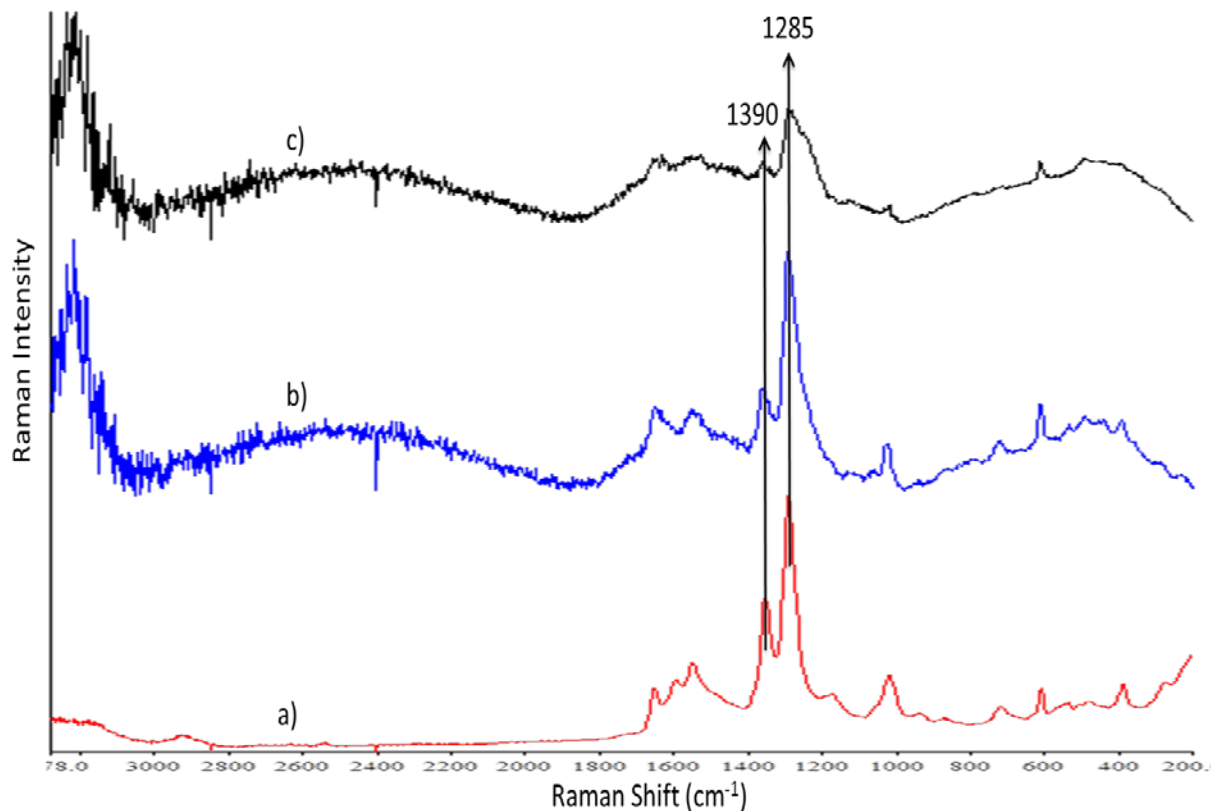


Fig. 27: Stability of RAD54 SERS sensor. The SERS sensor, functionalized with targeting and delivery peptides, after 3 hours (a) 6 hours (b) and 12 hours (c). Stability of sensor decreases with time, as indicated by decrease in peaks characteristics to MMT linker at 1285 cm^{-1} and carboxylic group of proteins at 1390 cm^{-1} .

The intense and distinct peaks characteristic to the MMT linker at $\sim 1285\text{ cm}^{-1}$ and protein's carboxylic group at $\sim 1390\text{ cm}^{-1}$ indicate stability of the SERS sensor. The decrease in characteristic peaks over time indicates a decrease in stability of the sensor. The stability of the AgNP-Lk-MAb conjugate is evident from the metal-sulphur bond between Ag NP and MMT in range of $400\text{-}600\text{ cm}^{-1}$, and the peptide bond between MMT and MAb ranging from $1500\text{-}1700\text{ cm}^{-1}$.

Although the SERS sensor with targeting and delivery peptides was stable and generated reproducible extracellular signals, no reproducible signals were obtained intracellularly

from CBB-SIST (Fig. 28). Reproducibility of intracellular signals from the sensor is critical towards development of a CBB-SIST. The chemical fingerprint of the sensor is qualitatively almost similar to the protein of interest, in this case RAD54 and HSP70 (Fig. 19). The only reliable basis to measure proteins intracellularly is to accurately quantitate the difference in Raman intensities of the SERS sensor (background) and the proteins.

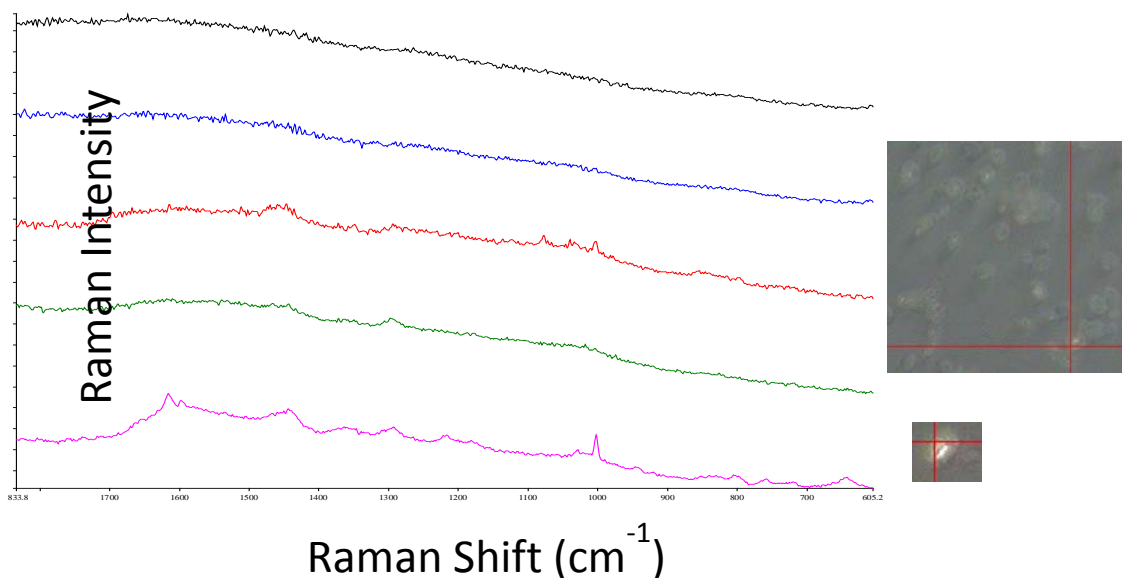


Fig. 28: Raman spectra of the CBB-SIST. CBB-SIST are the yeast cells internalizing SERS sensors functionalized with targeting and delivery peptides. Intersecting lines in images on right show point of focus where the Raman spectro-microscope laser was focused (50x objective, laser spot size 20 μm and depth of focus 40 μm). The laser was focussed on aggregates of the sensor molecules, visible under the microscope. Signal generation was negligible and irreproducible.

Direct analysis of peak intensities as well as chemometrics failed to discriminate analyte signals from background.

7.4 SUMMARY

A SERS sensor was delivered efficiently and uniformly into yeast cells with > 4000 sensor

molecules in 3 hours without any significant toxicity. All of these characteristics and are pre-requisites for the development of the first CBB-SIST. The sensor was stable for at least 3 hours and produced strong and reproducible Raman signals extracellularly. However, signal generation and reproducibility was not achievable inside the cell. Direct analysis as well as chemometrics completely failed to discriminate analyte signals from background. Development of the proposed first portable and high throughput CBB-SIST will require overcoming these obstacles. The discussion section gives detail on the possible changes in the technical design of the sensor to develop first CBB-SIST.

REFERENCES

- Bhardwaj V., Srinivasan S., et al. (2015). Efficient intracellular delivery and improved biocompatibility of colloidal silver nanoparticles towards intracellular SERS immunosensing. *Analyst*, 140: 3929-3934
- Chithrani B. D., Ghazani A. A., et al. (2006). Determining the size and shape dependence of gold nanoparticle uptake into mammalian cells. *Nano Lett.*, 6(4): 662-668
- Cho E. C., Au L. et al. (2010). The effects of size, shape, and surface functional group of gold nanostructures on their adsorption and internalization by cells. *Small*, 6(4): 517-522
- Govorov A. O., Richardson H. H. (2007). Generating heat with metal nanoparticles. *Nano Lett.*, 2(1): 30-38
- Takami A., Kurita H., et al. (1999). Laser-induced size reduction of noble metal particles. *J. Phys. Chem. B.*, 103(8): 1226-1232
- Wadia J. S., Stan R. V., et al. (2004). Transducible TAT-HA fusogenic peptide enhances escape of TAT-fusion proteins after lipid raft macropinocytosis. *Nat. Med.*, 10(3): 310-315
- Xiu Z. M., Zhang Q-bo, et al. (2012). Negligible particle-specific antibacterial activity of silver nanoparticles. *Nano Lett.*, 12(8): 4271-4275
- Ye S. F., Tian M. M., et al. (2012). Synergistic effect of cell-penetrating peptide Tat and fusogenic peptide HA2-enhanced cellular internalization and gene transduction of organosilica nanoparticles. *Nanomedicine*, 8(6): 833-841
- Yen H. J., Hsu H. S., et al. (2009). Cytotoxicity and immunological response of gold and

silver nanoparticles of different sizes. *Small*, 5(13): 1553-1561

Yu Y., Lin J., et al. (2011). Optimizing electroporation assisted silver nanoparticle delivery into living C666 cells for surface-enhanced Raman spectroscopy. *Spectroscopy*, 25(1): 13-21

Yu Y., Lin J., et al. (2011). Improved electroporation parameters of delivering silver nanoparticles into living C666 cells for surface-enhanced Raman scattering. *J. Phys. Conf. Ser.* 277, pages 5

Zhu Z. J., Ghosh P. S., et al. (2008). Multiplexed screening of cellular uptake of gold nanoparticles using laser desorption/ionization mass spectrometry. *J. Am. Chem. Soc.*, 130(43): 14139-14143

CHAPTER 8 A CASE STUDY: ON-CHIP SLISA

The purpose of this chapter is to describe the development of a portable on-chip SLISA prototype and translate its application to the environmental surveillance of chemical toxins, known as well as unknown. The H₂O₂/RAD54 dose-response relationship is correlated to the EPA's three-tiered scheme of exposure to dangerous chemicals (IDLHs) to signify applications of the on-chip SLISA in resource-limited settings. This work has been published as a full-length research article in SPIE DSS proceedings (Bhardwaj et al. 2015). My on-chip SLISA prototype invention is also under patent submission by the FIU Technology Management and Commercialization. Written permission (e-mail) to use this publication and patent content in my dissertation has been obtained from the journal editor and from the licensing manager of FIU Technology Management and Commercialization. Copies of the e-mails are incorporated in the appendix IV.

Materials and methods for this specific aim #5 are discussed in chapter III, section 3.5.

8.1 FABRICATION OF A PROTOTYPE MICROCHIP

The SERS microchip design is robust, small, ergonomic and/or offers technical advantages over current designs (Fig. 29). For example, portable microfluidic SERS chip designs are expensive and complex, as they require separate loading, mixing and detection zones (Quang et al. 2008). Paper-based anSERS designs by contrast are simple and inexpensive, but can only be used once (Diagnostic anSERS, Inc. USA, Yu et al. 2013). Additionally, almost all commercial plates or microchips used for ELISA and SERS detection are manufactured using polystyrene or polypropylene, which are inexpensive but have high Raman background signals.

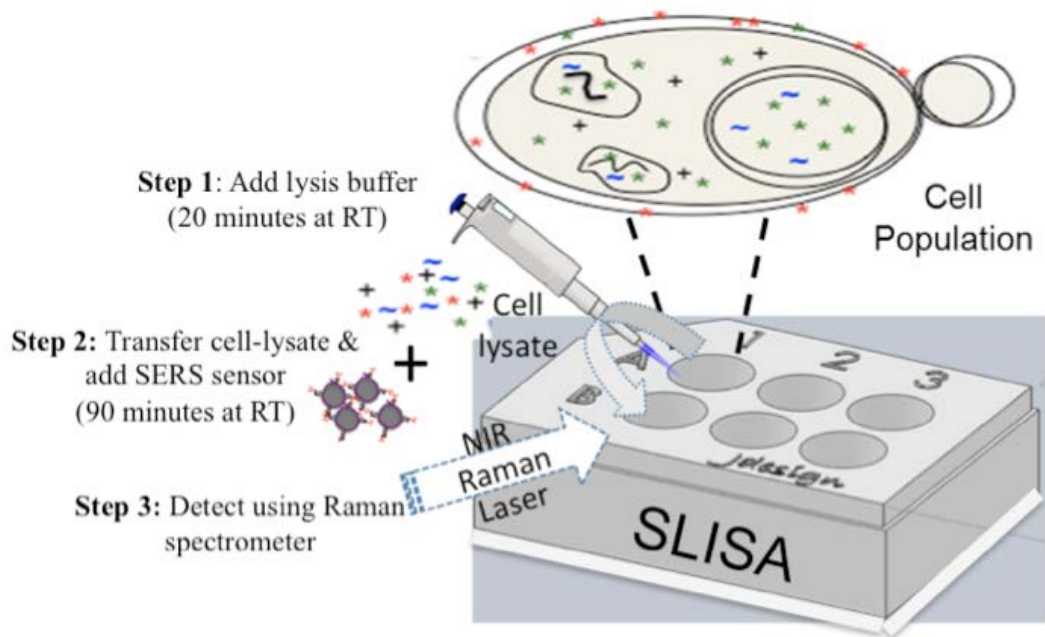


Fig. 29: Schematic of on-chip SLISA. A six-well glass-bottom reusable microchip (dimensions LxWxH is 30.5x25.5x1 mm) that offers RISE detection of proteins in just 3-steps and 2 hours (after Bhardwaj et al. 2015).

Glass has a negligible Raman signal and therefore it is a better choice to fabricate plates for RS/SERS applications (Marz et al. 2011). However, glass is expensive as compared to the aforementioned polymers and complicates the fabrication of the plate. Instead of using a whole-glass SERS chip design (Marz et al. 2011), a glass-bottom fabrication approach is economical as well as technically sound, as the Raman laser focuses on the bottom of the plate. A Commercial 8-well chip fabricated by Applied BioPhysics Inc., USA uses a somewhat similar design, microscope slide to mount plexiglass wells. However, the edges of glass slides protruding from corners of the chip are not safe and robust to handle and

transport. Additionally, the BioPhysics chip is specific for adherent mammalian cells and ECIS applications. The on-chip six-well microchip design (Fig. 28) is inspired from a PerkinElmer glass-bottom 96 well-plate (poly-D-lysine coated glass-bottom, Cat#6005530) that was used for high throughput screening in specific aims, and the BioPhysics 8-well chip design.

8.2 A CASE STUDY

Applications of SLISA for first responders in resource-limited settings were demonstrated using a six-well glass-bottom microchip (Fig. 29). H_2O_2 and RAD54 were chosen as model toxin and stress protein, respectively for the case study. H_2O_2 is a chemical toxin on the EPA's priority list and was a better choice over UV toxin, as it is a chemical toxin and a simulant of TICs and CWAs. Three levels of dangerous H_2O_2 concentrations have been examined, but not yet clearly defined by the EPA and ATSDR. The first tier is ≤ 75 ppm and is defined as tolerable, with transient health effects. The second tier of ≤ 1000 ppm has long-lasting, disabling effect, while third tier is > 1000 ppm and is life-threatening (Fig. 30). Doses up to 5000 ppm dose of H_2O_2 have been reported to be tolerated by organisms, therefore the tier II dose might be revised in the near future.

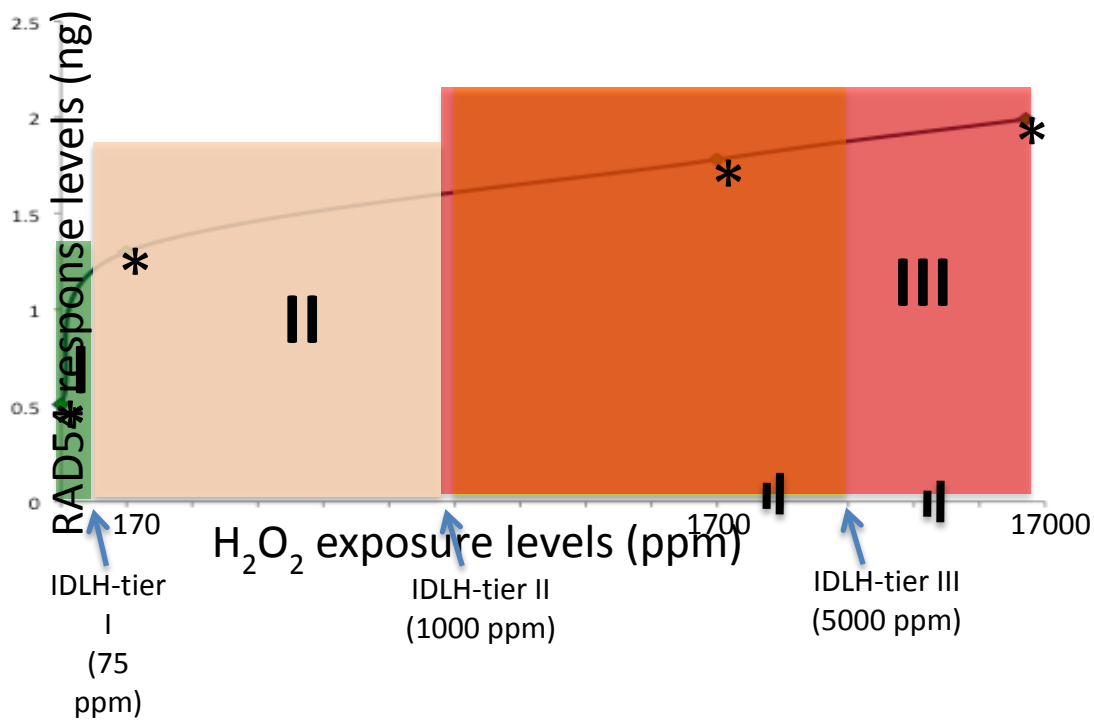


Fig. 30: Translation of dose-response relationship to assess environmental risk of toxins. The H₂O₂-RAD54 dose-response curve is translated to three-tiered guideline levels, IDLHs, defined by EPA-ATSDR-CDC. The color code indicates the severity of health effects, guided by levels of RAD54 proteins expressed in response to H₂O₂ toxin. The asterisks represent the levels of RAD54 expressed in response to H₂O₂ (after Bhardwaj et al. 2015).

Stereotypically, on-chip SLISA can be a potential global biosensor for pre-regulatory or primary screening of toxins, as its H₂O₂-RAD54 dose-response relationship curve can be used to translate the information from diverse classes of toxins, known as well as unknown (Cahill et al. 2000 and Gasch et al. 2000). A comprehensive screening validation program, which successfully assessed a yeast-based GreenScreen Assay to study expression of RAD54 in response to 102 environmental toxins, support a wide market of on-chip SLISA developed in this project (Cahill et al. 2000). Yet another federally-funded genomic expression program explored ~ 900 genes involved in the environmental stress responses of

yeast to diverse environmental toxins (Gasch et al. 2000). Please note, on-chip SLISA to measure RAD54 might not be a good choice to monitor stress conditions including non-genotoxic oxidative stress, reductive stress, heat, osmotic shock and amino acids starvation, as RAD54 does not show reciprocal response to these environmental stressors (Gasch et al. 2000). Measurement of HSP70 in response to these stress conditions could help overcome this limitation.

A critical consideration when establishing dose-response curves for environmental risk characterization is that the response of proteins to the toxins is assumed to be monotonic, i.e., increasing dose of stress toxins increases the stress proteins. However, the latest findings of non-monotonic dose-response (NMDR) curves has implications for environmental screening/surveillance and risk characterization, which is based on the EPA's monotonic model using a slope factor to characterize environmental risk (Savitz 2014). A more detailed study is required to develop a robust and stable monotonic dose-response curve for decision making to avoid NMDR or extrapolating information by developing correct quantitative models from NMDR curves (Savitz 2014). The multi-phasic response of NSMase to H₂O₂ observed in this study (data not reported) is an example of an NMDR curve, which was the reason for not using the NSMase stress marker protein in this study (Jaffrezou et al. 1998). Development of a robust and reproducible dose-response relationship will require a comprehensive study to investigate a wide range of doses, primarily in the lower range if the aim is to quantitate, and determine kinetics. Undoubtedly, yeast is an excellent choice of human surrogate for the proposed environmental application, to achieve portability and long shelf-life compared to a mammalian cell-based-biosensor technology (Baronian 2004). However, it is apparent that differences in chemical-specific

and organism-specific dose-response curves will exhibit discordance when translating the data to untested toxins and organisms, such as from yeast to human as in this application (Cahill et al. 2004).

8.3 SUMMARY

The SLISA demonstration discussed in chapter 5 was translated to a proof-of-concept portable technology using a six-well microchip. The microchip design is simple, small, robust, inexpensive and reusable as compared to current ELISA, SERS and many other plate designs. The on-chip SLISA requires a three-step assay, which can measure proteins within 2 hours. The H₂O₂-RAD54 dose-response relationship was translated to the EPA's three-tiered scheme of toxin guidance levels to potentially help first responders and minimize human health-risks in event of suspected environmental contamination.

REFERENCES

- Baronian K. H. (2004). The use of yeast and moulds as sensing elements in biosensors. *Biosens. Bioelectron.*, 19(9): 953-964
- Bhardwaj V., Srinivasan S., et al. (2015). On-chip surface-enhanced Raman spectroscopy (SERS)-linked immunosensor assay (SLISA) for rapid environmental surveillance of chemical toxins. *Proc. SPIE* 9486, pages 8
- Cahill P.A., Knight A. W., et al. (2004). The GrenScreen Genotoxicity Assay: A screening validation programme. *Mutagenesis*, 19(2): 105-119
- Gasch A. P., Spellman P. T., et al. (2000). Genomic expression programs in the response of yeast cells to environmental changes. *Mol. Biol. Cell*, 11: 42541-4257
- Jaffrezou J. P., Maestre N., De mas-mansat V. et al. (1998). Positive feedback control of neutral sphingomyelinase activity by ceramide. *FASEB*, 12(11): 999-1006
- Marz A., Bocklitz T., et al. (2011). Online calibration for reliable and robust lab-on-a-chip surface-enhanced Raman spectroscopy measurement in a liquid/liquid-segmented flow.

Anal. Chem., 83: 8337-8340

Quang L. X., Lim C., et al. (2008). A portable surface-enhanced Raman scattering sensor integrated with a lab-on-a-chip for field analysis. *Lab on a chip*, 8: 2214-2219

Savitz D. A. (2014). Review of the Environmental protection Agency's state-of-the-science evaluation of nonmonotonic dose-response relationships as they apply to endocrine disruptors. *National Academy of Sciences*, pp 64

Yu W. W., White I. M. (2013). Inkjet-printed paper-based SERS dipsticks and swabs for trace chemical detection. *Analyst*, 13: 1020-1025

SUMMARY AND FUTURE WORK

The on-chip SLISA developed in this project is primarily designed for environmental surveillance of toxins. The project represents a rapid and simple proof-of-concept yes/no detection model, and a semi-quantification of very specific proteins generated in response to model toxins. SLISA is capable of the qualitative and semi-quantitative detection required for primary screening to characterize environmental risk.

The SLISA is developed using Ag NP colloids that offer several fold SERS enhancement factor (~ 250x greater than Au NPs), which enable sensitive detection of proteins at pico levels. As compared to the competing industry-standard ELISA technology, SLISA allows the RISE detection of proteins without using any label and also provides qualitative information on the immunosensing, such as fabrication, stability and antigen-antibody interaction. However, ELISA is more reproducible than SLISA, probably because SLISA is an aggregation-based technique. Although lithography to control inter-particle distance between sensor molecules can improve SERS reproducibility (Lin et al. 2009; Lee et al. 2011), lithographed substrates cannot be used for intracellular immunosensing, as the delivery will be invasive and damaging. Colloidal substrates are flexible and capable of penetrating cell membranes without damaging cell. TATHA2-facilitated delivery of colloidal Ag NPs offer efficient intracellular uptake into yeast over passive diffusion and electroporation strategies. TATHA2-facilitated delivery is rapid, and allows high and largely uniform cell uptake of Ag NPs without any significant cytotoxicity. Although the SERS sensor was stable and was successfully delivered into cells, it failed to detect intracellular signals from sensor and the development of the proposed first CBB-SIST was

not achieved.

SLISA was demonstrated on a microchip (on-chip SLISA) for portability and ease-of-use, pre-requisites for applications in resource-limited settings. Additionally, the H₂O₂-RAD54 dose-response relationships were correlated to the three-tiered levels of toxicity established by the EPA, CDC and ATSDR. As a critical consideration, the biomarkers' response to toxins is assumed to be monotonic, i.e., increasing dose of stress toxins increases the amount stress proteins. The EPA's guideline levels are based on a monotonic model to derive a slope factor towards characterizing environmental risk. However, the latest findings of non-monotonic dose-response (NMDR) curves have implications for environmental screening/surveillance and risk characterization (Savitz 2014). A more detailed study is required to develop a robust and stable monotonic dose-response curve needed for making decision.

Use of yeast as sensor organism in the SLISA design confers portability and robustness to the CBB compared to the mammalian CBB designs (Baronian 2004; Banerjee et al. 2009). In the future, SLISA can easily be translated to a portable biomedical and environmental sensor technology using an on-chip SLISA design and a portable handheld point-and-shoot Raman spectrometer (Zheng et al. 2014). However, the SLISA developed in this study needs further optimization and a change in technical design from immunosensor to aptasensor to be capable of quantifying proteins with high accuracy, which is a major requirement in biomedical diagnostic assays, may be needed. SLISA and CBB-SIST cannot replace the industry-standard ELISA and cytogenetics for comprehensive screening and quantitation of proteomic and genomic biomarkers in organisms responding to stress toxins.

An antibody-based SERS design is likely not the best choice for a SERS sensor-based detection of proteins, either in the extracellular or the intracellular environments. Antibodies are very large protein molecules with molecular weights of several hundred KDs, similar to its target antigen. However, agglutination of antibody with antigen requires only a small chain of amino acids, the antibody's paratope interacts to antigen's epitope. The remaining redundant amino acid sequences limit the number of targeting sites that can be functionalized on the SERS sensor. Additionally, the resemblance of structural unit, amino acids in antibody and antigen result in a similar Raman signature, as noticed in this study. This complicates the discrimination of signals from background (SERS substrate functionalized with antibody) and analyte (antigen). The other major limitations of using antibodies are their sensitivity to temperature, which technically limits their shelf-life, and that of any immunosensor, including SLISA and ELISA to just few months. In last decade aptamers have emerged as an ideal alternate to antibodies (Keefe et al. 2010). Aptamers are very small and stable synthetic oligonucleotide or peptide sequences that bind to specific targets and have entirely different fingerprints (background) than antigens. Aptamers are easily modified to stably conjugate to almost any substrate without any need of a linker, unlike a SERS immunosensor, which require a bifunctional linker to conjugate antibody to the SERS substrate. Furthermore the metal-thiol bond in an aptasensor is far more stable than a typical peptide bond in an immunosensor design. A linker molecule also increases the distance between a SERS substrate and the antibody. This extra distance not only decreases sensitivity of the SERS sensor, but also increases the size of the sensor, limiting its cellular uptake. Therefore, replacement of the targeting peptide-antibody with an aptamer (Pang et al. 2014; Zheng et al. 2014) can be an alternative towards development

of the first SERS sensor for intracellular detection of proteins, and can possibly also increase sensitivity of the SERS sensor. Indeed, a SERS aptasensor has been developed for the sensitive, multiplex and simultaneous detection of four analytes using a single aptamer (Zheng et al. 2014).

REFERENCES

- Banerjee P., Bhunia A. K. (2009). Mammalian cell-based biosensors for pathogens and toxins. *Trends Biotechnol.*, 27(3): 179-188
- Baronian K. H. (2004). The use of yeast and moulds as sensing elements in biosensors. *Biosens. Bioelectron.*, 19(9): 953-962
- Keefe A. D., Pai S., et al. (2010). Aptamers as therapeutics. *Nat. Rev. Drug Discovery*, 9: 537-550
- Lee M., Lee S., et al. (2011). Highly reproducible immunoassay of cancer markers on a gold-patterned microarray chip using surface-enhanced Raman scattering imaging. *J. Biosens. Bioelectron.*, 26: 2135-2141
- Lin X. M., Cui Y., et al. (2009). Surface-enhanced Raman spectroscopy: substrate-related issues. *Anal. Bioanal. Chem.*, 394: 1729-1745
- Pang S., Labuza T. P., et al. (2014). Development of a single aptamer-based surface enhanced Raman scattering method for rapid detection of multiple pesticides. *Analyst*, 139(8): 1895-1901
- Savitz D. A. (2014). Review of the Environmental protection Agency's state-of-the-science evaluation of nonmonotonic dose-response relationships as they apply to endocrine disruptors. National Academy of Sciences, pp 64
- Zheng J., Pang S., et al. (2014). Evaluation of surface-enhanced Raman scattering detection using a handheld and a bench-top Raman spectrometer: a comparative study. *Talanta*, 129: 79-85

APPENDICES

I. Y-PER

INSTRUCTIONS



Y-PER™ Yeast Protein Extraction Reagent

78990 78991

0826.4

Number	Description
78990	Y-PER Yeast Protein Extraction Reagent, 500mL, sufficient reagent for 100-200g of wet cell pellet
78991	Y-PER Yeast Protein Extraction Reagent, 200mL, sufficient reagent for 40-80g of wet cell pellet

Storage: Store product at room temperature.

Introduction

The Thermo Scientific Y-PER Yeast Protein Extraction Reagent is a mild detergent formulation that is superior to the classical methods of protein isolation from yeast. In studies with *Saccharomyces cerevisiae*, yields of soluble protein typically exceed those achieved by glass bead disruption. Y-PER Reagent is effective for extracting soluble proteins from *Saccharomyces cerevisiae*, *Schizosaccharomyces pombe*, *Bacillus subtilis* and *Escherichia coli* as well as a variety of gram-positive bacteria.

Yeast protein extraction and purification has traditionally been difficult and time consuming. The yeast cell is difficult to lyse because of its complex proteinaceous cell wall that provides rigidity to the weak plasma membrane. Techniques for protein extraction from yeast often involve harsh mechanical treatment while using strong reducing agents, chemicals and pH and temperature extremes. The popular glass bead lysis protocol requires special equipment and must be performed at 4°C. The low yields of protein commonly obtained with this technique are the result of denaturation and proteins nonspecifically binding to the glass beads. In contrast, Y-PER Reagent uses a simple room temperature protocol that can be completed in 20 minutes and requires no special equipment.

General Guidelines for Yeast Cell Disruption

- **Fresh Cells and Frozen Cells:** Y-PER Reagent is capable of extracting proteins equally well from recently harvested cells and frozen cells.
- **Cell Density and Strain Variation:** Differences in growth rate among organisms, growth temperature and media composition can have dramatic effects on the number of cells harvested from a given volume of culture. For this reason, several suggestions for the amount of Y-PER Reagent to use for a given cell pellet (wet cell paste) weight are provided.
- ***Saccharomyces cerevisiae*:** Y-PER Reagent is equally effective on cells grown to saturation or cells isolated from log-phase growth in either rich or synthetic defined media.
- ***Schizosaccharomyces pombe*:** Y-PER Reagent performs best on cells grown in synthetic defined media such as Edinburgh Minimal Media (EMM). To achieve adequate results from cells grown in rich media such as YES, cells must be harvested during log-phase growth. To increase protein yield from *S. pombe* cultures grown past log-phase, increase temperature to 45°C during lysis and use protease inhibitors.
- ***Bacillus subtilis*:** Y-PER Reagent will not lyse *B. subtilis* spores. When using sporulating strains, cells must be harvested during log-phase growth. For strains unable to sporulate, cells may be grown to saturation before harvesting.
- **Enzyme Activity:** Because all proteins differ in structure, solubility and stability, there is no guarantee that a particular protein will retain optimal activity in the presence of Y-PER Reagent. However, Y-PER Reagent does not interfere with the activity of β -galactosidase. Y-PER Reagent is also compatible with affinity-based purification protocols for glutathione S-transferase (GST) and histidine-tagged fusion proteins.

Note: Y-PER Reagent contains detergent and, therefore, is not compatible with protein assays that are incompatible with detergents.

Pierce Biotechnology PO Box 117 (815) 968-0747 www.thermoscientific.com/yper
3747 N. Meridian Road Rockford, IL 61105 USA (815) 968-7316 fax

Procedure for Protein Extraction

1. Pellet cells by centrifugation at approximately $3000 \times g$ (e.g., 5000 rpm for Beckman JA-20 rotor) for 5 minutes at 4°C.

Note: Cells may be processed immediately after centrifugation or the cell pellet may be frozen at -20°C or -80°C.

2. Resuspend cells in an appropriate amount of Y-PER Reagent as indicated in Table 1. Vortex gently or pipette up and down until the mixture is homogeneous.

Note: To prevent degradation of proteins, add protease inhibitors (e.g., Thermo Scientific Halt Protease Inhibitor Cocktail, EDTA-Free, Product No. 87785) to the sample.

Table 1. Volume of Thermo Scientific Y-PER Reagent to add per milligram of cell pellet.

Wet Cell Pellet Weight (mg)	Y-PER Reagent Volume (μL)
50	125-250
100	250-500
250	625-1250
500	1250 - 2500

3. Agitate the mixture at room temperature for 20 minutes.

4. Pellet the cell debris by centrifuging at $14,000 \times g$ for 10 minutes.

Note: Typically, greater than 90% of the soluble protein is extracted at this point and may be used for further purification or analysis. A second extraction may increase yield, but is usually not necessary.

5. Reserve the supernatant (i.e., lysate) for analysis, further purification and/or protein concentration determination.

Note: Y-PER Reagent contains detergent and, therefore, is not compatible with protein assays that are incompatible with detergents.

Related Thermo Scientific Products

89835	DNase I, 5000 units
87785	Halt™ Protease Inhibitor Cocktail, EDTA-Free (100X), 1mL
87786	Halt Protease Inhibitor Cocktail, contains sufficient reagents to treat 100mL of sample
78248	B-PER™ Bacterial Protein Extraction Reagent, 500mL
77720	Bond-Breaker™ CEP Solution, 5mL, enhances lysis of stationary-phase yeast cells
78870	Yeast DNA Extraction Kit, for extraction of genomic and plasmid DNA from <i>S. cerevisiae</i>
75768	Yeast β-Galactosidase Assay Kit

This product ("Product") is warranted to operate or perform substantially in conformance with published Product specifications in effect at the time of sale, as set forth in the Product documentation, specifications and/or accompanying package inserts ("Documentation") and to be free from defects in material and workmanship. Unless otherwise expressly authorized in writing, Products are supplied for research use only. No claim of suitability for use in applications regulated by FDA is made. The warranty provided herein is valid only when used by properly trained individuals. Unless otherwise stated in the Documentation, this warranty is limited to one year from date of shipment when the Product is subjected to normal, proper and intended usage. This warranty does not extend to anyone other than the original purchaser of the Product ("Buyer").

No other warranties, express or implied, are granted, including without limitation, implied warranties of merchantability, fitness for any particular purpose, or non infringement. Buyer's exclusive remedy for non-conforming Products during the warranty period is limited to replacement of or refund for the non-conforming Product(s).

There is no obligation to replace Products as the result of (i) accident, disaster or event of force majeure, (ii) misuse, fault or negligence of or by Buyer, (iii) use of the Products in a manner for which they were not designed, or (iv) improper storage and handling of the Products.

Current product instructions are available at www.thermoscientific.com/pierce. For a faxed copy, call 800-874-3723 or contact your local distributor.

© 2012 Thermo Fisher Scientific Inc. All rights reserved. Unless otherwise indicated, all trademarks are property of Thermo Fisher Scientific Inc. and its subsidiaries. Printed in the USA.

INSTRUCTIONS



Pierce™ BCA Protein Assay Kit

23225 23227

1296.9

Number	Description
23225	Pierce BCA Protein Assay Kit, sufficient reagents for 500 test-tube or 5000 microplate assays
23227	Pierce BCA Protein Assay Kit, sufficient reagents for 250 test-tube or 2500 microplate assays

Kit Contents:

BCA Reagent A, 1000mL (in Product No. 23225) or 500mL (in Product No. 23227), containing sodium carbonate, sodium bicarbonate, bicinchoninic acid and sodium tartrate in 0.1M sodium hydroxide

BCA Reagent B, 25mL, containing 4% cupric sulfate

Albumin Standard Ampules, 2mg/mL, 10 × 1mL ampules, containing bovine serum albumin (BSA) at 2mg/mL in 0.9% saline and 0.05% sodium azide

Storage: Upon receipt store at room temperature. Product shipped at ambient temperature.

Note: If either Reagent A or Reagent B precipitates upon shipping in cold weather or during long-term storage, dissolve precipitates by gently warming and stirring solution. Discard any kit reagent that shows discoloration or evidence of microbial contamination.

Table of Contents

Introduction	1
Preparation of Standards and Working Reagent (required for both assay procedures).....	2
Test Tube Procedure (Sample to WR ratio = 1:20)	3
Microplate Procedure (Sample to WR ratio = 1:8)	3
Troubleshooting.....	4
Related Thermo Scientific Products	5
Additional Information	5
References	6

Introduction

The Thermo Scientific™ Pierce™ BCA Protein Assay is a detergent-compatible formulation based on bicinchoninic acid (BCA) for the colorimetric detection and quantitation of total protein. This method combines the well-known reduction of Cu^{2+} to Cu^{+} by protein in an alkaline medium (the biuret reaction) with the highly sensitive and selective colorimetric detection of the cuprous cation (Cu^{+}) using a unique reagent containing bicinchoninic acid.¹ The purple-colored reaction product of this assay is formed by the chelation of two molecules of BCA with one cuprous ion. This water-soluble complex exhibits a strong absorbance at 562nm that is nearly linear with increasing protein concentrations over a broad working range (20-2000 $\mu\text{g}/\text{mL}$). The BCA method is not a true end-point method; that is, the final color continues to develop. However, following incubation, the rate of continued color development is sufficiently slow to allow large numbers of samples to be assayed together.

The macromolecular structure of protein, the number of peptide bonds and the presence of four particular amino acids (cysteine, cystine, tryptophan and tyrosine) are reported to be responsible for color formation with BCA.² Studies with di-, tri- and tetrapeptides suggest that the extent of color formation caused by more than the mere sum of individual color-producing functional groups.² Accordingly, protein concentrations generally are determined and reported with reference to standards of a common protein such as bovine serum albumin (BSA). A series of dilutions of known concentration are prepared from the protein and assayed alongside the unknown(s) before the concentration of each unknown is determined based on the standard curve. If precise quantitation of an unknown protein is required, it is advisable to select a protein

standard that is similar in quality to the unknown; for example, a bovine gamma globulin (BGG) standard (see Related Thermo Scientific Products) may be used when assaying immunoglobulin samples.

Two assay procedures are presented. Of these, the Test Tube Procedure requires a larger volume (0.1mL) of protein sample; however, because it uses a sample to working reagent ratio of 1:20 (v/v), the effect of interfering substances is minimized. The Microplate Procedure affords the sample handling ease of a microplate and requires a smaller volume (10-25µL) of protein sample; however, because the sample to working reagent ratio is 1:8 (v/v), it offers less flexibility in overcoming interfering substance concentrations and obtaining low levels of detection.

Preparation of Standards and Working Reagent (required for both assay procedures)

A. Preparation of Diluted Albumin (BSA) Standards

Use Table 1 as a guide to prepare a set of protein standards. Dilute the contents of one Albumin Standard (BSA) ampule into several clean vials, preferably using the same diluent as the sample(s). Each 1mL ampule of 2mg/mL Albumin Standard is sufficient to prepare a set of diluted standards for either working range suggested in Table 1. There will be sufficient volume for three replications of each diluted standard.

Table 1. Preparation of Diluted Albumin (BSA) Standards

Dilution Scheme for Standard Test Tube Protocol and Microplate Procedure (Working Range = 20-2,000µg/mL)			
<u>Vial</u>	<u>Volume of Diluent</u> (µL)	<u>Volume and Source of BSA</u> (µL)	<u>Final BSA Concentration</u> (µg/mL)
A	0	300 of Stock	2000
B	125	375 of Stock	1500
C	325	325 of Stock	1000
D	175	175 of vial B dilution	750
E	325	325 of vial C dilution	500
F	325	325 of vial E dilution	250
G	325	325 of vial F dilution	125
H	400	100 of vial G dilution	25
I	400	0	0 = Blank

Dilution Scheme for Enhanced Test Tube Protocol (Working Range = 5-250µg/mL)			
<u>Vial</u>	<u>Volume of Diluent</u> (µL)	<u>Volume and Source of BSA</u> (µL)	<u>Final BSA Concentration</u> (µg/mL)
A	700	100 of Stock	250
B	400	400 of vial A dilution	125
C	450	300 of vial B dilution	50
D	400	400 of vial C dilution	25
E	400	100 of vial D dilution	5
F	400	0	0 = Blank

B. Preparation of the BCA Working Reagent (WR)

1. Use the following formula to determine the total volume of WR required:

$$(\# \text{ standards} + \# \text{ unknowns}) \times (\# \text{ replicates}) \times (\text{volume of WR per sample}) = \text{total volume WR required}$$

Example: for the standard test-tube procedure with 3 unknowns and 2 replicates of each sample:

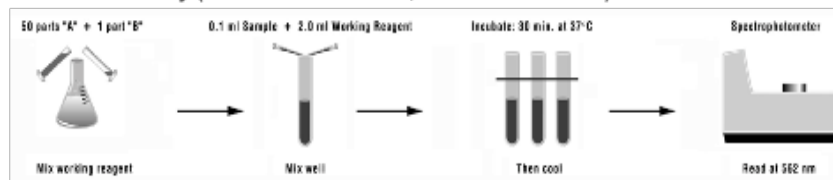
$$(9 \text{ standards} + 3 \text{ unknowns}) \times (2 \text{ replicates}) \times (2\text{mL}) = 48\text{mL WR required}$$

Note: 2.0mL of the WR is required for each sample in the test-tube procedure, while only 200 µl of WR reagent is required for each sample in the microplate procedure.

2. Prepare WR by mixing 50 parts of BCA Reagent A with 1 part of BCA Reagent B (50:1, Reagent A:B). For the above example, combine 50mL of Reagent A with 1mL of Reagent B.

Note: When Reagent B is first added to Reagent A, turbidity is observed that quickly disappears upon mixing to yield a clear, green WR. Prepare sufficient volume of WR based on the number of samples to be assayed. The WR is stable for several days when stored in a closed container at room temperature (RT).

Procedure Summary (Test-tube Procedure, Standard Protocol)



Test-tube Procedure (Sample to WR ratio = 1:20)

- Pipette 0.1mL of each standard and unknown sample replicate into an appropriately labeled test tube.
 - Add 2.0mL of the WR to each tube and mix well.
 - Cover and incubate tubes at selected temperature and time:
 - Standard Protocol: 37°C for 30 minutes (working range = 20-2000µg/mL)
 - RT Protocol: RT for 2 hours (working range = 20-2000µg/mL)
 - Enhanced Protocol: 60°C for 30 minutes (working range = 5-250µg/mL)
- Notes:**
- Increasing the incubation time or temperature increases the net 562nm absorbance for each test and decreases both the minimum detection level of the reagent and the working range of the protocol.
 - Use a water bath to heat tubes for either Standard (37°C incubation) or Enhanced (60°C incubation) Protocol. Using a forced-air incubator can introduce significant error in color development because of uneven heat transfer.
- Cool all tubes to RT.
 - With the spectrophotometer set to 562nm, zero the instrument on a cuvette filled only with water. Subsequently, measure the absorbance of all the samples within 10 minutes.

Note: Because the BCA assay does not reach a true end point, color development will continue even after cooling to RT. However, because the rate of color development is low at RT, no significant error will be introduced if the 562nm absorbance measurements of all tubes are made within 10 minutes of each other.
 - Subtract the average 562nm absorbance measurement of the Blank standard replicates from the 562nm absorbance measurement of all other individual standard and unknown sample replicates.
 - Prepare a standard curve by plotting the average Blank-corrected 562nm measurement for each BSA standard vs. its concentration in µg/mL. Use the standard curve to determine the protein concentration of each unknown sample.

Microplate Procedure (Sample to WR ratio = 1:8)

- Pipette 25µL of each standard or unknown sample replicate into a microplate well (working range = 20-2000µg/mL) (e.g., Thermo Scientific™ Pierce™ 96-Well Plates, Product No. 15041).

Note: If sample size is limited, 10µL of each unknown sample and standard can be used (sample to WR ratio = 1:20). However, the working range of the assay in this case will be limited to 125-2000µg/mL.
- Add 200µL of the WR to each well and mix plate thoroughly on a plate shaker for 30 seconds.
- Cover plate and incubate at 37°C for 30 minutes.
- Cool plate to RT. Measure the absorbance at or near 562nm on a plate reader.

Notes:

- Wavelengths from 540-590nm have been used successfully with this method.
- Because plate readers use a shorter light path length than cuvette spectrophotometers, the Microplate Procedure requires a greater sample to WR ratio to obtain the same sensitivity as the standard Test Tube Procedure. If higher 562nm measurements are desired, increase the incubation time to 2 hours.
- Increasing the incubation time or ratio of sample volume to WR increases the net 562nm measurement for each well and lowers both the minimum detection level of the reagent and the working range of the assay. As long as all standards and unknowns are treated identically, such modifications may be useful.

5. Subtract the average 562nm absorbance measurement of the Blank standard replicates from the 562nm measurements of all other individual standard and unknown sample replicates.
6. Prepare a standard curve by plotting the average Blank-corrected 562nm measurement for each BSA standard vs. its concentration in $\mu\text{g/mL}$. Use the standard curve to determine the protein concentration of each unknown sample.

Note: If using curve-fitting algorithms associated with a microplate reader, a four-parameter (quadratic) or best-fit curve will provide more accurate results than a purely linear fit. If plotting results by hand, a point-to-point curve is preferable to a linear fit to the standard points.

Troubleshooting

Problem	Possible Cause	Solution
No color in any tubes	Sample contains a copper chelating agent	Dialyze, desalt or dilute sample Increase copper concentration in working reagent (e.g., use 50:2, Reagent A:B) Remove interfering substances from sample using Product No. 23215
Blank absorbance is OK, but standards and samples show less color than expected	Strong acid or alkaline buffer, alters working reagent pH	Dialyze, desalt, or dilute sample
	Color measured at the wrong wavelength	Measure the absorbance at 562nm
Color of samples appears darker than expected	Protein concentration is too high	Dilute sample
	Sample contains lipids or lipoproteins	Add 2% SDS to the sample to eliminate interference from lipids ¹ Remove interfering substances from sample using Product No. 23215
All tubes (including blank) are dark purple	Buffer contains a reducing agent	Dialyze or dilute sample
	Buffer contains a thiol	Remove interfering substances from sample using Product No. 23215
	Buffer contains biogenic amines (catecholamines)	
Need to measure color at a different wavelength	Spectrophotometer or plate reader does not have 562nm filter	Color may be measure at any wavelength between 540nm and 590nm, although the slope of standard curve and overall assay sensitivity will be reduced

A. Interfering substances

Certain substances are known to interfere with the BCA assay including those with reducing potential, chelating agents, and strong acids or bases. Because they are known to interfere with protein estimation at even minute concentrations, avoid the following substances as components of the sample buffer:

Ascorbic acid	EGTA	Iron	Impure sucrose
Catecholamines	Impure glycerol	Lipids	Tryptophan
Creatinine	Hydrogen peroxide	Melibiose	Tyrosine
Cysteine	Hydrazides	Phenol Red	Uric acid

Other substances interfere to a lesser extent with protein estimation using the BCA assay, and these have only minor (tolerable) effects below a certain concentration in the original sample. Maximum compatible concentrations for many substances in the Standard Test Tube Protocol are listed in Table 2 (see last page of Instructions). Substances were compatible at the indicated concentration in the Standard Test Tube Protocol if the error in protein concentration estimation caused by the presence of the substance was less than or equal to 10%. The substances were tested using WR prepared immediately before each experiment. Blank-corrected 562nm absorbance measurements (for a 1000 $\mu\text{g/mL}$ BSA standard + substance) were compared to the net 562nm measurements of the same standard prepared in 0.9% saline. Maximum compatible concentrations will be lower in the Microplate Procedure where the sample to WR ratio is 1:8 (v/v).

Furthermore, it is possible to have a substance additive affect such that even though a single component is present at a concentration below its listed compatibility, a sample buffer containing a combination of substances could interfere with the assay.

III ELISA, A. RAD54



SER945Hu 96 Tests
Enzyme-linked Immunosorbent Assay Kit
For RAD54 Like Protein 2 (RAD54L2)
Organism Species: Homo sapiens (Human)
Instruction manual

FOR IN VITRO AND RESEARCH USE ONLY
NOT FOR USE IN CLINICAL DIAGNOSTIC PROCEDURES

11th Edition (Revised in July, 2013)

[INTENDED USE]

The kit is a sandwich enzyme immunoassay for in vitro quantitative measurement of RAD54L2 in human tissue homogenates and other biological fluids.

[REAGENTS AND MATERIALS PROVIDED]

Reagents	Quantity	Reagents	Quantity
Pre-coated, ready to use 96-well strip plate	1	Plate sealer for 96 wells	4
Standard	2	Standard Diluent	1×20mL
Detection Reagent A	1×120μL	Assay Diluent A	1×12mL
Detection Reagent B	1×120μL	Assay Diluent B	1×12mL
TMB Substrate	1×9mL	Stop Solution	1×6mL
Wash Buffer (30 × concentrate)	1×20mL	Instruction manual	1

[MATERIALS REQUIRED BUT NOT SUPPLIED]

1. Microplate reader with 450 ± 10nm filter.
2. Precision single or multi-channel pipettes and disposable tips.
3. Eppendorf Tubes for diluting samples.
4. Deionized or distilled water.
5. Absorbent paper for blotting the microtiter plate.
6. Container for Wash Solution

[STORAGE OF THE KITS]

1. **For unopened kit:** All the reagents should be kept according to the labels on vials. The **Standard, Detection Reagent A, Detection Reagent B** and the **96-well strip plate** should be stored at -20°C upon receipt while the others should be at 4 °C.
2. **For opened kit:** When the kit is opened, the remaining reagents still need to be stored according to the above storage condition. Besides, please return the unused wells to the foil pouch containing the desiccant pack, and reseal along entire edge of zip-seal.

Designed by Cloud-Clone Corp., Assembled by Usckn Life Science Inc. ISO9001:2008, ISO13485:2003
11271 Richmond Avenue, Suite H194, Houston, TX 77062, USA | Toll free: 001-888-960-7402 | Fax: 001-432-538-0088 | Http://www.cloud-clone.us | E-mail: mail@cloud-clone.us
Export Processing Zone Building F, Wuhan, Hubei 430036, PRC | Toll free: 0086-800-880-0687 | Fax: 0086-27-8425-8551 | Http://www.usckn.com | E-mail: mail@usckn.com

Note:

It is highly recommended to use the remaining reagents within 1 month provided this is within the expiration date of the kit. For the expiration date of the kit, please refer to the label on the kit box. All components are stable until this expiration date.

[SAMPLE COLLECTION AND STORAGE]

Tissue homogenates - The preparation of tissue homogenates will vary depending upon tissue type. For this assay, tissues were rinsed in ice-cold PBS(0.01mol/L,pH 7.0-7.2) to remove excess blood thoroughly and weighed before homogenization. Minced the tissues to small pieces and homogenized them in 5-10mL of PBS with a glass homogenizer on ice(Micro Tissue Grinders woks, too). The resulting suspension was sonicated with an ultrasonic cell disrupter or subjected to two freeze-thaw cycles to further break the cell membranes. After that, the homogenates were centrifugated for 5 minutes at 5000×g. Remove the supernate and assay immediately or aliquot and store at ≤-20°C.

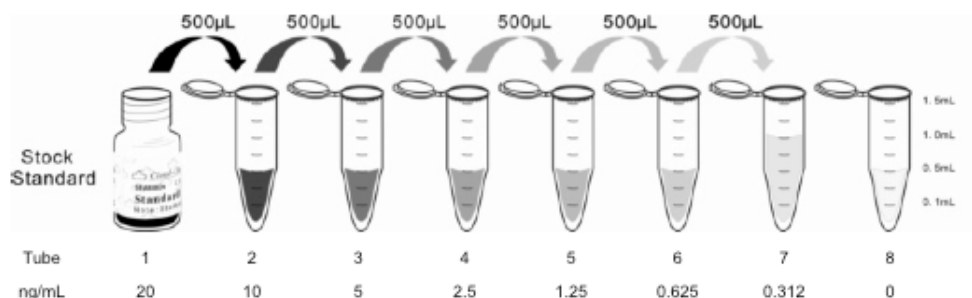
Other biological fluids - Centrifuge samples for 20 minutes at 1000×g. Remove particulates and assay immediately or store samples in aliquot at -20°C or -80°C for later use. Avoid repeated freeze/thaw cycles.

Note:

1. Samples to be used within 5 days may be stored at 4°C, otherwise samples must be stored at -20°C (≤1 month) or -80°C (≤2 months) to avoid loss of bioactivity and contamination.
2. Sample hemolysis will influence the result, so hemolytic specimen should not be detected.
3. When performing the assay, bring samples to room temperature.

[REAGENT PREPARATION]

1. Bring all kit components and samples to room temperature (18-25°C) before use.
2. **Standard** - Reconstitute the **Standard** with 1.0mL of **Standard Diluent**, kept for 10 minutes at room temperature, shake gently(not to foam). The concentration of the standard in the stock solution is 20ng/mL. Please prepare 7 tubes containing 0.5mL Standard Diluent and produce a double dilution series according to the picture shown below. Mix each tube thoroughly before the next transfer. Set up 7 points of diluted standard such as 20ng/mL, 10ng/mL, 5ng/mL, 2.5ng/mL, 1.25ng/mL, 0.625ng/mL, 0.312ng/mL, and the last EP tubes with **Standard Diluent** is the blank as 0ng/mL.



3. **Detection Reagent A and Detection Reagent B** - Briefly spin or centrifuge the stock Detection A and Detection B before use. Dilute to the working concentration with **Assay Diluent A and B**, respectively (1:100).
4. **Wash Solution** - Dilute 20mL of Wash Solution concentrate (30×) with 580mL of deionized or distilled water to prepare 600mL of Wash Solution (1×).
5. **TMB substrate** - Aspirate the needed dosage of the solution with sterilized tips and do not dump the residual solution into the vial again.

Note:

1. Making serial dilution in the wells directly is not permitted.
2. Prepare standard within 15 minutes before assay. Please do not dissolve the reagents at 37°C directly.
3. Please carefully reconstitute Standards or working Detection Reagent A and B according to the instruction, and avoid foaming and mix gently until the crystals are completely dissolved. To minimize imprecision caused by pipetting, use small volumes and ensure that pipettors are calibrated. It is recommended to suck more than 10µL for once pipetting.
4. The reconstituted Standards, Detection Reagent A and Detection Reagent B can be **used only once**.
5. If crystals have formed in the Wash Solution concentrate (30×), warm to room temperature and mix gently until the crystals are completely dissolved.
6. Contaminated water or container for reagent preparation will influence the detection result.

[SAMPLE PREPARATION]

1. Cloud-Clone Corp. is only responsible for the kit itself, but not for the samples consumed during the assay. The user should calculate the possible amount of the samples used in the whole test. Please reserve sufficient samples in advance.
2. Please predict the concentration before assaying. If values for these are not within the range of the standard curve, users must determine the optimal sample dilutions for their particular experiments. Sample should be diluted by 0.01mol/L PBS(PH=7.0-7.2).
3. If the samples are not indicated in the manual, a preliminary experiment to determine the validity of the kit is necessary.
4. Tissue or cell extraction samples prepared by chemical lysis buffer may cause unexpected ELISA results due to the impacts from certain chemicals.
5. Due to the possibility of mismatching between antigen from other origin and antibody used in our kits (e.g., antibody targets conformational epitope rather than linear epitope), some native or recombinant proteins from other manufacturers may not be recognized by our products.
6. Influenced by the factors including cell viability, cell number or sampling time, samples from cell culture supernatant may not be detected by the kit.
7. Fresh samples without long time storage is recommended for the test. Otherwise, protein degradation and denaturalization may occur in those samples and finally lead to wrong results.

[ASSAY PROCEDURE]

1. Determine wells for diluted standard, blank and sample. Prepare 7 wells for standard, 1 well for blank. Add 100µL each of dilutions of standard (read Reagent Preparation), blank and samples into the appropriate wells. Cover with the Plate sealer. Incubate for 2 hours at 37°C.

2. Remove the liquid of each well, don't wash.
3. Add 100µL of **Detection Reagent A** working solution to each well. Incubate for 1 hour at 37°C after covering it with the Plate sealer.
4. Aspirate the solution and wash with 350µL of 1× Wash Solution to each well using a squirt bottle, multi-channel pipette, manifold dispenser or autowasher, and let it sit for 1–2 minutes. Remove the remaining liquid from all wells completely by snapping the plate onto absorbent paper. Totally wash 3 times. After the last wash, remove any remaining Wash Buffer by aspirating or decanting. Invert the plate and blot it against absorbent paper.
5. Add 100µL of **Detection Reagent B** working solution to each well. Incubate for 30 minutes at 37°C after covering it with the Plate sealer.
6. Repeat the aspiration/wash process for total 5 times as conducted in step 4.
7. Add 90µL of **Substrate Solution** to each well. Cover with a new Plate sealer. Incubate for 15 - 25 minutes at 37°C (Don't exceed 30 minutes). Protect from light. The liquid will turn blue by the addition of Substrate Solution.
8. Add 50µL of **Stop Solution** to each well. The liquid will turn yellow by the addition of Stop solution. Mix the liquid by tapping the side of the plate. If color change does not appear uniform, gently tap the plate to ensure thorough mixing.
9. Remove any drop of water and fingerprint on the bottom of the plate and confirm there is no bubble on the surface of the liquid. Then, run the microplate reader and conduct measurement at 450nm immediately.

Note:

1. **Assay preparation:** Keep appropriate numbers of wells for each experiment and remove extra wells from microplate. Rest wells should be resealed and stored at -20°C.
2. **Samples or reagents addition: Please use the freshly prepared Standard.** Please carefully add samples to wells and mix gently to avoid foaming. Do not touch the well wall. For each step in the procedure, total dispensing time for addition of reagents or samples to the assay plate should not exceed 10 minutes. This will ensure equal elapsed time for each pipetting step, without interruption. Duplication of all standards and specimens, although not required, is recommended. To avoid cross-contamination, change pipette tips between additions of standards, samples, and reagents. Also, use separated reservoirs for each reagent.
3. **Incubation:** To ensure accurate results, proper adhesion of plate sealers during incubation steps is necessary. Do not allow wells to sit uncovered for extended periods between incubation steps. Once reagents are added to the well strips, DO NOT let the strips DRY at any time during the assay. Incubation time and temperature must be controlled.
4. **Washing:** The wash procedure is critical. Complete removal of liquid at each step is essential for good performance. After the last wash, remove any remaining Wash Solution by aspirating or decanting and remove any drop of water and fingerprint on the bottom of the plate. Insufficient washing will result in poor precision and false elevated absorbance reading.
5. **Controlling of reaction time:** Observe the change of color after adding **TMB Substrate** (e.g. observation once every 10 minutes), if the color is too deep, add **Stop Solution** in advance to avoid excessively strong reaction which will result in inaccurate absorbance reading.
6. **TMB Substrate** is easily contaminated. Please protect it from light.

7. The environment humidity which is less than 60% might have some effects on the final performance, therefore, a humidifier is recommended to be used at that condition.

[TEST PRINCIPLE]

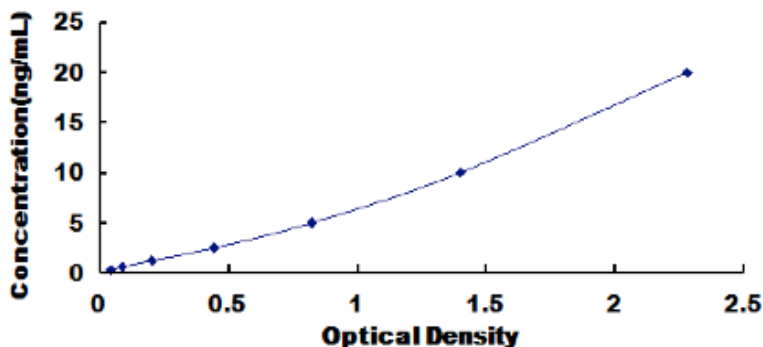
The microtiter plate provided in this kit has been pre-coated with an antibody specific to RAD54L2. Standards or samples are then added to the appropriate microtiter plate wells with a biotin-conjugated antibody specific to RAD54L2. Next, Avidin conjugated to Horseradish Peroxidase (HRP) is added to each microplate well and incubated. After TMB substrate solution is added, only those wells that contain RAD54L2, biotin-conjugated antibody and enzyme-conjugated Avidin will exhibit a change in color. The enzyme-substrate reaction is terminated by the addition of sulphuric acid solution and the color change is measured spectrophotometrically at a wavelength of $450\text{nm} \pm 10\text{nm}$. The concentration of RAD54L2 in the samples is then determined by comparing the O.D. of the samples to the standard curve.

[CALCULATION OF RESULTS]

Average the duplicate readings for each standard, control, and samples and subtract the average zero standard optical density. Construct a standard curve by plotting the mean O.D. and concentration for each standard and draw a best fit curve through the points on the graph or create a standard curve on log-log graph paper with RAD54L2 concentration on the y-axis and absorbance on the x-axis. Using some plot software, for instance, curve expert 1.30, is also recommended. If samples have been diluted, the concentration read from the standard curve must be multiplied by the dilution factor.

[TYPICAL DATA]

In order to make the calculation easier, we plot the O.D. value of the standard (X-axis) against the known concentration of the standard (Y-axis), although concentration is the independent variable and O.D. value is the dependent variable. However, the O.D. values of the standard curve may vary according to the conditions of assay performance (e.g. operator, pipetting technique, washing technique or temperature effects), plotting log of the data to establish standard curve for each test is recommended. Typical standard curve below is provided for reference only.



Typical Standard Curve for RAD54L2, Human ELISA.

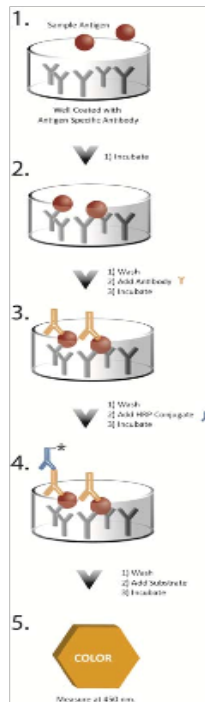
Designed by Cloud-Clone Corp., Assembled by Usck Life Science Inc. ISO9001:2008; ISO13485:2003
 11271 Richmond Avenue Suite H104, Houston, TX 77062, USA | Toll free: 001-888-960-7402 | Fax: 001-832-838-0088 | Http://www.cloud-clone.us | E-mail: mail@cloud-clone.us
 Export Processing Zone Building F, Wuhan, Hubei 430096, PRC | Toll free: 0086-800-880-8687 | Fax: 0086-27-4425-8051 | Http://www.usck.com | E-mail: mail@usck.com

B. HSP70



Product Manual

INTRODUCTION



The HSP70 high sensitivity ELISA kit is a complete kit for the quantitative determination of inducible Heat Shock Protein 70 (Hsp70) in serum and plasma samples of human, mouse, and rat origin. It does not detect other Hsp70 family members such as Hsc70 (Hsp73), Grp78, DnaK (*E. coli*), or Hsp71 (*M. tuberculosis*). Please read the entire kit insert before performing this assay.

Hsp70 is a molecular chaperone whose expression is induced upon exposure of the cell or organism to conditions of stress. It prevents protein aggregation and promotes the refolding of proteins that become damaged in response to environmental insults, pathogens, and disease. Its activity is essential for cellular survival and recovery under stress conditions, as well as for the maintenance of normal cellular function under non-stress conditions¹⁻³. Hsp70 has been implicated to play a role in a variety of disease and physiological processes such as hyperthermia,⁴ hypertension,⁵ toxic exposure to chemical agents,⁶ hypoxia,⁷ ischemia,^{8,9} inflammation,¹⁰ autoimmunity,^{5, 11} apoptosis,^{12, 13} cancer,¹³ organ transplantation,¹⁴ and bacterial^{15,16} and viral¹⁷ infections. Hsp70 is also a key regulator of many normal physiological processes including aging,^{12,18} spermatogenesis,^{19,20} menstruation,²¹ and physical activity such as exercise²². The Hsp70 High Sensitivity ELISA kit is designed to evaluate and monitor Hsp70 in these processes, providing a key research tool to understand the role of Hsp70 in physiology and disease.



Bring all reagents except the standard and assay buffer to room temperature for at least 30 minutes prior to opening.



Plastic tubes must be used for standard preparation.

REAGENT PREPARATION

1. Wash Buffer

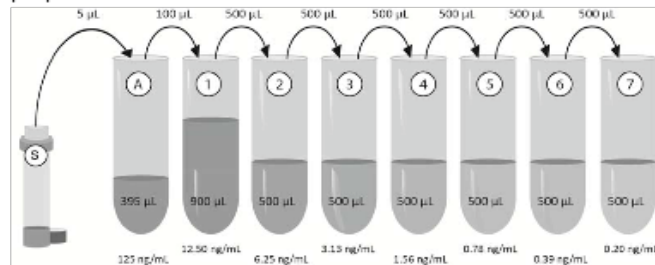
Prepare the wash buffer by diluting 50 mL of the supplied Wash Buffer Concentrate with 950 mL of deionized water. This can be stored at room temperature until the kit expiration, or for 3 months, whichever is earlier.

2. 125ng/ml Hsp70 Intermediate Standard

Label one 12x75 mm polypropylene tube as A. Pipet 400 μ l of the assay buffer into tube A. Remove 5 μ l of the assay buffer from the tube for a final volume of 395 μ l. Add 5 μ l of the Hsp70 High Sensitivity Standard stock solution. Vortex gently. Keep the intermediate standard on ice for optimal performance.

3. Hsp70 Standard Curve

The assay buffer as well as diluted standards and samples should be kept on ice and used within 60 minutes of preparation for optimal performance. If ice is not available, room temperature assay buffer may be used and the diluted standards and samples should be used within 20 minutes of preparation.



Label seven 12x75 mm polypropylene tubes #1 through #7. Pipet 900 μ l of the assay buffer into tube#1. Pipet 500 μ l of the assay buffer into tubes #2 through #7. Add 100 μ l of the 125ng/ml Hsp70 Intermediate Standard from tube A into tube #1. Vortex gently. Add 500 μ l of tube #1 to tube#2 and vortex gently. Continue this for tubes #3 through #7.



Product Manual



Bring all reagents except the standard and assay buffer to room temperature for at least 30 minutes prior to opening.



All standards and samples should be run in duplicate.



Pre-rinse each pipet tip with reagent. Use fresh pipet tips for each sample, standard, and reagent.



Pipet the reagents to the sides of the wells to avoid possible contamination.



Prior to the addition of antibody, conjugate or substrate, ensure there is no residual wash buffer in the wells. Remaining wash buffer may cause variation in assay results.

Serum and Plasma Preparation

1. Collect whole blood in either clotting tubes for serum or EDTA tubes for plasma.
2. Allow serum to clot for 30 minutes.
3. Centrifuge at 1000 x g for 15 minutes at 4°C.
4. Place supernatants in a clean tube.
5. The supernatant may be aliquotted and stored at or below -20°C, or used immediately in the assay.

ASSAY PROCEDURE

Refer to the Assay Layout Sheet to determine the number of wells to be used. Remove the wells not needed for the assay and return them, with the desiccant, to the mylar bag and seal. Store unused wells at 4°C.

1. Pipet 100µl of the assay buffer into the S0 (0ng/ml standard) wells.
2. Pipet 100µl of Standards #1 through #7 to the bottoms of the appropriate wells.
3. Pipet 100µl of the samples to the bottoms of the appropriate wells.
4. Seal the plate. Incubate for 2 hours shaking* at room temperature.
5. Empty the contents of the wells and wash by adding 400µl of wash buffer to every well. Repeat 3 more times for a total of 4 washes. After the final wash, empty or aspirate the wells and firmly tap the plate on a lint free paper towel to remove any remaining wash buffer.
6. Pipet 100µl of yellow antibody into each well except the blank.
7. Seal the plate. Incubate for 1 hour shaking* at room temperature.
8. Wash as above (Step 5).
9. Add 100µl of blue conjugate to each well except the blank.
10. Seal the plate. Incubate for 1 hour shaking* at room temperature.
11. Wash as above (Step 5).
12. Pipet 100µl of substrate solution into each well.
13. Incubate for 30 minutes shaking* at room temperature.
14. Pipet 100µl of stop solution into each well.



Product Manual

15. After zeroing the plate reader against the substrate blank, read optical density at 450nm. If plate reader is not capable of adjusting for the blank, manually subtract the mean OD of the substrate blank from all readings.

*Shaking is preferably carried out on a suitable plate or orbital shaker set at a speed to ensure adequate mixing of the contents of the wells. The optimal speed for each shaker will vary and may range from 120-700rpm.

CALCULATION OF RESULTS

Several options are available for calculating the concentration of Hsp70 in the samples. We recommend that the data be handled by an immunoassay software package utilizing a 4-parameter logistic curve fitting program. If data reduction software is not readily available, the concentrations may be calculated as follows:

1. Calculate the average Net OD for each standard and sample by subtracting the average blank OD from the average OD for each standard and sample.

$$\text{Average Net OD} = \text{Average OD} - \text{Average Blank OD}$$

2. Plot the average Net OD for each standard versus Hsp70 concentration in each standard. Approximate a straight line through the points. The concentration of the unknowns can be determined by interpolation.

Samples with concentrations outside of the standard curve range will need to be re-analyzed using a different dilution.



Multiply sample concentrations by the dilution factor used during sample preparation.

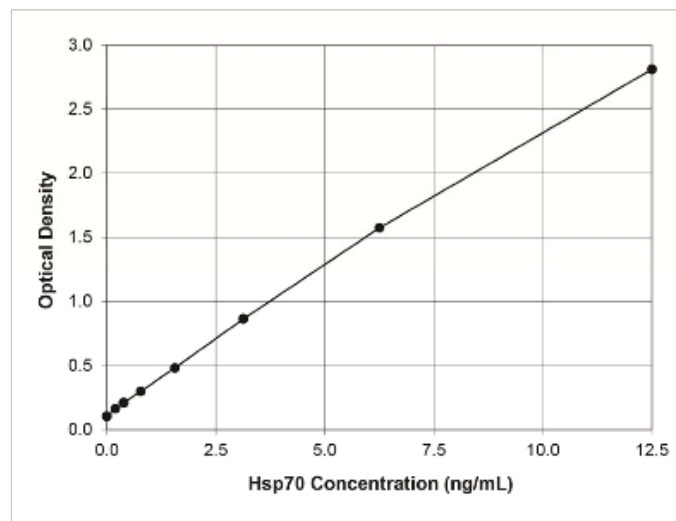


Product Manual

TYPICAL RESULTS

The results shown below are for illustration only and should not be used to calculate results from another assay.

Sample	Net OD	Hsp70 (ng/ml)
S0	0.104	0
S1	2.810	12.50
S2	1.574	6.25
S3	0.864	3.13
S4	0.481	1.56
S5	0.299	0.78
S6	0.211	0.39
S7	0.163	0.20
Unknown 1	1.291	4.98
Unknown 2	0.372	1.08



IV Permission emails A. OMICS Publishing Group

Vinay Bhardwaj <vbhar002@fiu.edu> Fri, Sep 4, 2015 at 4:47 PM
To: editor.jbsbe@omicsonline.org, contact@omicsonline.org

Dear OMICS Representative,

I am the first author of a manuscript published in OMICS Journal of Biosensors Bioelectronics (JBSBE).

Bhardwaj V, Srinivasan S, McGoron AJ (2013) AgNPs-based Label-Free Colloidal SERS Nanosensor for the Rapid and Sensitive Detection of Stress-Proteins Expressed in response to Environmental-Toxins. J Biosens Bioelectron S12: 005

The work in the manuscript was completed as a part of my PhD dissertation. I am now writing my dissertation towards graduating this year. **Please grant me permission to use this article in my PhD dissertation to be submitted to Florida International University.** Although my common sense tells that using the material in my dissertation with proper citation is okay, but i thought of asking you first.

Please forward my request to the concerned person if you are not the one to be contacted for such a request.

Regards,
Vinay Bhardwaj, PhD Dissertation year Fellow
Department of Biomedical Engineering
Florida International University
10555 W Flagler Street
Miami-FL 33174
Voice: 786-479-1281

"RULE OUT CANCER BEFORE IT RULES US OUT"

[Quoted text hidden]

Biosensors & Bioelectronics <editor.jbsbe@omicsinc.com> Sat, Sep 5, 2015 at 9:21 AM
To: Vinay Bhardwaj <vbhar002@fiu.edu>

Dear. Dr. Vinay Bharadwaj,

We are happy to answer your query.

You can use your article to cite since it is already published.

With thanks & regards,
Margret Wilson
Editorial Assistant
Journal of Biosensors and Bioelectronics
731 Gull Ave, Foster City
CA 94404, USA
Phone: +1-650-268-9744
Fax: +1-650-618-1414

B. Photon Foundation Publishing



Vinay Bhardwaj <vbhar002@fiu.edu>

Request for permission to use my manuscript in my dissertation

2 messages

Vinay Bhardwaj <vbhar002@fiu.edu>

Fri, Sep 4, 2015 at 5:06 PM

To: Photon Journal <photonjournal@yahoo.com>, Photon Journals <photonjournals@gmail.com>

Dear Photon Foundation Representative,

I am the first author of a manuscript published in Photon Journal of Biomedical Engineering.

Bhardwaj V, McGoron AJ (2014). Biosensor technology for chemical and biological toxins: progress and prospects. Photon 112, 380-392.

The work in the manuscript was completed as a part of my PhD dissertation. I am now writing my dissertation towards graduating this year. **Please grant me permission to use this article in my PhD dissertation to be submitted to Florida International University.** Although my common sense tells that using the material in my dissertation with proper citation is okay, but i though of asking you first.

Please forward my request to the concerned person if you are not the one to be contacted for such a request.

Regards,
Vinay Bhardwaj, PhD Dissertation year Fellow
Department of Biomedical Engineering
Florida International University
10555 W Flagler Street
Miami-FL 33174
Voice: 786-479-1281

"RULE OUT CANCER BEFORE IT RULES US OUT"

Photon Journal <photonjournal@yahoo.com>

Sat, Sep 5, 2015 at 12:12 AM

Reply-To: Photon Journal <photonjournal@yahoo.com>

To: Vinay Bhardwaj <vbhar002@fiu.edu>

Dear Dr. Vinay Bhardwaj
Welcome at [Photon](#).

Reference to your mail permission is granted.

With Best Wishes from [International Library for Thesis](#)

International Library for Thesis - Photon eBooks

International Library for Thesis International Library for Thesis is Top Most international platform for publication of world's best research work.

Tim Haggerty
Editorial Office
[Photon Journal of Biomedical Engineering](#)
[Photon](#)

[Quoted text hidden]

C. Royal Society of Chemistry

Vinay Bhardwaj <vbhar002@fiu.edu>

Request for the permission to use my manuscript in my dissertation
2 messages

Vinay Bhardwaj <vbhar002@fiu.edu>Fri, Sep 4, 2015 at 4:55 PM

To: "<analyst@rsc.org>" <analyst@rsc.org>, Royal Society of Chemistry <RSC1@rsc.org>

Dear RSC Representative,

I am the first author of a manuscript published in Royal Society of Chemistry - Analyst.

Bhardwaj V, Srinivasan S, McGoron AJ. Efficient Intracellular Delivery and Improved Biocompatibility of colloidal silver nanoparticles towards intracellular SERS immuno-sensing. 2015, 140(12): 3929-34

The work in the manuscript was completed as a part of my PhD dissertation. I am now writing my dissertation towards graduating this year. **Please grant me permission to use this article in my PhD dissertation to be submitted to Florida International University.** Although my common sense tells that using the material in my dissertation with proper citation is okay, but i thought of asking you first.

Please forward my request to the concerned person if you are not the one to be contacted for such a request.

Regards,
Vinay Bhardwaj, PhD Dissertation year Fellow
Department of Biomedical Engineering
Florida International University
10555 W Flagler Street
Miami-FL 33174
Voice: 786-479-1281

"RULE OUT CANCER BEFORE IT RULES US OUT"

RSC1 (shared) <RSC1@rsc.org>Mon, Sep 7, 2015 at 9:45 AM

To: Vinay Bhardwaj <vbhar002@fiu.edu>

Dear Vinay,

Thank you for your email.

With regards to being able to reproduce parts of your manuscript and/or the figure files in your doctoral dissertation there is no problem with this and you do not require formal permission – its covered in the licence to publish:

(a) The Author(s) may republish the final (PDF) version of the Paper in theses of the Author(s) in printed form and may make available this PDF in the theses of Author(s) via any website(s) that the university(ies) of the Author(s) may have for the deposition of theses. No embargo period applies.

Hope that helps clear up the issue. Please let me know if you have any further queries.

Jamie Long

Publishing Assistant - Editorial Production

Royal Society of Chemistry,

Thomas Graham House,

Science Park, Milton Road,

Cambridge, CB4 0WF, UK

Tel +44 (0) 1223 432144

www.rsc.org

Winner of The Queen's Award for Enterprise, International Trade 2013

D. SPIE

Vinay Bhardwaj <vbhar002@fiu.edu>

reprint permission

1 message

Nicole Harris <nicoleh@spie.org>
To: "vbhar002@fiu.edu" <vbhar002@fiu.edu>

Fri, Sep 4, 2015 at 5:53 PM

Dear Vinay Bhardwaj,

Thank you for seeking permission from SPIE to reprint material from our publications. As author, SPIE shares the copyright with you, so you retain the right to reproduce your paper in part or in whole.

Publisher's permission is hereby granted under the following conditions:

- (1) the material to be used has appeared in our publication without credit or acknowledgment to another source; and
- (2) you credit the original SPIE publication. Include the authors' names, title of paper, volume title, SPIE volume number, and year of publication in your credit statement.

Sincerely,

Nicole Harris
Administrative Editor, SPIE Publications
1000 20th St.
Bellingham, WA 98225
+1 360 685 5586 (office)
nicoleh@spie.org

SPIE is the international society for optics and photonics. <http://SPIE.org>



SPIE.



INTERNATIONAL
YEAR OF LIGHT
2015

VITA

VINAY BHARDWAJ

- 2006 Bachelor of Sciences (Hons.) in Zoology, University of Delhi, India
- 2008 Master of Sciences in Biotechnology, Kurukshetra University, India
- 2008-2009 Research Fellow, Nano-Biotech Lab, University of Delhi, India
- 2009-2010 Assistant Professor, Department of Biotechnology and Bioinformatics, Geeta Vidya Mandir Girl's College, Sonapat-HR, India
- 2010-2010 Visiting Research Scholar, Florida International University (FIU), Department of Biomedical Engineering (BME), Miami-FL USA
- 2010-2015 Graduate Teaching Certification, FIU-CATE (Center for the Advancement of Teaching)
- 2010-Present Pursuing Doctorate in BME with specialization in Bio-nanotechnology for biomedical applications, in particular cancer and CNS theranostics
- 2010-Present Graduate Teaching/Research Assistant*, FIU-BME, Miami-FL USA.

* For my excellence in teaching and research I was awarded Provost Outstanding Graduate Teaching Assistant Award-2015 and FIU-UGS Dissertation Year Fellowship-2015

Patent: On-chip assay for environmental surveillance. Ref. FIU.153 (Status: US patent filed in November 2015).

PUBLICATIONS AND PRESENTATIONS, * denotes presenting author

1. Kaushik A., Jayant R. D., Nikkah R., Bhardwaj V., Roy U., Huang Z., Ruiz A., Yndart A., Sagar V., Atluri V. and Nair M. (2015) "Magnetically-guided on-demand delivery and toxicity evaluation of magneto-electric nanoparticles (MENs) for CNS delivery: in vitro and in vivo study" Nature Methods (status: submitted)

2. Srinivasan S., Bhardwaj V. and McGoron A. J. (2015) "SERS-guided pH triggered doxorubicin delivery for cancer theranostics" *J. Biomedical Nanotechnology* (status: submitted, under review)
3. Bhardwaj V., Srinivasan S. and McGoron A. J. (2015) "On-chip surface-enhanced Raman spectroscopy (SERS)-Linked ImmunoSensor Assay (SLISA) for rapid and global environmental surveillance of chemical toxins" *Proc. SPIE 9486*, 2015, pages 8
4. Bhardwaj V., Srinivasan S. and McGoron A. J. (2015) "Efficient intracellular delivery and improved biocompatibility of colloidal silver nanoparticles towards intracellular SERS immunosensing" *Analyst (The Royal Society of Chemistry Journal)*, 140, 3929-34
5. Bhardwaj V. and McGoron A. J. (2013) "Biosensor technology for chemical and biological toxins: progress and prospects" *P. J. Biomedical Engineering*, 112, ISJN: 6275-3754
6. Bhardwaj V., Srinivasan S., Dua R. and McGoron A. J. (2013) "SERS biosensor for label-free monitoring of environmental stress" *IEEE Explore* 79. Doi: 10.1109/SBEC.2013.48
7. Bhardwaj V., Srinivasan S. and McGoron A. J. (2013) "AgNPs-based label-free colloidal SERS nanosensor for rapid and sensitive detection of stress proteins expressed in response to environmental toxins" *J. Biosensors & Bioelectronics*, S12: 005. Doi: 10.4172/6155-6210.S12-005
8. Bhardwaj V.*, Srinivasan S. and McGoron A. J. "Towards development of first LF-CBB-SIST (Label-Free Cell-Based Biosensor using SERS ImmunoSensor Technology for intracellular proteins detection" *BMES 2015*, Oct 7-10, Tampa-FL (Abstract #120 accepted for poster presentation)
9. Kaushik A.*, Jayant R. D., Nikkhah R., Bhardwaj V. et al. "In vitro & in vivo cytotoxic evaluation of magneto-electric nanoparticles for CNS delivery" *21st Scientific Conference*, April 22-25 2015, Miami-FL (Poster Presentation)
10. Bhardwaj V.*, Srinivasan S. and McGoron A. J. "On-chip surface-enhanced Raman spectroscopy (SERS)-Linked ImmunoSensor Assay (SLISA) for rapid and global environmental surveillance of chemical toxins" *SPIE Defense, Security and Sensing Technology (DSS)*, April 20-24 2015, Baltimore-MD (Poster Presentation)
11. Bhardwaj V.*, Srinivasan S., Dua R. and McGoron A. J. "SERS biosensor for label-free monitoring of environmental stress" *IEEE 29th Southern Biomedical Engineering Conference (SBEC)*, Miami-FL, May 3-5 2013 (Oral Presentation)
12. Bhardwaj V.*, Srinivasan S. and McGoron A. J. "SERS over ELISA for rapid and label free detection of response of stress markers to environmental toxins" *2nd International Conference & Exhibition on Biosensors & Bioelectronics*, Chicago-IL, June 17-19 2013 (Oral Presentation)